Design and Investigation of Vinylcyclopropanes (VCPs) as Fast Curing Resins

DISSERTATION

zur Erlangung des akademischen Grades
eines Doktors der Naturwissenschaften (Dr. rer. nat.)
an der Bayreuther Graduiertenschule für Mathematik und
Naturwissenschaften (BayNAT) der Universität Bayreuth

vorgelegt von

Paul Pineda Contreras

aus *Ruda*

Bayreuth, 2016

Die vorliegende Arbeit wurde in der Zeit von *04/2013* bis *07/2016* in Bayreuth am Lehrstuhl *Makromolekulare Chemie II* unter Betreuung von Frau Professorin Dr. *Seema Agarwal* angefertigt.

Dissertation eingereicht am: 19.07.2016

Zulassung durch das Leitungsgremium: 26.07.2016

Wissenschaftliches Kolloquium: 19.01.2017

Amtierender Direktor: Prof. Dr. Stephan Kümmel

Prüfungsausschuss:

Prof. Dr. Seema Agarwal	(Erstgutachterin)
Prof. Dr. Hans-Werner Schmidt	(Zweitgutachter)
Prof. Dr. Birgit Weber	(Vorsitz)
Jun.-Prof. Dr. Markus Retsch	

“If you don't design your own life plan, chances are you'll fall into someone else's plan. And guess what they have planned for you? Not much.”

by Jim Rohn

Dedicated to my mother Jadwiga Ksionsko (†)

Table of Contents

Summary 1

Zusammenfassung 3

1 Introduction 5

1.1 Volume change of polymeric materials 5

1.1.1. Extent of volume shrinkage 6

1.1.2. Theoretical background of volume shrinkage 8

1.1.3. Techniques for shrinkage reduction 10

1.2 Ring opening polymerization (ROP) 11

1.2.1. Types of ROP 12

1.2.2. Radical ring opening polymerization (RROP) 13

1.2.3. Application of low shrinking materials 15

1.3 Vinylcyclopropanes (VCPs) 17

1.3.1. Access and function of VCPs in synthetic chemistry 17

1.3.2. VCPs as low shrinking monomers and resins 19

1.4 Photo-polymerization 23

1.5 Research progress of VCPs beyond low shrinking monomers 28

2 References 30

3 Thesis Overview 38

3.1 Publication 1: Low volume shrinkage of polymers by photopolymerization of 1,1-bis(ethoxycarbonyl) 2-vinylcyclopropanes 39

3.2 Publication 2: Renaissance for low shrinking resins: all-in-one solution by bi-functional vinylcyclopropane-amides 41

3.3 Publication 3: Photo-polymerizable, low shrinking modular construction kit with high efficiency based on vinylcyclopropanes 44

3.4 Individual Contributions to Joint Publications 48

4 Reprints of Publications 50

4.1 Low volume shrinkage of polymers by photopolymerization of 1,1-bis(ethoxycarbonyl) 2-vinylcyclopropanes 50

4.2 Renaissance for low shrinking resins: all-in-one solution by bi-functional vinylcyclopropane-amides 74

4.3 Publication 3: Photo-polymerizable, low shrinking modular construction kit with high efficiency based on vinylcyclopropanes 104

5 Outlook 123

6 List of Publications 124

7 Conference Participations 125

8 List of Abbreviations and Symbols 126

9 Acknowledgements 130

10 (Eidesstattliche) Versicherung und Erklärung 132

Summary

The volume shrinkage during curing is to a certain extent a general issue of all cross-linkable systems and has not been sufficiently improved so far. But in particular for applications, like dental fillings, coatings and adhesives low volume shrinkage is of high significance, since within these applications final textures have to match very precisely the requirements on the spot. Thereby, especially the radical ring opening polymerization (RROP) of vinylcyclopropane (VCP) monomers have set in the past a promising concept to overcome this drawback. However until now, the general low reactivity of VCP monomers restricted their overall use. Therefore, the focus of this thesis was to investigate the polymerization behavior of light induced VCP monomers, as well as to design novel VCP systems with high reactivity, complete conversion and tunable properties.

In the first part of the work the emphasis laid on evaluating the impact of mono-functional VCPs on the polymerization kinetic, using different combinations of photo-initiators. Further, since the substitution pattern might allow further influence on the reactivity, different methyl-substituted VCP derivatives were prepared. A reduction in RROP reactivity, according to the sequence VCP>MeVCP>>DiMeVCP, was observed by methyl substitution in α- and β-position to the vinyl group. Thereby, for the MeVCP the participation of a constitution isomer could be confirmed, which was used to prove the formation of cyclobutane units by 2D-NMR measurements. Generally, the cyclobutane formation occurs as unwanted side reaction during the RROP of VCPs. Nevertheless, by comparing thermal and photo-initiated polymerizations with binary, as well as with ternary photo-initiators, an enhanced reactivity and ring-opening could be achieved. Thereby, the addition of the onium salt DPIHFP enhanced the initiation process. Further, as a consequence of the enhanced thermodynamic control, due to the photo-polymerization, a significant higher amount of 1,5-ring-opened units, and vice versa lower amount of cyclobutane-units could be obtained, reducing the overall shrinkage of VCPs significantly.

In contrast to the mono-functional VCP monomers, for bi-functional VCP resins a novel approach, introducing H-bond forming amide-groups into the system was explored. Thereby, a novel VCP resin “VCPMe$_3$hexAmid” was synthesized, which

incorporated intermolecular H-bonds into the VCP system. For comparison, a further VCP resin "VCPhexEster" was synthesized, which served as reference for bi-functional VCP resins reported in literature. Thereby, curing experiments with KSCN as chaotropic additive as well as temperature dependent NMR measurements confirmed the H-bond participation for VCPMe$_3$hexAmid, whereas not for VCPhexEster. In consequence, a significant difference in reactivity between both VCP resins was observed, analyzed by conventional curing-, as well as by photo-DSC- and dielectric analysis (DEA) experiments. Hereby, for the first time a fast bulk curing within seconds and high overall conversions (>95%) could be obtained for a VCP resin. Additionally, further characteristics like mechanical strength, cytoxicity and optical refraction were balanced in optimum ranges. As overall result, VCPMe$_3$hexAmid showed low viscosity and a reduction by 45% in volume shrinkage, compared to the well-known and abundantly used urethane-dimethacrylate (UDMA) resin.

Based on the H-bond concept, the effective partial self-assembly was explored to a universal applicability. In this regard, uniformity within the intermolecular hydrogen bond strength was proven, providing an excellent control of constant high reactivity, nearly regardless of the chosen spacer-unit. This offered the system a possible application as modular construction kit for low shrinking resins. According to the uniformity within the H-bond strength, it was demonstrated by two entirely different VCP ester-amide systems that, *e.g.*, a modulation of the mechanical properties was easy to achieve, without sacrificing reactivity. For this purpose, one flexible, high molar mass macro-monomer and two rigid, low molar mass monomers were prepared. Both, extremely low volume shrinkages between 1.4 - 4.5%, and a wide range of E-moduli for the resulting polymer networks could be obtained. Finally, an easy control of final characteristics by varying the co-monomer content in co-networks was shown; without obtaining any significant disadvantage within curing behavior.

In summary, for the first time a suitable and efficient concept regarding VCPs was developed, which provided high reactivity and conversion during RROP. Thereby, the key to success was based on the use of photo-polymerization techniques, and by including selective intermolecular H-bonds to the VCP systems. Further, the resulting concept of modulation offers VCPs a sustainable and improved alternative to the commonly used methacrylate systems, especially since the volume shrinkage on polymerization is significantly reduced.

Zusammenfassung

Der Polymerisationsschrumpf von Monomeren ist zu einem gewissen Maß ein allgemeingültiges Problem aller Polymerisationsverfahren und wurde bislang noch nicht ausreichend verbessert. Dabei ist ein geringer Volumenschwund in Anwendungen, wie Zahnfüllungen, Beschichtungen und Klebstoffen von hoher Bedeutung, da innerhalb dieser Applikationen die endgültigen Texturen sehr genau den entsprechenden Anforderungen entsprechen müssen. Zur Überwindung dieses Nachteils stellte die radikalisch ringöffnende Polymerisation (RROP) von Vinylcyclopropanen (VCP) in der Vergangenheit ein vielversprechendes Konzept dar. Jedoch beschränkte die geringe Reaktivität der VCP-Monomere deren Verwendung. Daher war das Ziel dieser Arbeit die Untersuchung des lichtinduzierten Polymerisationsverhaltens, sowie die Entwicklung eines neuartigen VCP-Systems mit hoher Reaktivität, hohen Reaktionsumsätzen und einstellbaren Eigenschaftsprofil.

Im ersten Teil dieser Arbeit lag der Schwerpunkt in der Bewertung des kinetischen Polymerisationsverhaltens monofunktioneller VCP-Monomere, wobei verschiedene Kombinationen von Photoinitiatoren untersucht wurden. Da das Substitutionsmuster einen Einfluss auf die Reaktivität ermöglichte, wurden verschiedene VCP-Derivate hergestellt. Dabei wurde eine Verminderung der Reaktivität mit steigender methyl-Substitution in α- und β-Position zur Vinylgruppe, entsprechend der Reihenfolge VCP>MeVCP>>DiMeVCP, festgestellt. Ferner wurde für das MeVCP die Präsenz eines Konstitutionsisomers bestätigt. In 2D-NMR Untersuchungen konnte dieses die Bildung von Cyclobutan-Addukten während der RROP bestätigen. Gleichwohl konnte bei einem direkten Vergleich von thermischen und lichtinduzierten Polymerisationsmethoden mit binären als auch ternären Initiatorsystemen, eine verbesserte Reaktivität und Ringöffnung erreicht werden. Dabei konnte durch die Zugabe des Oniumsalzes DPIHFP der Initiierungsprozess erhöht werden. Im Weiteren konnte aufgrund der verbesserten thermodynamischen Kontrolle der Photopolymerisation ein erhöhter Anteil an 1,5-ringgeöffneten-, und umgekehrt verminderter von Cyclobutan-Einheiten, erzielt werden, wodurch der Volumenschrumpf der VCP-Polymerisation signifikant verringert wurde.

Im Gegensatz zu den monofunktionellen VCP Monomeren wurde für bifunktionelle VCP-Harze ein neues Konzept von Amid Wasserstoffbrücken (H-Brücken) untersucht.

Dazu wurde ein neuartiges VCPMe$_3$hexAmid-Harz entwickelt, welches erstmalig intermolekulare H-Brücken einbaute. Für einen Vergleich wurde ein weiteres VCP-Harz VCPhexEster synthetisiert, welches als Referenz galt und kennzeichnend für alle bisherigen bifunktionellen VCP-Harze stand. Durch Härtungsuntersuchungen mit KSCN als chaotropem Additiv, sowie temperaturabhängiger NMR Messungen, konnten die H-Brücken für VCPMe$_3$hexAmid bestätigt werden. Als Resultat wurde ein signifikanter Unterschied in der Reaktivität beider VCP-Systeme beobachtet. Dabei wurden sowohl konventionellen Härtungsreaktionen, als auch Photo-DSC und dielektrischen Analyse (DEA) Experimente durchgeführt. Erstmalig wurde für ein VCP-Harz eine schnelle Substanzpolymerisation innerhalb weniger Sekunden und mit hohen Umsätzen (>95%) erreicht. Weitere Untersuchungen zur mechanischen Festigkeit, Zytotoxizität und optischer Brechung zeigten zudem ein ausgewogenes Leistungsverhältnis. Ferner wurde für das VCPMe$_3$hexAmid eine niedrige Zähigkeit und 45%ige Verminderung im Schrumpf, verglichen zum häufig verwendeten Urethandimethacrylat (UDMA) erzielt.

Basierend auf den H-Brücken wurde die partielle Selbstorganisation der VCP zu einem universell Konzept untersucht. Unabhängig von der verwendeten Spacer-Einheit konnte eine Einheitlichkeit der intermolekularen H-Brücken nachgewiesen werden, wodurch eine exzellente Kontrolle und hohe Reaktivität erfolgte. Dieses ermöglichte eine Applikation als modularisierter Synthesebaukasten. Entsprechend der Gleichheit der H-Brücken wurde anhand zweier unterschiedlicher VCPs gezeigt, dass die Steuerung der mechanischen Eigenschaften einfach zu erzielen war. Zu diesem Zweck wurden sowohl ein flexibles Makromonomerharz, sowie zwei biegesteife, niedrigmolekulare VCP-Harze synthetisiert. Dabei wurden sehr niedrige Schrumpfung zwischen 1.4 – 4.5%, als auch eine große Vielfalt von E-Moduli erreicht. Zuletzt ermöglichte die Co-Härtungen mit den anderen VCP-Comonomeren eine einfache Kontrolle der Eigenschaften; ohne signifikante Nachteile innerhalb der Härtungseigenschaft zu erhalten.

Zusammengefasst wurde erstmalig ein effizientes und anwendbares VCP-System entwickelt, welches eine hohe Reaktivität und Härtungsausbeute bereitstellte. Zum wesentlichen Erfolg dieser Arbeit führte sowohl die Anwendung der Photopolymerisation als auch das Einbringen spezifischer H-Brücken. Ferner bat das Konzept der VCP-Modularisierung die Möglichkeit nachhaltig eine verbesserte Alternative zu den derzeitig verwendeten Methacrylaten bereitzustellen, vor allem, da die Volumenschrumpfung der Polymerisation deutlich reduziert ist.

1 Introduction

This thesis addresses the design and investigation of mono- and bi-functional vinylcyclopropane (VCP) systems, being capable as low shrinking monomers and resins. Thereby, the ring opening polymerization (ROP) of the VCPs was used as powerful tool to accomplish an effective counter measure to the commonly observed volume shrinkage during polymerization. Further, in order to solve the issue of low reactivity obtained by VCPs, enhanced photo-polymerization methods and novel VCP resins were prepared and studied.

In the following chapter the theoretical background, according to the knowledge about the volume shrinkage, low shrinking materials as well as their polymerization techniques, are described. Furthermore, a short general overview about the synthetic procedures and applications of VCPs is given. Finally, Section 1.5 reviews additional research progresses of VCPs in the field of material science. The reviewed fundamentals and state-of-the-art literature summary are indispensable to put the achieved results and the observed phenomena reported in this thesis into context.

1.1 Volume change of polymeric materials

Polymeric materials, whether organic, inorganic or as composites are extremely versatile due to their characteristics and application range. Thus, polymeric materials are encountered in everyday life and meanwhile applied across all sectors from private purposes to industrial and medical fields. Thereby, adjustable specific characteristics as shape, appearance, physical state, mechanical strength or electric properties, just to mention a few, made polymeric materials suitable for almost all purpose applications, whether on land, on water or in the air. Especially by adjustments of several influencing factors like the selection of specific monomers, chemical synthesis, polymerization conditions, processing steps, physical-chemical interactions and many other factors, the final properties can be adapted for the end application.[1]

However, one factor that is often neglected, but can influence the above-mentioned material properties strongly, is the volume change. Neglecting the evaporation of any component and focusing on solvent-free processes, two different phenomena for the

volume change are reasonable. First, for the processing within a temperature range the volumetric coefficient of thermal expansion, which is given by

$$\alpha_V = \frac{1}{V}\left(\frac{\partial V}{\partial T}\right)_p \quad (1)$$

has to be taken into consideration.[2] Thereby the coefficient determines the proportional variation of volume within the temperature variation. The larger the value α_v, the more pronounced the effect is. Due to the fact that α_v is very dependent on the material and varies even between thermoplastic polymers, the degree to which a material expands or contracts (contraction ≙ negative expansion) during the processing to its final state is an important factor, which has to be engineered in advance.[3]

The second observed phenomenon of volume change is caused by the polymerization and curing process itself and describes primarily the problem for unprocessable thermosets, since these are in a cross-linked and unchangeable form after curing.[3] Thereby, in accordance with the polymerization an increase in density a reduction in volume occurs. For all current vinyl polymerizations this negative volume change, henceforth described as shrinkage, is to some degree inevitable.[4] Therefore, due to the non-availability of alternative monomers, reducing or eliminating the shrinkage, several processing strategies have been developed, such as

- increasing the molecular weight of the monomer units ≙ reduction of reactive units per volume, *e.g.* applying of prepolymers
- manufacturing of composite-materials
- applying mixtures of different types of monomers and resins, *e.g*. reactive diluents
- adjusted application procedures, such as layer-by-layer, gradient initiations etc.

However, at a certain level also these strategy improvements find their limitation and new concepts shift into the spotlight, with the objective of reducing shrinkage by alternative monomer structures. Thereby, shrinkage reduction by ROP of compact ring molecules defines the most promising method and forms the basis of this scientific work.[5,6]

1.1.1. Extent of volume shrinkage

Shrinkage is observed during both, the monomer polymerization as well as the curing. Especially when a distinction between mono – and multifunctional monomers has to be defined, the following slight difference is worth to mention. Whereas mono-

functional monomers form linear or branched polymers, which are still processable, the use of multi-functional monomers can lead to elastomers (wide-meshed) and thermosets (close-meshed) of fixed shapes (see Fig. 1).[7,8]

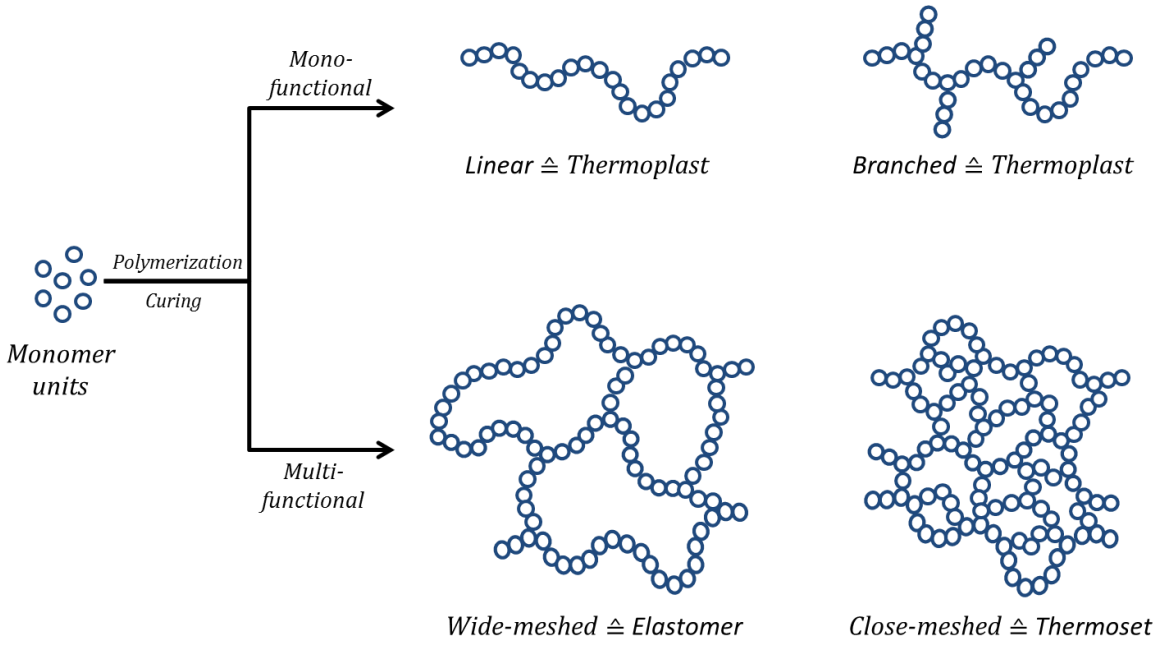

Figure 1: Schematic description of linear, branched, wide- and close-meshed polymers describing the chain configuration of thermoplastics, elastomers and thermosets. Thermoplastic elastomers (TPE) have a particular status and are not included.

As a result, in particular thermosets with their high degree of cross-linking are very prone to high shrinkage.[9] Depending on the reaction conditions, the multi-functionality and the monomer itself the general curing process can be separated into a pre-gelation (liquid) and post-gelation (solid) stage. Thereby, the point in time when the monomer/polymer solution becomes insoluble (cross-linked) defines the "gel-point" (see Fig. 2), representing the transition of pre- and post-gelation.[10,11] Thus, with an ongoing curing, after the gel-point is reached, further density changes (≙ shrinkage) become more and more restricted. As a result, internal stress within the network can be produced. Thereby, high internal stress may cause many different problems, such as reduction of adhesion, bad mechanical properties, micro-voids, delayed micro-fractures, accelerated aging, delamination and warping.[12,13]

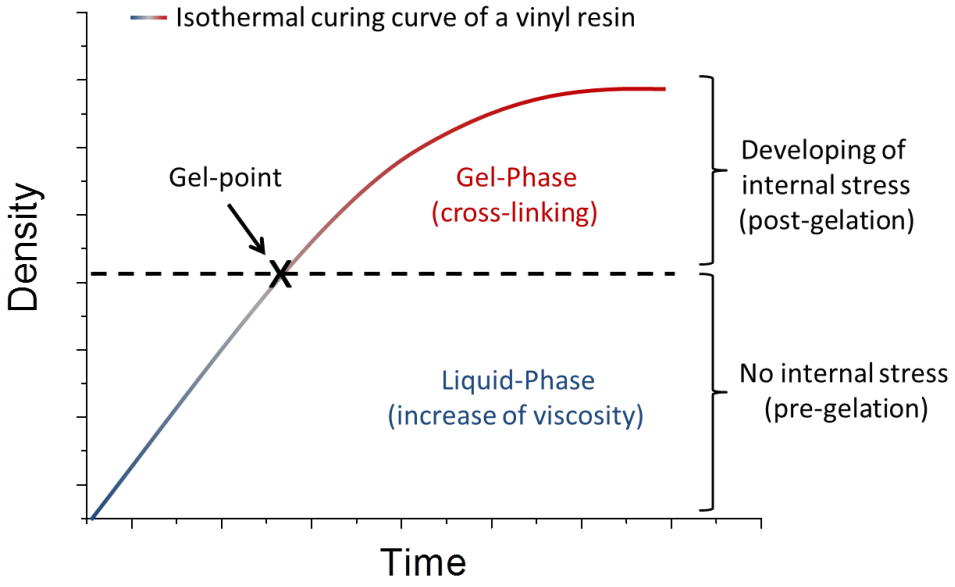

Figure 2: Schematic curing curve of a vinyl resin, cured at isothermal conditions. The curve is an exemplary representation and not representative to a single experiment. Shape and slope can vary depending on reaction conditions (chain-growth or step-reaction), the multi-functionality and the monomer itself.

Hence, several methods seem apparent to avoid this problem, as for instance, a postponing of the gelation point and a general reduction or elimination of the shrinkage.[14] A postponing of gelation can be achieved by decreasing the initiator concentration or applying selective chain-transfer reactions.[15,16] In photo-polymerizations, also the so called "intensity cycle", slowing and fastening the polymerization by light intensity, is used.[17,18] Further, by applying a reversible cleavage of the cross-linked polymer upon light exposure, a photo-induced plasticity can be achieved allowing a chain rearrangement and exhibiting stress relaxation.[19] Moreover, within non isothermal curing processes both the introduction of hyper-branched resins, showing a low Newtonian viscosity, as well as adjustments of the temperature profiles are common.[20,21] However, despite these manifold concepts, each strategy has a drawback as well, being not appropriate to solve the fundamental challenges of internal stress for overall applications. Thus, only a shrinkage reduction/elimination seem suitable to result in more reliable and durable cross-linked networks.

1.1.2. Theoretical background of volume shrinkage

As mentioned before, polymerization shrinkage is a universally shared attribute among all polymerization methods as any monomer conversions is accompanied with a formation of covalent bonds.[4] Thereby, within the monomeric form predominantly van

der Waals (v.d.W.) forces define the distance between two and more molecules, while within the polymeric form especially the covalent bonds are responsible for distances.[22] For two vinyl bonds for instance, the v.d.W. distance corresponds to ~340 pm, whereas the joined C-C bond accounts to a length of only 154 pm (see Fig. 3a).[3] Hence, an approximately shrinkage of 50% could be expected for this sole bond change. Yet, further effects have to be taken into consideration as well. This is partly due to the fact that the distance of the C=C double bond (134 pm) changes to a single C-C bond (154 pm) too, reflecting an expansion in bond length of about 15%.[3] With regard to additional factors, like content of vinyl groups, entropy reduction, formation of free volume (amorphous polymers), tacticity, entanglements, phase transition changes and formation of small by-product molecules (polycondensation reactions), the overall shrinkage is a cumulative value of all these factors (see Fig. 3b).[3,23]

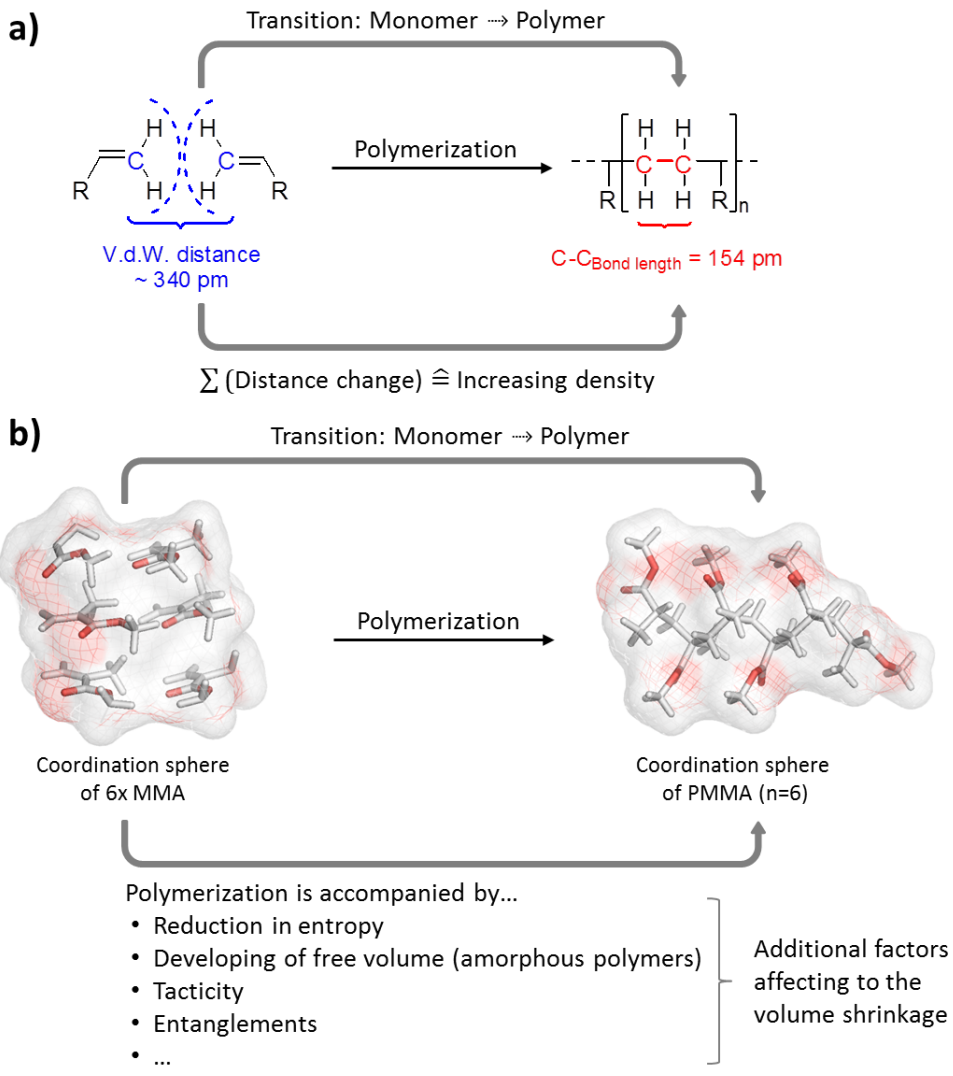

Figure 3: a) Illustration of the volume shrinkage by bond changes of any vinyl monomer. b) Example of a methyl methacrylate (MMA) polymerization to illustrate the other factors affecting to the overall volume shrinkage.

As a result, during the polymerization process of methyl methacrylate (MMA) the density at 25 °C increases from 0.940 g cm^{-3} to 1.189 g cm^{-3} for the poly(methyl methacrylate) (PMMA), yielding a shrinkage of 21.4% (values measured by a 1 mL pycnomter at the liquid stage and by Archimedes Principle for the solid state).[24] However, the complexity of shrinkage becomes easily illustrated by comparing the shrinkage values of *n*-butyl- and *i*-butyl methacryl esters, differing in 15.7% and 13.3% respectively, although the molar masses are identical.[25,26]

1.1.3. Techniques for shrinkage reduction

Within Section 1.1.1 already several techniques have been introduced to handle or reduce the shrinkage during polymerization. In the following, an extended concept and explanation is provided. For instance, the use of prepolymers or monomers of larger molar volumes, such as macro-monomers, is a widely spread method across diverse applications, whether for coatings, dental resins or adhesives.[27–30] Thereby, prepolymers are often polymerized to a conversion prior to the gel-point, to remain in a processable state, utilizing them in pure forms or as mixtures with other monomers and resins. Since these prepolymers have an increased molecular weight, less shrinkage during the final curing is observed.[5,31]

The formulation of resins to composites with additional materials is a further exploitable method.[32] However, as the use of composite materials, whether with inert or active fillers, organic or inorganic additives and fibers, colorants and many other ingredients, aims also other issues as improved mechanical properties by reinforcements, optical properties, heat resistant and so on.[27] Hence, a detailed discussion of this methods is not made within this work. The range of formulation possibilities to choose is obviously enormous, and the number of combinations quasi limitless.[8] However, it is apparent that the amount of shrinkage reduces with increasing content of any filler, since these generally exhibit only low dimensional change during the curing.[33]

Where feasible, addition of reactive diluents with lower shrinkage is preferred as well. For instance, styrene is applied in polyester moldings and casting formulations to reduce and control the cumulative shrinkage.[34]

With regard to photo-curing applications, where initiation and rate of polymerization can be easily controlled by light intensity and duration, new concepts of photo-

polymerizations at low temperatures, reducing the overall shrinkages by vitrification processes, are carried out.[35] Thereby, a combinatorial effect is used, combining low conversions, due to low temperature polymerizations, with the effect of thermal expansion (see volumetric coefficient in Section 1.1), counteracting the additional shrinkage, when the temperature is raised and the previously trapped radicals continue to initiate the polymerization.

Likewise, for low cross-linked systems and gels volume changes initialized by light irradiation were described, offering a potential control in reversible shrinkage and expansion. In this process, light as external stimulus initiates a photochemical ionization, changing the internal osmotic pressure and charge repulsion of the network.[36,37]

Another alternative, representing these days the most widespread concept of shrinkage reduction is incumbent upon the ring-opening polymerization (ROP), which was examined for the first time in 1966 by *I. S. Klaus* and *W. S. Knowles* by an anhydride polymerization. Both, an effect of the ring size as well as an effect of rigidity and free volume was described.[38] On this basis, especially *W. J. Bailey* developed many concepts and theories on new monomers, providing a reduced shrinkage or even volume expansion.[3,39] Thereby, *W. J. Bailey* extended the general concept of ROP, opening up new possibilities into the previously unexplored research field of low shrinking and expandable monomers.[22,39]

1.2 Ring opening polymerization (ROP)

Nowadays, many different types of cyclic compounds have been developed and are spread across numerous application fields.[40,41] But in particular those, which are capable to participate in ROP process are of high interest for the development of low shrinking monomers.[42] Thereby, the most apparent advantage of the ROP is its possibility to transform a cyclic monomer directly to a ring-opened, linear repeat unit. Hence, the ring-opened bond turns from a previously covalent distance to a near v.d.W. distance, reducing the overall shrinkage to a certain extent (see Fig 4a). Furthermore, cyclic aliphatic compounds possess generally higher densities than their linear aliphatic equivalents, which is presented in a simplified manner within Figure 4b.[3] As a result, the change in density within the polymerization process of ring-opened polymers is reduced, compared for instance to a linear vinyl monomer, forming the same polymer.

a)

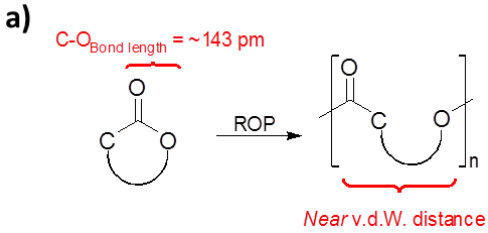

b)

Linear aliphatic	Density / g cm^{-3}	Cyclic aliphatic	Density / g cm^{-3}
n-Pentane	0.63	Cyclopentane	0.75
n-Heptane	0.68	Cycloheptane	0.81
n-Decane	0.73	Cyclodecane	0.87

Figure 4: a) Schematic illustration of the ring-opening, demonstrating the impact of the ring opening effect. b) Exemplary densities of some linear aliphatic alkanes and their cyclic counterparts.[43]

Moreover, from Figure 4b a ring-size effect can be observed, too. The density difference increases with increasing the ring size, suggesting that the larger ring, the smaller the shrinkage. This seems rationale, as the larger the ring, the closer a "true" v.d.W. distance is obtained during ROP. However, for any real world application the general reactivity or driving force has to be taken into consideration as well. But unfortunately reactivity reduces for most monomers with increasing ring sizes, as the ring strain reduces, too.[3,44] Consequently, focusing on the radical initiated ring-opening, especially ring strained monomers up to five-membered rings attracted the interest of researchers.[45]

1.2.1. Types of ROP

From a more general perspective as described in the previous section, it should be noted that cyclic monomers offer a high variety of polymer structures, polymerization techniques and application fields beyond the issue of pure volume shrinkage reduction. However, due to the size and complexity of the overall topic of ROP, for a more intense view the reader is kindest referred to some review articles of *O. Nuyken* and other authors.[41,44] It is merely emphasized that ROP is mainly employed via anionic (AROP),[46] cationic (CROP),[47] metal catalyzed[48] (for instance like the ring olefin metathesis polymerization, ROMP) as well as radical polymerization (RROP),[49,50] which are illustrated in the simplified Scheme 1.

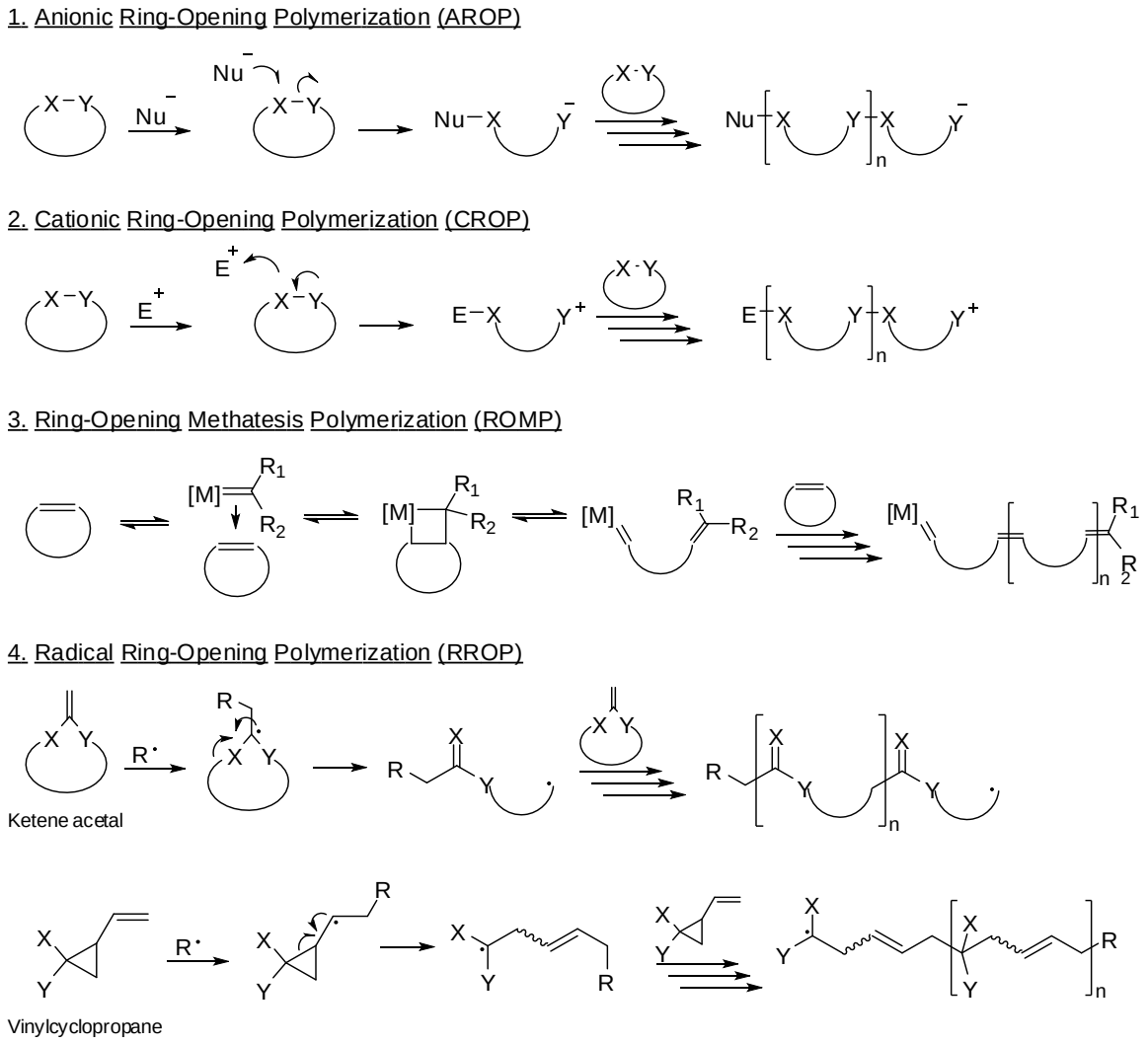

Scheme 1: Simplified mechanisms of the ROP via anionic, cationic, metal catalyzed and radical initiation. X and Y depict heteroatoms or electron withdrawing group, respectively for vinylcylopropanes, Nu^- a nucleophile, E^+ an elektrophile, [M] a metal complex and $R^\bullet$ a radical, respectively. For the RROP the two monomer classes, the cyclic ketene acetals and the vinylcylopropanes were selected as example.

1.2.2. Radical ring opening polymerization (RROP)

Whereas in the beginning especially innovative concepts in the field of AROP and ROMP were developed, producing industrially important polymers as, for instance, block-co-polymers or poly(norbornene),[51,52] in the meantime also radical-initiated RROP increased in significance, as it provides an easy access to design co-polymerizations of vinyl monomers and cyclic monomers, combining the characteristics and advantages of both polymerization processes. As a result, for instance co-polymerizations of conventional monomers like styrene, methyl methacrylate and other vinyl monomers with cyclic ketene acetals could be achieved, providing bio-degradable and hydrolysable polymers,[50,53,54] as well as a decrease in the volume shrinkage.[55] Moreover, a palette of

potential RROP monomers is shown in Figure 5. However, with regard to a commercial implementation particularly cyclic ketenacetals and vinylcyclopropanes attracted recently great attention, due to their relatively simple synthetic access, promising properties and modification possibilities.[50,56–63]

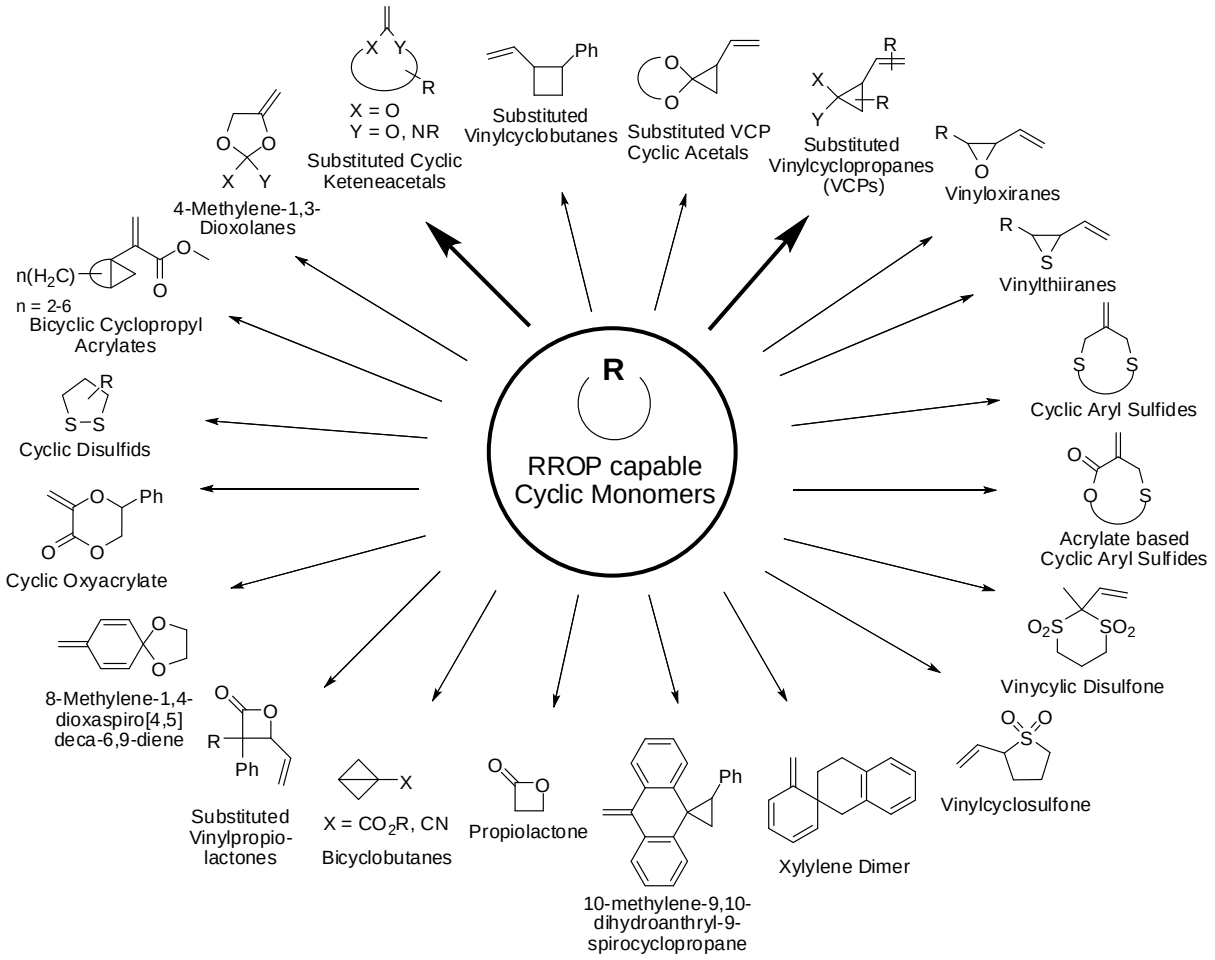

Figure 5: Portfolio of RROP capable cyclic monomers (R depicts a wide range of different chemical structures, X and Y represent predominantly heteroatoms or electron withdrawing groups, unless otherwise noted). Especially cyclic ketenacetals and vinylcyclopropanes gained considerable scientific attention; hence these are marked in bold. The illustrated monomers serve only for orientation of capable RROP functional groups, as more complex, multifunctional and hybrid systems of these monomers are likewise possible.

Moreover, synthetically highly specific RROP capable monomers such as vinycyclobutanes,[64] bicyclic cyclopropyl acrylates,[65,66] cyclic oxyacrylates,[67] vinylpropiolactones,[39] vinyloxiranes and –thiiranes,[68–72] cyclic aryl sulfides,[73–75] vinylcyclic sulfones and disulfones,[76–78] xyxlene dimers,[79] the 8-Methylene-1,4-dioxaspiro[4,5]deca-6,9-diene[80] and the 10-methylene-9,10-dihydroanthryl-9-spirocyclopropane[81] have been developed, too. Further, whereas most cyclic monomers require at least one double bond for the radical initiation, cyclic disulfides,[82–84] bicyclobutanes[85] and β-propiolactones[86,87] can be mentioned as exceptional monomers,

as these monomers are also capable for radical initiation due to light activation or their ring strain. However, according to their complexity and cost-benefit assessment none of these has yet made major inroads into the market.

In addition, it is worth to mention that monomer systems like spiro orthocarbonates (SOC) and spiro orthoesters (SOE), providing a double ring-opening polymerization with near zero-shrinkage or expansion, became very popular as well.[42,88,89] However, since SOCs and SOEs showed a low reactivity, their commercial implementation was restricted. Further, the strong discrepancy within the double ring-opening, the low storage stability as well as the sensitivity against moisture, acids and many additives were additional disadvantages.[39,90–92] Moreover, these systems are not capable for radical initiation, but rather for CROP, which is described in Section 1.4.

1.2.3. Application of low shrinking materials

As mentioned previously, for many current high-precision applications, especially where final devices have to match very specifically the projected dimensions and shapes, characteristics of shrinkage and internal stress obtained during photo-polymerizations are of great significance. Thereby, the polymerization and curing process of thermosets is characterized by a complex interplay of various parameters like the material processing, conversion, gelation, cross-linking and so on. To illustrate this complexity, especially in terms of shape fidelity for high-precision applications, in Figure 6a schematic drawing of this complex interplay is shown. It thus becomes very clear, that to improve the performance and the durability of dental composites,[93] electronical coatings,[7,94–96] adhesives,[97,98] lithographic based 3D laser writing systems[99–102] and optical/holographic data storages[74,75,103,104] the goal is to reduce volume shrinkage. Only in this way upcoming internal stress can be avoided, in order to achieve highest precision on this type of thermosets. A universally applicable monomer system, suiting the common requirements of stability, synthetic access and variability would be of course preferable.

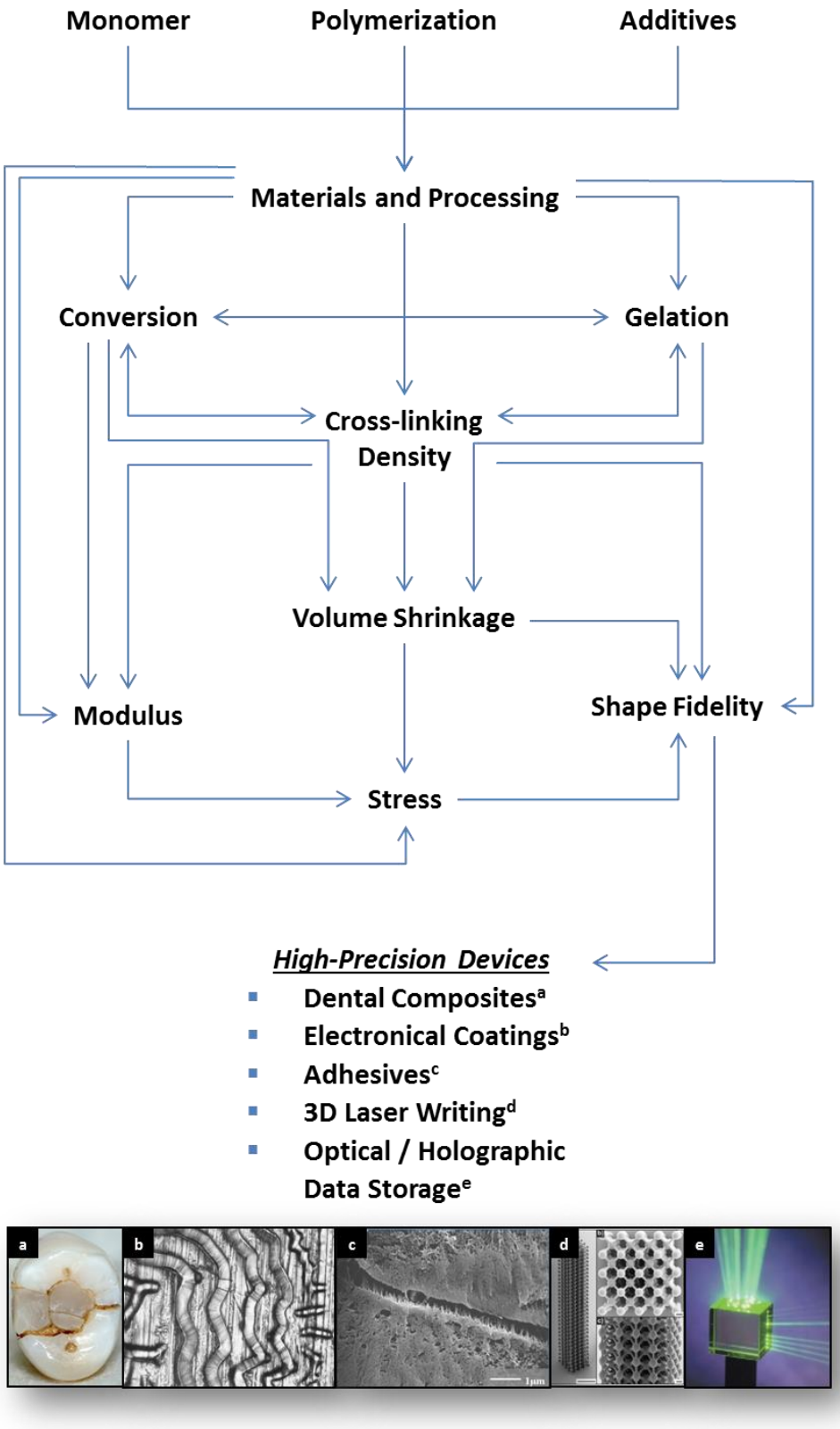

Figure 6: Schematic illustration of the complex interplay between various polymerization and curing parameters having significant impact on the shape fidelity of polymers for high-precision applications such as dental composites, electronical coatings, adhesives, 3D laser writing systems and optical data storages. The images a) and c) are reprints from online based open access publications from the Ref. 105,106, the images d) and e) are reprints from Ref. 102 and 103, respectively with permission. Copyright by John Wiley & Sons and by the Nature Publishing Group. The microscopy image b) is from own production and illustrates the self-wrinkling process of resins induced by high shrinkage and internal stress during photo-polymerizations.[107]

In the view of such potential low shrinking monomer systems, the possibilities offered by VCPs are wide-ranging and described in the following section more in detail.

1.3 Vinylcyclopropanes (VCPs)

In general, vinylcyclopropanes (VCPs) have been applied across many different fields of chemistry, as these molecules can undergo various useful transformations, serving not only the research field of volume shrinkage during polymerization, but rather the field of synthetic chemistry. Thus, a very short state-of-the-art excerpt is described in the following.

1.3.1. Access and function of VCPs in synthetic chemistry

Since VCPs have been successfully introduced in 1922 to the chemical community by *Demjanov* and *Dojarenko*,[108] for a long time only minor attention was paid to this highly interesting class of molecules. In fact, the existence of VCPs was long disputed.[109,110] Since then, the structure of VCPs was studied in detail[111] and investigated by numerous experiments. Thereby, Figure 7 provides an overview of the different categories and research fields VCPs were part of research.

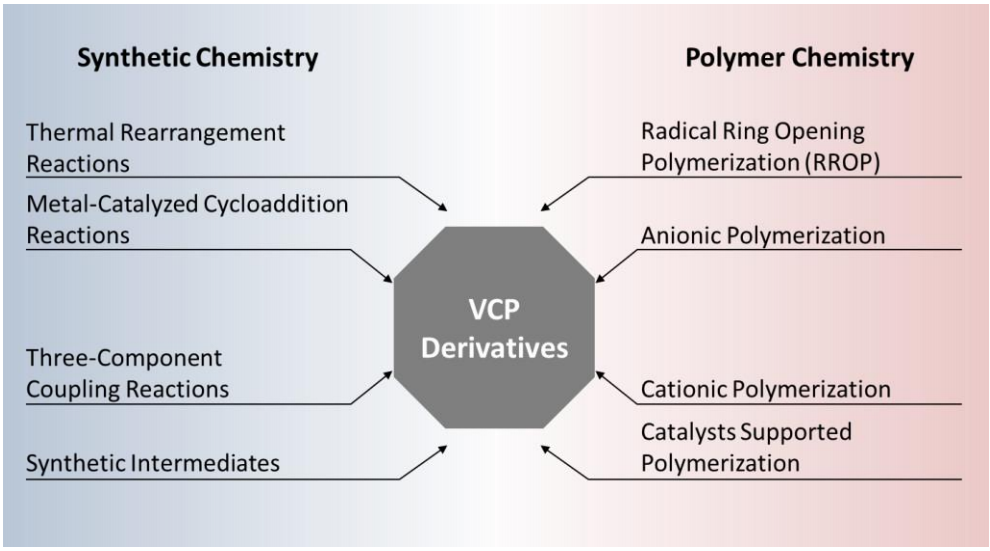

Figure 7: Potential fields of research interests available for a utilization of VCP derivatives.

Among organic chemists, especially beginning from 1960s, thermal rearrangement experiments of VCPs were carried out,[112–114] opening the issue of stereochemistry for VCP molecules. Subsequently, due to their characteristics *Woodward* and *Hoffmann* used VCPs to explain the phenomena of pericyclic reactions, whereby the Woodward-

Hoffmann rules were postulated, illustrating the molecular orbital theory in a simple manner.[115,116] Hence, VCPs gained considerable attention and importance in synthetic applications, and are nowadays considered as one of the precursors of the modern stereochemistry.[117] However, since by now such a number of variants of rearrangement reactions relating to VCPs is disclosed, several detailed reviews provide a more extensive report and overview over the relevant literature.[118–120]

Within cycloaddition transformations a variety of metal catalyzed reactions are known, producing five- to eight-membered carbocycles out of VCPs (see Fig. 8).[121] Since such cycloaddition reactions are mostly catalyzed by transition metals (*e.g.* rhodium), providing an insertion, complexation, reductive elimination or an oxidative cyclometalation, the substitution pattern of VCPs has a strong influence on the addition mode.[122] Thereby, in particular the eight-membered carbocycles represent an important synthetic intermediate for the natural product synthesis, as methodologies and strategies are limited,[123] for instance within the total synthesis of Paclitaxel, one of most potent anticancer drug.[124] However, VCPs have been utilized in numerous of natural product synthesis, just to review a few.[125–129] Thus, VCP chemistry has nowadays a strong impact and served several times as a key reaction in natural product synthesis. The complexity and variation of these reactions is *e.g.* nicely reviewed by *Zhi-Xiang Yu*.[121,122]

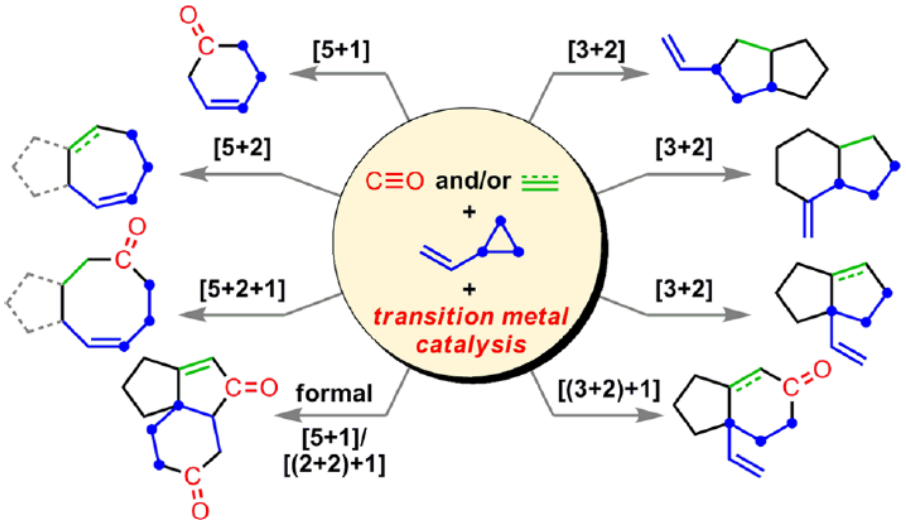

Figure 8: Reaction modes of various cycloadditions, VCPs are capable to undergo. Reprinted with permission from Ref. 121. Copyright by American Chemical Society.

Moreover, in 2015 for the first time a Pd-catalyzed three component coupling of terminal alkynes and a VCP has been described in an one pot synthesis, combining the ring-opening chemistry of VCPs with an *in situ* generated aryne.[130]

1.3.2. VCPs as low shrinking monomers and resins

In material science, just like in synthetic chemistry, for a long time only limited attention was paid to VCPs, although their first polymerization was described in 1949.[131] Thus, until the 1990s only few publications have been published concerning VCPs in the field of polymer chemistry (see Fig. 9a). But henceforth, especially the research groups of *T. Endo* and *N. Moszner* reported within several publications and patents about the advantageous use of VCPs as low shrinking monomer.[132–138] Thereby, as mentioned within Section 1.2, during ROP of VCPs the ring-opened bond turns from a previously covalent distance to a near v.d.W. distance (see Fig. 9b), reducing the cumulative shrinkage.

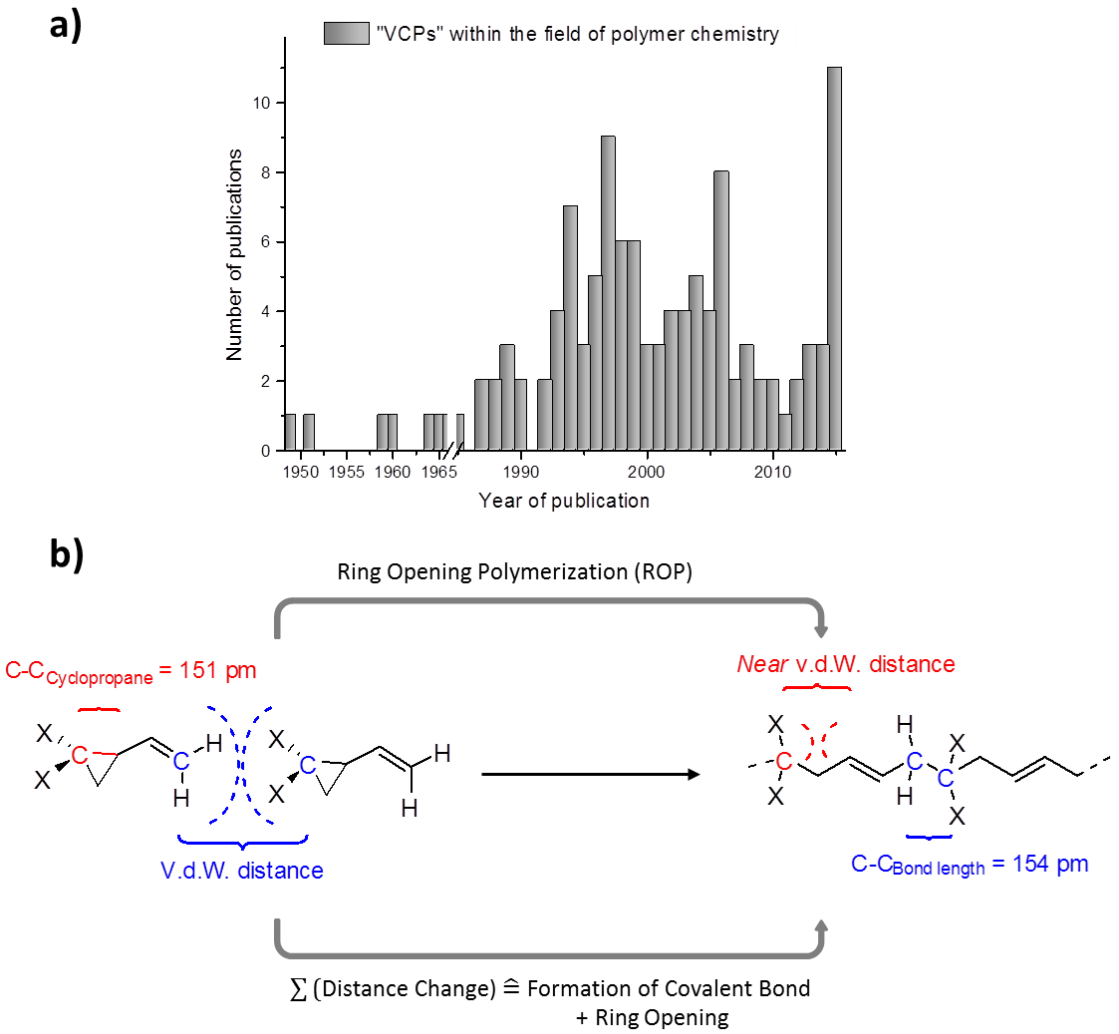

Figure 9: a) Number of publications per year concerning VCPs in the field of polymer chemistry (based on a SciFinder search on May 05, 2016 with the keyword: "Vinylcyclopropane"; the field of synthetic chemistry was excluded). b) Illustration of the reduced volume shrinkage of a basic VCP monomer. The ring-opening counteracts the general shrinkage, as the carbon atom (marked red) moves from a covalent and strained distance to a near v.d.W. distance.

However, for a sustainable and successful utilization monomers and resins have to fulfill a number of complex specifications, in which the reduced shrinking is only one component. Hence, the research interest for VCPs decreased to the year 2011, since VCPs could not meet the additional basic requirements, like *e.g.* rate of polymerization.[139] To obtain an improved curing- and crosslinking-behavior, as well as to widen the application range, new concepts have been developed, raising nowadays (in 2015) the interest for VCPs (see Fig. 9a).

In general, VCP structures can be synthesized by various methods; however it is attempted to establish procedures that provide a reasonable quantity and product yield. Thereby, the most frequently applied synthetic route is based on a condensation-cyclization of an unsaturated *trans*-1,4-dihalogene-butene with an active-hydrogen compound, like for instance a malonate (Scheme 2).[129,133,140–143]

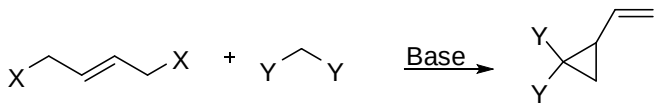

X = Cl or Br
Y = COOR, CN, COR, CONR, SO_2R

Scheme 2: Synthesis of VCPs based on S_N-cyclization reaction.

Another important and well known route is based on the addition of carbenes to diene compounds, like butadiene.[144,145] Thereby, by variation of the carbene species as well as the diene different substituted VCPs may be synthesized.[146,147] One example is the synthesis of 1,1-dichloro-2-vinylcylopropane, using chloroform as carbene source (Scheme 3).

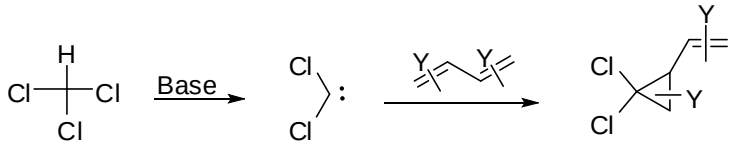

Y= Electron Donting Group (EDG)

Scheme 3: Synthesis of VCPs by applying carbene chemistry to dienes. The unspecified electron donating group Y can be interpreted as variable. Hence, it is not assigned to an individual carbon atom.

Furthermore, there are other multi-step procedures to apply substituted and unsubstituted VCPs, too.[148,149] In contrast to the other methods, these allow the introduction of selective substitutions, for instance if first a cyclopropanation followed by a Wittig-reaction is executed (Scheme 4).[150–154]

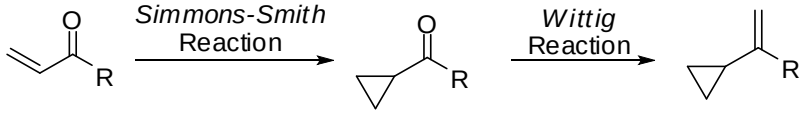

Scheme 4: Exemplary synthesis of VCPs by applying a multi-step reaction.

Due to these and other syntheses, meanwhile a variety of complex polymerizable VCP derivatives were developed. Further, with regard to reactivity VCPs are less reactive than corresponding methacrylate systems. Yet, in many applications methacrylates serve as reference system and benchmark. Therefore, several different approaches were made to enhance the reactivity of VCPs, which are illustrated in Figure 10.

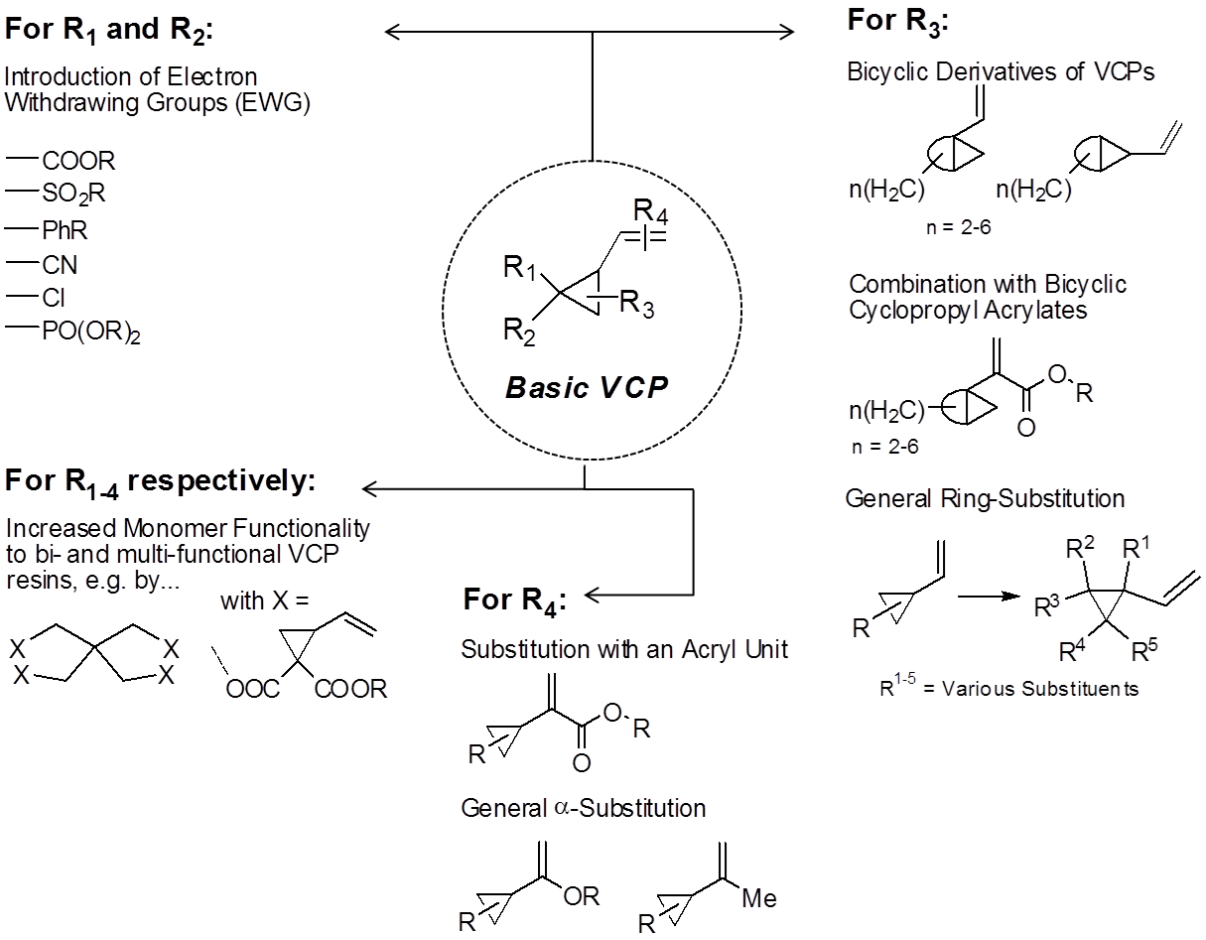

Figure 10: Schematic description of synthetic approaches varying VCP structure in order to enhance the reactivity and outcome of the RROP. Since VCPs are generally less reactive than corresponding methacrylate resins, an improvement in reactivity is a basic requirement for a possible real-market application. The unspecified R group can be interpreted as variable. Hence, it is not assigned to an individual carbon atom.

Thereby, by varying the VCP structures significant reactivity improvements were achieved. However, the substitution patterns still did not result in sufficient reactive VCP system. There are several reasons for this.

First, as illustrated in Figure 11, the polymerization mechanism of VCPs is more complex as for instance of methacrylates. In the beginning the initiating radical attacks the vinyl bond, forming a cyclopropylcarbinyl radical, which then isomerizes and ring-opens to an allylcarbinyl radical. As the allylcarbinyl radical represents the propagating radical, it seemed reasonable that strong electron withdrawing groups (EWG) are of crucial importance to provide a radical stabilization effect, in order to achieve a 1,5-RROP.[155,156] However, besides the intended 1,5-ring opening process, the allylcarbinyl radical can undergo a cyclobutane formation as well. Thereby, steric effects have an effect as well. Thus, both the stabilizing and steric effect of the EWGs have to be considered. Furthermore, a balance in the stabilizing effect of allylcarbinyl radical must be struck. If allylcarbinyl radical is only rarely stabilized, the polymerization will result predominately in 1,2-repeat units, but if the allylcarbinyl radical is excessively stabilized, the polymerization will fail at all. An enhanced reactivity was for example achieved with nitrile groups.[49,140,157] However, the introduction of nitrile groups reduced the possibility to apply additional multi-functionality, which defined a major drawback in order to synthesize thermosets.

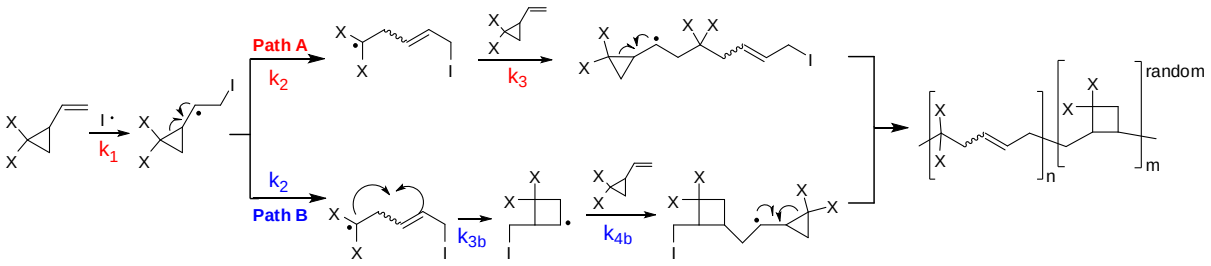

Figure 11: Polymerization mechanism of the RROP of a basic VCP monomer. Apparently, in the polymerization process of VCPs two reaction pathways seem possible. Besides the intended 1,5-ring opening process (Path A), the propagating ring-opened radical can undergo a cyclobutane formation (Path B) via a backbiting reaction as well. This cyclobutane formation (Path B) is considered as a drawback as it causes higher shrinkage values. As both pathways are generally involved in the RROP the overall polymerization process of VCPs is more complex than for a 1,2-vinyl polymerization.

Further, by creating high steric hindrance the recyclization and cyclobutane formation of the allylcarbinyl radical could be suppressed. Therefore, bulky ester groups like adamantyl groups have been introduced.[158,159] However, since these bulky groups generated crystalline monomers, their practical application as resin was restricted.

Moreover, whereas for most radical polymerizable systems an increase of the number of vinyl units generally ends with a rapid increase in reactivity, known as the gel effect, a similar pronounced observation was not observed for VCPs (except for the

results of this cumulative thesis; for this purpose please see Section 4.2 and 4.3).[139] Likewise, hybrid monomers of VCPs and (methyl)-methacrylates did not sufficiently improve the reactivity, since almost exclusively the (methyl)-methacrylates were involved in the polymerization process.[160]

In addition, it was reasonable that the α-substitution of the vinyl bond of VCPs, obtaining *e.g.* acrylic modified VCPs, enhances the propagation rate, too. Thereby, a selective α-substitution has a direct impact on the rate constants k_1, k_2 as well as k_3 and k_{4b} (see Fig. 11).[66,161] In this context, promising results were achieved with acrylic modified bicyclic VCP derivatives, where reactivity similar to that of methacrylates was observed. However, because of incomplete homopolymerization in bulk, these monomers were only capable of radical copolymerizations.[65,162]

In summary, although high efforts have been directed towards optimizing the polymerization behavior of VCPs, so far not a single VCP derivative could be utilized to a practical application, predominately because they could not meet the requirements of high polymerization rates.

1.4 Photo-polymerization

Since light-induced polymerizations and curing reactions were introduced in the 1970s,[163–165] this technology became highly versatile and rapidly expanding, meanwhile applied in a variety of industrial applications, like coatings and paints, adhesives, 3D-printing methods, as well as different type of photoresists.[94,99,101,166–168] Depending on the processing and application, both the radiation source as well as its intensity can vary, for instance by applying UV or IR radiations at different outputs.[18,167]

Besides the fact that photo-polymerizations offer unique advantages, which include for instance an easy control of initiation and processing, the main reason for the strong technology development was the possibility of a rapid curing, for example of solvent-free resins at ambient temperature. As a result, both reduction of operation costs and release of volatile organic compounds (VOCs) is possible, which makes this technique environmentally friendly over conventional thermal processes.[169,170]

Indeed, with further diversification of applications and novel developments of initiators and light sources, which are *e.g.* adapted to LED excitation, today's photo-polymerization technique is rated among the green technology.[171] Moreover, as an

excess of heating can be avoided, reducing local heat toxicity, especially the fields of biomedical applications and tissue engineering benefit from this technique.[172,173]

Within most photo-polymerization processes the reactive units undergo a light-initiated free radical or cationic polymerization.[7,174] Hence, these reactions are predominantly described as conventional chain-growth polymerizations. A rather marginal number of step-growth photo-polymerizations is known, where the irradiation is used to trigger an addition or condensation reaction between comonomers.[175] Thus, Scheme 5 represents schematically the overall photo-polymerization and curing process.

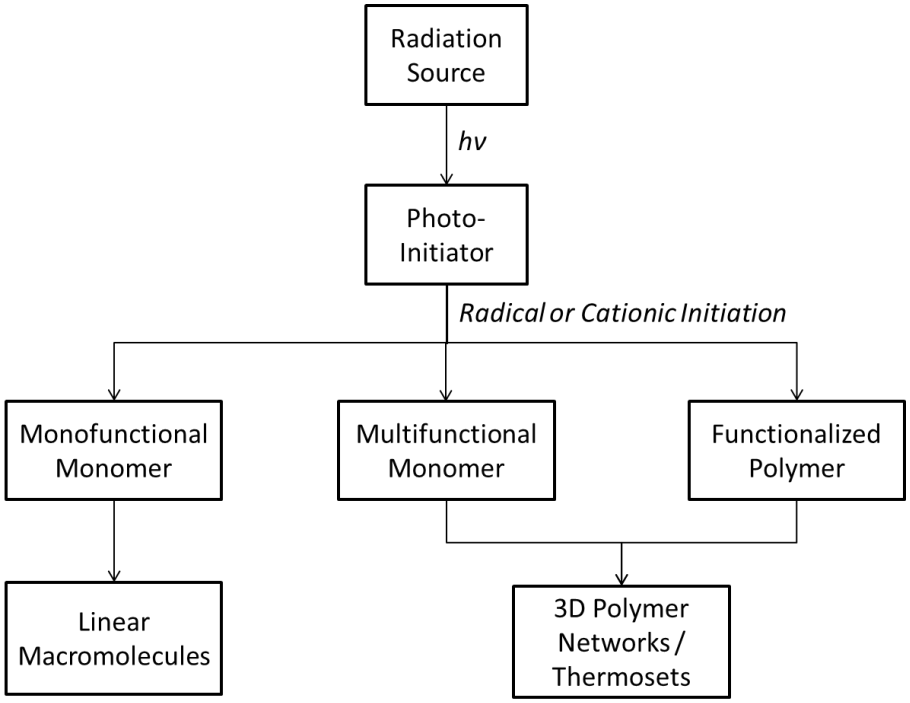

Scheme 5: Schematic illustration of the light induced polymerization and curing process.

Since most monomers are not capable to initiate the polymerization when they are exposed to a radiation source, suitable photo-initiators have to be added. Thereby, the photo-initiators absorb the radiated light, yielding in an excited species, which generate in subsequent reaction(s) reactive radicals or ions, that subsequently initiate the chain reaction.[7,174] However, although the most important applications are characterized by the curing of mono- and multifunctional liquid monomers and resins, the crosslinking of functionalized polymers to 3D networks receives more and more attention as post-polymerization modification method. Thereby, either suitable photo-initiators have to be incorporated into the polymer chain, allowing *e.g.* chain transfer reactions,[176,177] or a photo-curable initiator has to be formulated into a polymer composite, which bears further reactive units.[178]

As introduced above, two main classifications are made whether the polymerization proceeds by a radical-type or a cationic-type mechanism.[168,174,179–181] Thereby, the radical-type initiation is by far the most widely used in today's photo-polymerization processes, mainly because of its high reactivity and large choice of monomers and resins.[99] Further, the radical initiation can be subdivided into a *type I* and a *type II* reaction.[168] The so called *Norrish type I* reaction (see Scheme 6) is characterized by the α-cleavage of a C-C bond, which can be observed in general for all carbonyl group systems.[182] However, especially the aromatic carbonyl compounds are most employed within photo-polymerizations, as these provide higher absorption coefficients as well as a preferred absorption range of >250 nm combined with a relatively slow termination process.[99,183]

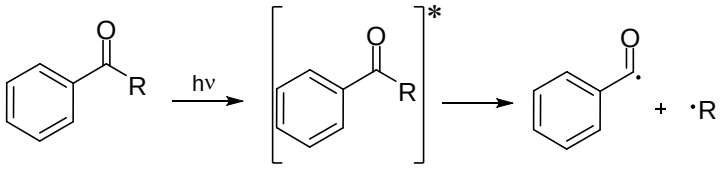

R = predominantly derivatives of benzoin ether, benzil ketals, α–hydroxyalkylphenones and aminoalkylphenones, α–oximinoketones as well as acylphospine oxides

Scheme 6: Photo-initiation of a radical-type I polymerization.

In contrast to the *type I* systems, *type II* initiators normally consist of two or more components, whereby first a primary radical (non-initiating species) is obtained, which undergoes a bimolecular hydrogen abstraction, generating subsequently the initiating radical.[184] Benzophenone for instance, a fully aromatic ketone abstracts a hydrogen atom from a suitable hydrogen-donor (H-donor), instead of undergoing α-cleavage (see Scheme 7). Since the hydrogen abstraction reaction is essential for *type II* initiators, the hydrogen-donors are also called co-initiators, and have to be available in sufficient quantities.[7,183]

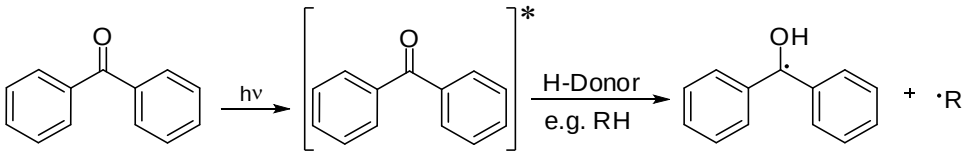

Scheme 7: Photo-initiation of a radical-type II polymerization for the example of benzophenone.

Besides benzophenone, various other types of carbonyl and 1,2-dicarbonyl compounds are suitable obtaining typical hydrogen abstraction reactions, like

xanthones and thioxanthones, α-ketocoumarins, phenylglyoxylates, etc.[7,183] However, since the co-initiator/H-donor compound is responsible for an efficient initiation process, the resulting ketyl radical is predominately terminated by recombination or other radical couplings, by selection and control of stoichiometric quantity of the H-donor, polymerization rate and efficiency may vary. Further, although many compounds like ethers and alcohols may be used as H-donors, many studies have been dedicated to tertiary amines, as by excitation of these *type II* systems an excited electron transfer (ET) exciplex is formed.[7,183,185,186] Further, as the ET exciplex generates radicals almost without intervention of oxygen, tertiary amines are less susceptible to be deactivated by oxygen than alcohols and ethers, which do not form an ET exciplex, and are therefore more often quenched.[183] The overall *type II* initiation mechanism can be nicely illustrated by the system of camphorquinone/amine (see Scheme 8), an initiator system which is widely used for biological and dental applications, and which was predominantly applied within the experimental part of this thesis (see Section 4.1 - 4.3). Thereby, in contrast to most aromatic ketone initiators, which show only weak absorption in the visible range, the absorption maximum of camphorquinone (CQ) lies at 467 nm, making it in terms of radiation more safe and non-hazardous.[187–191]

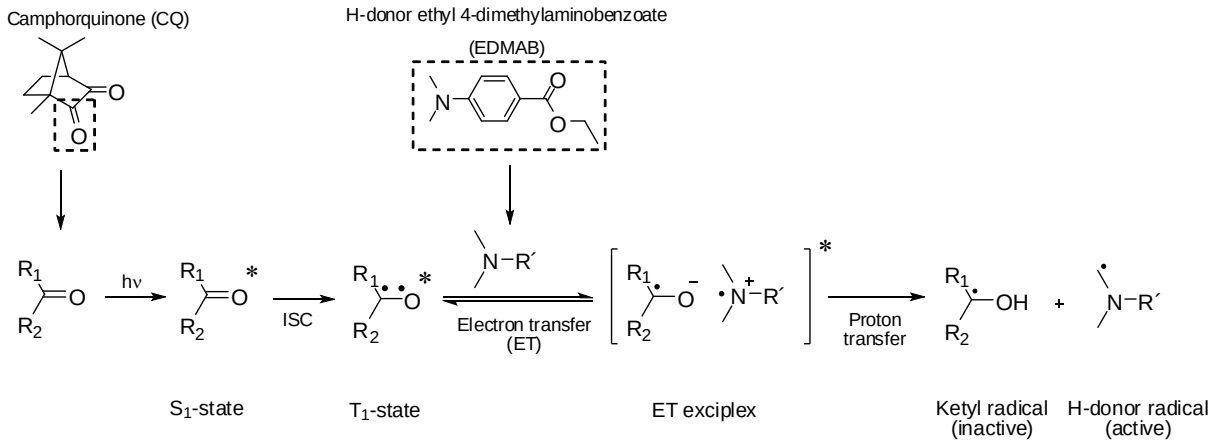

Scheme 8: Schematic illustration of camphorquinone/amine initiation. By absorption of a photon camphor-quinone is promoted to the first excited singlet state (S_1), which is subsequent promoted by an intersystem crossing (ISC) of the electrons into the first excited triplet state (T_1), where the electrons are unpaired with parallel spin. Hereupon, the co-initiator may induce an electron transfer (ET), forming an exciplex, which leads to a proton transfer (H-abstraction), providing an inactive ketyl radical and an active H-donor radical, which starts radical initiation.

Indeed, today a variety of initiator systems besides the camphorquinone/amine one are known to be capable of visible light initiation.[192–194] In dental applications for instance, several organometallic ketones containing germanium are known (see

Scheme 9), providing *type I* photo-initiators with significantly higher reactivity than conventional CQ systems.[195,196] Further, these types of initiators show high quantum yields for photodecomposition, strong absorption in the visible region of the spectrum, as well as excellent photo bleaching, making them highly interesting for polymerizations and curings in biological and dental applications, in particular where a depth radiation penetration is necessary.[197]

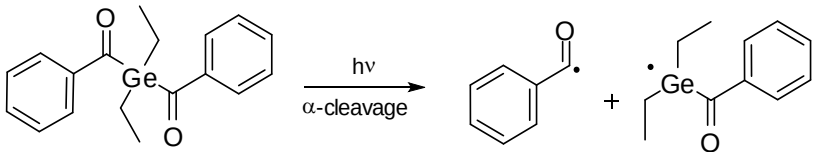

Scheme 9: Example of a benzoylgermanium derivative *type I* photo-initiator.

However, since most radical-initiated applications are carried out under atmospheric conditions, oxygen inhibition is an omnipresent phenomenon, independent whether *type I* or *type II* initiator is utilized.[198] Hence, especially for surface applications with unfavorable surface-to-volume ratios like coatings, a retardation as well as incomplete conversion has to be taken into account.[174,179,198,199] Moreover, not only the initiators, but also various monomers and resins are susceptible to oxygen inhibition. Acrylates are more sensitive than methacrylates[200] and high viscous resins showed less susceptibility than low viscous ones.[7] Thus, in order to achieve high initiation and deep-through cure various components and processing conditions, like *e.g.* type and concentration of the photo-initiator, chemical structure of monomer/resin as well as exposure time and illumination intensity have to be adjusted.[201,202]

In contrary to radical-type photo-initiations, the photo-initiated cationic polymerization is mainly used for vinyl ether systems,[174] which do not homopolymerize in the presence of radicals, due to their electron-rich double bond, as well as cyclic monomer systems, like the epoxy-functionalized and the previously described SOCs and SOEs systems (see Chapter 1.2.2).[39,42,88,89,174,203–205] Thereby, the photolysis of onium salts generate both, free aryl radicals and highly reactive aryliodo radical cations (see Scheme 10).[206,207] Thereby, the highly reactive radical cations either initiate the monomers directly, since monomers are often capable H-donors, or the initiation proceeds via the resulting *Brønsted* acids (H^+), after the hydrogen transfer was carried with other H-donors.[183]

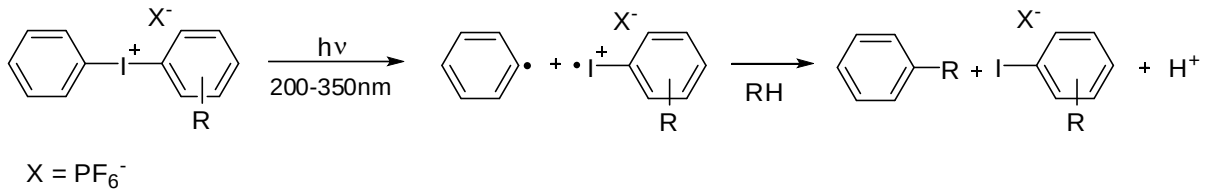

Scheme 10: Reaction mechanism of UV photo-initiation of diaryliodonium salts.

Generally, during the chain propagation in cationic polymerization transfer and chain termination reactions are observed. However, if these transfer and chain termination reactions of the cationic ring-opening polymerization are at low level, the photo-initiated polymerization may proceed even after the radiation exposure stopped, since a simple recombination of two propagating polymer cations is not possible.[208] To illustrate this, the cationic initiation of an epoxide derivative is described in Scheme 11.

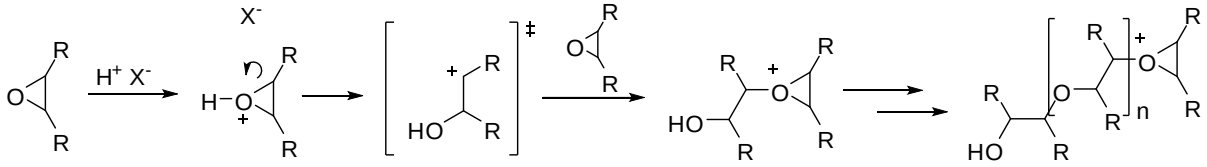

Scheme 11: Exemplary mechanism of cationic ring-opening polymerization of epoxides.

Moreover, the spectral response of onium salts can be extended to longer wavelengths into the visible spectral range by photo-sensitization.[207,209,210] Thereby, generally binary or ternary photo-initiator systems are formulated. Hence, such systems offer the possibility to accomplish cationic and concurrent radical polymerization in the visible spectral range, whereas hybrid polymerizations as well as initiation improvements are possible.[24,164,171,211]

Especially within dental applications, where the spectral excitation range is fixed to blue-light, ternary photo-initiator systems of camphorquinone/amine in combination with an onium salt are of growing importance.[5,24,212]

1.5 Research progress of VCPs beyond low shrinking monomers

As noted in the previous sections, the strong progress within RROP capable monomers as well as within photo-polymerization techniques enables a high potential of applying low shrinking resins, such as VCPs, within various fields and devices, which are hardly explored so far. However, looking to the long-term future of VCPs not only devices with a demand of high precision during photo-polymerization find a strong

attention, but also devices with a high specification variability of gels, thermosets, adhesives, coatings and thermoplastics. Thereby, already several new application possibilities for VCPs have been suggested.

Due to their low auto-polymerization temperature below 100 °C,[60] VCPs may find interest as direct thermo-crosslinkable resins, acting as volatile- as well as ion-free curing agents, for instance in a similar manner as known for Novolac resins, bearing functional groups.[213–215]

Further, recently *Théato et al.* demonstrated that VCP polymers can be easily modified by various synthetic post-polymerization procedures, as shown in Scheme 12.[61,62] A combination of such post-polymerization methods allows to equip VCPs with additional features. Thereby, linear VCP polymers and probably also VCP networks may be modified with additional functionalities. *Théato et al*. for instance demonstrated thermo-responsive behavior of a VCP polymer by an upper critical solution temperature (UCST) in the medium ethanol and ethanol–water.[61] Thereby, although the double bond of the polymerized VCPs is a non-activated and not terminal one, under harsher conditions both an epoxidation, a thiol-ene as well as a bromination reaction is possible, enabling further specific reactions.[63,216] This could help to achieve for instance low surface energy coatings as well as to generate other surface modifications, expanding the application range of VCPs.[217]

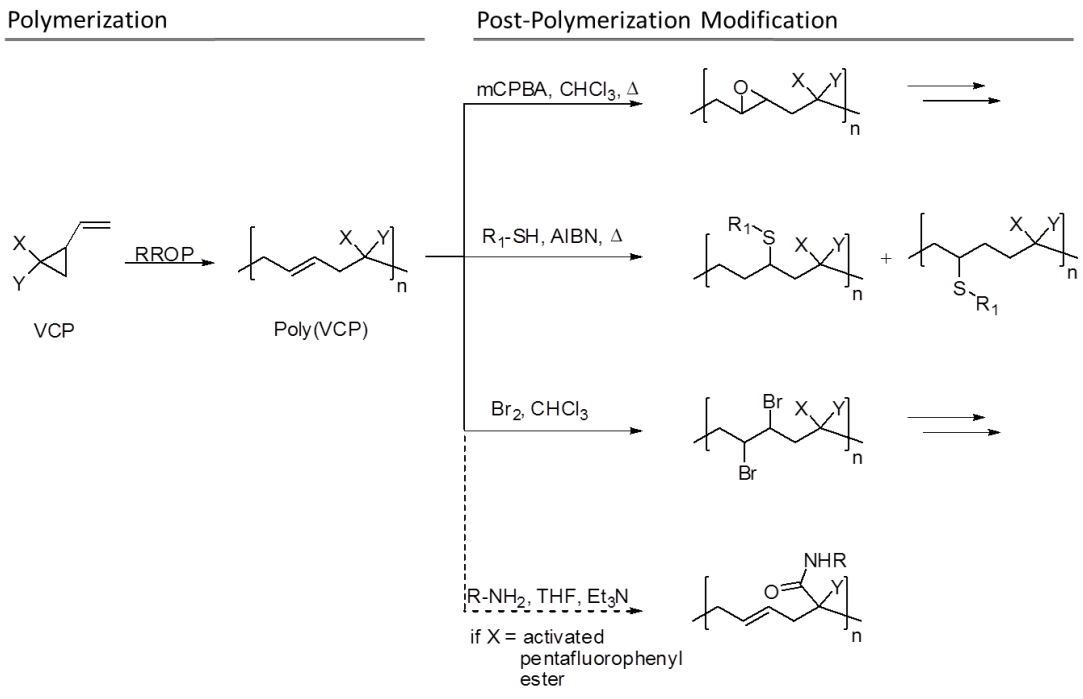

Scheme 12: RROP of VCPs and synthetic routes for post-polymerization modifications of poly(VCPs).

2 References

[1] A. Göthlich, S. Koltzenburg and G. Schornick, *Chemie in unserer Zeit*, 2005, **39**, 262–273.

[2] P. W. Atkins and Julio de Paula, *Physikalische Chemie*, Wiley-VCH, Weinheim, 4th edn., 2006.

[3] R. K. Sadhir and R. M. Luck, *Expanding monomers. Synthesis, characterization, and applications*, CRC Press, Boca Raton, Fla., 1992.

[4] F. Rueggeberg and K. Tamareselvy, *Dent. Mater.*, 1995, **11**, 265–268.

[5] W. Weinmann, C. Thalacker and R. Guggenberger, *Dent. Mater.*, 2005, **21**, 68–74.

[6] S. C. Ligon-Auer et al., *Polym. Chem.*, 2016, **7**, 257–286.

[7] E. Andrzejewska, *Prog. Polym. Sci.*, 2001, **26**, 605–665.

[8] T. Brock, M. Groteklaes and P. Mischke, *Lehrbuch der Lacktechnologie*, Vincentz Network, Hannover, 3rd edn., 2009.

[9] U. Boschert and I. Pratt, US3883612 A, 1975.

[10] K. Dušek and M. Dušková-Smrčková, *Prog. Polym. Sci.*, 2000, **25**, 1215–1260.

[11] J. W. Stansbury et al., *Dent. Mater.*, 2005, **21**, 56–67.

[12] N. R. G. Fróes-Salgado et al., *J. Appl. Polym. Sci.*, 2012, **123**, 2985–2991.

[13] J. Lange et al., *Polymer*, 1997, **38**, 809–815.

[14] C. S. Pfeifer et al., *Polymer*, 2011, **52**, 3295–3303.

[15] R. R. Braga and J. L. Ferracane, *J. Appl. Oral Sci.*, 2004, **12**, 1–11.

[16] S. Ye et al., *Macromolecules*, 2011, **44**, 9084–9090.

[17] D. M. Vaessen et al., *J. Appl. Polym. Sci.*, 2002, **84**, 2784–2793.

[18] N. Emami and K.-J. M. Söderholm, *J. Mater. Sci. Mater. Med.*, 2005, **16**, 47–52.

[19] T. F. Scott et al., *Science*, 2005, **308**, 1615–1617.

[20] Y. Eom et al., *Polym. Compos.*, 2002, **23**, 1044–1056.

[21] J. Lange et al., *Polymer*, 1995, **36**, 3135–3141.

[22] W. J. Bailey and T. Endo, *J. Polym. Sci., C Polym. Symp.*, 1978, **64**, 17–26.

[23] K. S. Anseth, C. N. Bowman and N. A. Peppas, *J. Polym. Sci. A Polym. Chem.*, 1994, **32**, 139–147.

[24] P. Pineda Contreras, P. Tyagi and S. Agarwal, *Polym. Chem.*, 2015, **6**, 2297–2304.

[25] T. G. Fox and S. Loshaek, *J. Polym. Sci.*, 1955, **15**, 371–390.

[26] Thomas Klabunde, *Neue Wege zur Herstellung von Dentalkompositen mit geringem Polymerisationsschrumpf auf (Meth-)Acrylat-Basis*, Dissertation (Universität Mainz) 2001.

[27] U. Poth, R. Schwalm and M. Schwartz, *Acrylatharze*, Vincentz Network, Hannover, 2011.

[28] M. P. Patel, M. Braden and K. Davy, *Biomaterials*, 1987, **8**, 53–56.

[29] J. E. Klee et al., *Macromol. Chem. Phys.*, 1999, **200**, 517–523.

[30] A. Szanka, G. Szarka and B. Iván, *Polymer*, 2013, **54**, 6073–6077.

[31] K. M. Choi and J. W. Stansbury, *Chem. Mater.*, 1996, **8**, 2704–2707.

[32] N. M. Mohsen, R. G. Craig and F. E. Filisko, *J. Biomed. Mater. Res.*, 1998, **40**, 224–232.

[33] C.-M. Chung et al., *Dent. Mater.*, 2002, **18**, 174–178.

[34] X. Cao and L. Lee, *Polymer*, 2003, **44**, 1507–1516.

[35] B. Lu et al., *J. Appl. Polym. Sci.*, 2007, **104**, 1126–1130.

[36] A. Suzuki and T. Tanaka, *Nature*, 1990, **346**, 345–347.

[37] S. Juodkazis et al., *Nature*, 2000, **408**, 178–181.

[38] I. S. Klaus and W. S. Knowles, *J. Appl. Polym. Sci.*, 1966, **10**, 887–889.

[39] W. J. Bailey, *Polym. J.*, 1985, **17**, 85–95.

[40] A.-C. Albertsson and I. K. Varma, *Biomacromolecules*, 2003, **4**, 1466–1486.

[41] P. Dubois, O. Coulembier and J.-M. Raquez, *Handbook of ring-opening polymerization*, Wiley-VCH, Weinheim, 2009.

[42] R. F. Brady, *Journal of Macromolecular Science, Part C: Polymer Reviews*, 1992, **32**, 135–181.

[43] D. R. Lide, *Handbook of chemistry and physics, 87th ed.*, CRC Press, Boca Raton, Fla., 2007.

[44] O. Nuyken and S. Pask, *Polymers*, 2013, **5**, 361–403.

[45] F. Sanda and T. Endo, *J. Polym. Sci. A Polym. Chem*, 2001, **39**, 265–276.

[46] N. Hadjichristidis et al., *Chem. Rev.*, 2001, **101**, 3747–3792.

[47] S. Penczek, P. Kubisa and K. Matyjaszewski, *Cationic ring-opening polymerization*, Springer-Verlag, Berlin, New York, 1985, Vol. 68/69.

[48] S. Sutthasupa, M. Shiotsuki and F. Sanda, *Polym. J.*, 2010, **42**, 905–915.

[49] I. Cho, *Prog. Polym. Sci.*, 2000, **25**, 1043–1087.

[50] S. Agarwal, *Polym. Chem.*, 2010, **1**, 953–964.

[51] K. Matyjaszewski and A. Müller, *Controlled and Living Polymerizations: From Mechanisms to Applications*, John Wiley & Sons, 2009.

[52] T. M. Trnka and R. H. Grubbs, *Acc. Chem. Res.*, 2001, **34**, 18–29.

[53] S. Im Chung and K. Matyjaszewski, *Macromolecules*, 2003, **36**, 2995–2998.

[54] Y. Zhang et al., *Polym. Chem.*, 2012, **3**, 2752–2759.

[55] T. Schulze and E. Klemm, *Macromol. Chem. Phys.*, 1995, **196**, 567–572.

[56] Y. Hiracuri and Y. Tokiwa, *J. Polym. Sci. A Polym. Chem.*, 1993, **31**, 3159–3163.

[57] Y. Hiraguri and Y. Tokiwa, *Macromolecules*, 1997, **30**, 3691–3693.

[58] N. Moszner, *Macromol. Symp.*, 2004, **217**, 63–76.

[59] P. Pineda Contreras et al., *Chem. Commun.*, 2015, **51**, 11899–11902.

[60] P. Pineda Contreras and S. Agarwal, *Polym. Chem.*, 2016, **7**, 3100–3106.

[61] D. H. Seuyep N., G. A. Luinstra and P. Theato, *Polym. Chem.*, 2013, **4**, 2724–2730.

[62] D. H. Seuyep Ntoukam, G. A. Luinstra and P. Theato, *J. Polym. Sci. A Polym. Chem.*, 2014, **52**, 2841–2849.

[63] P. Theato and H.-A. Klok, *Functional polymers by post-polymerization modification. Concepts, guidelines, and applications*, Wiley-VCH, Weinheim, 2013.

[64] Y. Hiraguri and T. Endo, *J. Polym. Sci. C Polym. Lett.*, 1989, **27**, 333–337.

[65] N. Moszner et al., *Macromol. Rapid Commun.*, 2003, **24**, 269–273.

[66] A. d. Meijere et al., *Eur. J. Org. Chem.*, 2004, **2004**, 3669–3678.

[67] Q. Smith et al., *Macromolecules*, 2005, **38**, 5581–5586.

[68] T. Endo and N. Kanda, *J. Polym. Sci. Polym. Chem. Ed.*, 1985, **23**, 1931–1938.

[69] T. Koizumi et al., *Polym. J.*, 1995, **27**, 757–761.

[70] O. Moriya et al., *J. Polym. Sci. A Polym. Chem.*, 2000, **38**, 3729–3735.

[71] F. Lautenschlaeger and H. Schnecko, *J. Polym. Sci. A-1 Polym. Chem.*, 1970, **8**, 2579–2594.

[72] K. Suga and T. Endo, *J. Polym. Sci. C Polym. Lett.*, 1989, **27**, 381–384.

[73] R. A. Evans et al., *Macromolecules*, 1994, **27**, 7935–7937.

[74] R. A. Evans and E. Rizzardo, *Macromolecules*, 1996, **29**, 6983–6989.

[75] K. Choi et al., *Adv. Funct. Mater.*, 2009, **19**, 3560–3566.

[76] I. Cho, S.-K. Kim and M.-H. Lee, *J. Polym. Sci., C Polym. Symp.*, 1986, **74**, 219–226.

[77] I. Cho and M.-H. Lee, *J. Polym. Sci. C Polym. Lett.*, 1987, **25**, 309–311.

[78] I. Cho and S. Y. Choi, *Makromol. Chem., Rapid Commun.*, 1991, **12**, 399–402.

[79] L. A. Errede, *J. Polym. Sci.*, 1961, **49**, 253–265.

[80] I. Cho and K. Y. Song, *Makromol. Chem., Rapid Commun.*, 1993, **14**, 377–381.

[81] H. Mori, S. Masuda and T. Endo, *Macromolecules*, 2006, **39**, 5976–5978.

[82] R. C. Thomas and L. J. Reed, *J. Am. Chem. Soc.*, 1956, **78**, 6148–6149.

[83] T. Suzuki, Y. Nambu and T. Endo, *Macromolecules*, 1990, **23**, 1579–1582.

[84] K. Endo, T. Shiroi and N. Murata, *Polym. J.*, 2005, **37**, 512–516.

[85] H. K. Hall and A. B. Padias, *J. Polym. Sci. A Polym. Chem.*, 2003, **41**, 625–635.

[86] S. Katayama, H. Horikawa and O. Toshima, *J. Polym. Sci. A-1 Polym. Chem.*, 1971, **9**, 2915–2932.

[87] Y. Shi, Z. Zheng and S. Agarwal, *Chem. Eur. J.*, 2014, **20**, 7419–7428.

[88] T. Takata and T. Endo, *Prog. Polym. Sci.*, 1993, **18**, 839–870.

[89] T. Endo, S. Maruoka and T. Yokozawa, *Macromolecules*, 1987, **20**, 2690–2693.

[90] N. Moszner, F. Zeuner and V. Rheinberger, *Macromol. Rapid Commun.*, 1995, **16**, 667–672.

[91] N. Moszner et al., *Macromol. Symp.*, 2000, **153**, 151–159.

[92] N. Moszner and U. Salz, *Prog. Polym. Sci.*, 2001, **26**, 535–576.

[93] K. L. van Landuyt et al., *Biomaterials*, 2007, **28**, 3757–3785.

[94] Y. Fuchs, O. Soppera and K. Haupt, *Anal. Chim. Acta*, 2012, **717**, 7–20.

[95] J. A. Payne, L. F. Francis and A. V. McCormick, *J. Appl. Polym. Sci.*, 1997, **66**, 1267–1277.

[96] Y. Jian et al., *Adv. Polym. Technol.*, 2013, **32**, 21331-n/a.

[97] H. Yu, S. G. Mhaisalkar and E. H. Wong, *J. Electron. Mater.*, 2005, **34**, 1177–1182.

[98] Y. Gan, J. Yin and X. Jiang, *J. Mater. Chem. A*, 2014, **2**, 18574–18582.

[99] C. Decker, *Macromol. Rapid Commun.*, 2002, **23**, 1067–1093.

[100] A. Amirsadeghi, J. J. Lee and S. Park, *J. Micromech. Microeng.*, 2011, **21**, 115013-n/a.

[101] C. Gorsche et al., *Polym. Chem.*, 2016, **7**, 2009–2014.

[102] A. S. Quick et al., *Adv. Funct. Mater.*, 2015, **25**, 3735–3744.

[103] M. Haw, *Nature*, 2003, **422**, 556–558.

[104] Y. Satoru, JP2009015163 A, 2007.

[105] M. Naraghi, *Carbon nanotubes. Growth and applications*. Chapter 14, MWCNT Used in Orthopaedic Bone Cements, By Nicholas Dunne and Ross W. Ormsby, InTech, Rijeka, Croatia, 2011.

[106] D. Clark, J. Khademi, E. Herbranson, Dentistry Today (Open Access), Category Restorative (Resource online 21.05.2016), *Fracture Resistant Endodontic and Restorative Preparations,* available at: http://www.dentistrytoday.com/articles /8693-february-2013.

[107] S. K. Basu et al., *Prog. Org. Coat.*, 2005, **53**, 1–16.

[108] N. J. Demjanow and M. Dojarenko, *Ber. Dtsch. Chem. Ges. A/B*, 1922, **55**, 2718–2727.

[109] C. K. Ingold, *J. Chem. Soc., Trans.*, 1923, **123**, 1706–1713.

[110] F. C. Whitmore, *Organic Chemistry;* D. Van Nostrand: New York, 1937, p 622.

[111] Z. Kisiel et al., *J. Chem. Soc., Faraday Trans.*, 1996, **92**, 907–911.

[112] E. Vogel, *Angew. Chem.*, 1960, **72**, 4–26.

[113] C. G. Overberger and A. E. Borchert, *J. Am. Chem. Soc.*, 1960, **82**, 1007–1008.

[114] W. V. E. Doering and W. R. Roth, *Angew. Chem.*, 1963, **75**, 27–35.

[115] R. B. Woodward and R. Hoffmann, *Angew. Chem. Int. Ed. Engl.*, 1969, **8**, 781–853.

[116] P. Geerlings et al., *Acc. Chem. Res.*, 2012, **45**, 683–695.

[117] J. E. Baldwin and A. P. Kostikov, *J. Org. Chem.*, 2010, **75**, 2767–2775.

[118] J. E. Baldwin, *Chem. Rev.*, 2003, **103**, 1197–1212.

[119] S. Vshyvenko et al., in *Comprehensive Organic Synthesis 5II6 (Second Edition)*, ed. P. Knochel, Elsevier, Amsterdam, 2014, pp. 999–1076.

[120] K. N. Houk, Y. Li and J. D. Evanseck, *Angew. Chem. Int. Ed. Engl.*, 1992, **31**, 682–708.

[121] L. Jiao and Z.-X. Yu, *J. Org. Chem.*, 2013, **78**, 6842–6848.

[122] Y. Wang and Z.-X. Yu, *Acc. Chem. Res.*, 2015, **48**, 2288–2296.

[123] N. A. Petasis and M. A. Patane, *Tetrahedron*, 1992, **48**, 5757–5821.

[124] F. Flam, *Science*, 1994, **263**, 911–914.

[125] H. Zhang and D. P. Curran, *J. Am. Chem. Soc.*, 2011, **133**, 10376–10378.

[126] L. Jiao et al., *Org. Lett.*, 2010, **12**, 2528–2531.

[127] P. A. Wender et al., *Org. Lett.*, 1999, **1**, 137–140.

[128] L. Jiao, C. Yuan and Z.-X. Yu, *J. Am. Chem. Soc.*, 2008, **130**, 4421–4430.

[129] G. Quinkert et al., *Liebigs Ann. Chem.*, 1981, **1981**, 2335–2371.

[130] L. K. B. Garve and D. B. Werz, *Org. Lett.*, 2015, **17**, 596–599.

[131] R. V. Volkenburgh et al., *J. Am. Chem. Soc.*, 1949, **71**, 3595–3597.

[132] T. Endo et al., *J. Polym. Sci. A Polym. Chem.*, 1987, **25**, 3039–3048.

[133] F. Sanda, T. Takata and T. Endo, *Macromolecules*, 1993, **26**, 1818–1824.

[134] F. Sanda, T. Takata and T. Endo, *Macromolecules*, 1995, **28**, 1346–1355.

[135] F. Zeuner, N. Moszner and V. Rheinberger, *Macromol. Chem. Phys.*, 1996, **197**, 2745–2752.

[136] N. Moszner, F. Zeuner and V. Rheinberger, *Macromol. Rapid Commun.*, 1997, **18**, 775–780.

[137] V. Rheinberger, F. Zeuner and N. Moszner, EP000000798286B1, 1997.

[138] N. Moszner, V. Rheinberger, T. Völkel and U. K. Arbon, DE19812888A1, 1999.

[139] N. Moszner and U. Salz, *Macromol. Mater. Eng.*, 2007, **292**, 245–271.

[140] R. W. Kierstead, R. P. Linstead and B. C. L. Weedon, *J. Chem. Soc.*, 1952, 3610–3616.

[141] J. M. Stewart and G. K. Pagenkopf, *J. Org. Chem.*, 1969, **34**, 7–11.

[142] S. Birch, R. Dean and N. Hunter, *J. Org. Chem.*, 1958, **23**, 1390–1392.

[143] K. Burgess, *J. Org. Chem.*, 1987, **52**, 2046–2051.

[144] R. C. Woodwortii and P. S. Skell, *J. Am. Chem. Soc.*, 1957, **79**, 2542–2544.

[145] W. von E. Doering and A. K. Hoffmann, *J. Am. Chem. Soc.*, 1954, **76**, 6162–6165.

[146] F. Sanda, T. Takata and T. Endo, *J. Polym. Sci. A Polym. Chem.*, 1994, **32**, 2517–2522.

[147] F. Cluet et al., *Synlett*, 1994, **11**, 913–915.

[148] W. F. Bailey and Y. Tao, *Tetrahedron Lett.*, 1997, **38**, 6157–6158.

[149] Y. Tang et al., *J. Org. Chem.*, 1996, **61**, 5762–5769.

[150] H. E. Simmons and R. D. Smith, *J. Am. Chem. Soc.*, 1959, **81**, 4256–4264.

[151] E. C. Friedrich and E. J. Lewis, *J. Org. Chem.*, 1990, **55**, 2491–2494.

[152] M. Mitani, Y. Yamamoto and K. Koyama, *J. Chem. Soc., Chem. Commun.*, 1983, 1446–1447.

[153] E. Wenkert, R. S. Greenberg and H.-S. Kim, *HCA*, 1987, **70**, 2159–2165.

[154] R. E. Ireland and J. P. Daub, *J. Org. Chem.*, 1983, **48**, 1303–1312.

[155] S. Danishefsky, *Acc. Chem. Res.*, 1979, **12**, 66–72.

[156] I. Cho and K.-D. Ahn, *J. Polym. Sci. Polym. Chem. Ed.*, 1979, **17**, 3169–3182.

[157] E. Ciganek, *J. Am. Chem. Soc.*, 1966, **88**, 1979–1988.

[158] J.-i. Sugiyama, N. Kayamori and S.-i. Shimada, *Macromolecules*, 1996, **29**, 1943–1950.

[159] H. Chiba et al., *J. Polym. Sci. A Polym. Chem.*, 2015, **54**, 39–43.

[160] Norbert Moszner et al., *Macromol. Rapid Commun.*, **1998**, 33–35.

[161] P. Ksionsko. *Darstellung, Charakterisierung und ringöffnende Polymerisation von Vinylcyclopropan-Derivaten für eine Applikation in der Dentalindustrie*, Masterarbeit (Philipps-Universität), Marburg, 2012.

[162] N. Moszner et al., *Macromol. Mater. Eng.*, 2006, **291**, 83–89.

[163] S. Pappas, *Radiat. Phys. Chem. (1977)*, 1985, **25**, 633–641.

[164] S. Pappas, *Prog. Org. Coat.*, 1985, **13**, 35–64.

[165] C. G. Roffey, *Photopolymerization of surface coatings*, Wiley, Chichester, New York, 1982.

[166] R. S. Davidson, *Exploring the science, technology and applications of UV and EB curing*, Sita Tecnology Limited, 1999.

[167] J.-P. Fouassier and J. F. Rabek, *Radiation curing in polymer science and technology*, Elsevier Applied Science, London, New York, 1993.

[168] B. M. Monroe and G. C. Weed, *Chem. Rev.*, 1993, **93**, 435–448.

[169] Y. Yagci, S. Jockusch and N. J. Turro, *Macromolecules*, 2010, **43**, 6245–6260.

[170] M. Sangermano, N. Razza and J. V. Crivello, *Macromol. Mater. Eng.*, 2014, **299**, 775–793.

[171] C. Dietlin et al., *Polym. Chem.*, 2015, **6**, 3895–3912.

[172] A. S. Sawhney, C. P. Pathak and J. A. Hubbell, *Macromolecules*, 1993, **26**, 581–587.

[173] J. L. Ifkovits and J. A. Burdick, *J. Tissue Eng.*, 2007, **13**, 2369–2385.

[174] C. Decker, *Prog. Polym. Sci.*, 1996, **21**, 593–650.

[175] M. Soto, R. M. Sebastián and J. Marquet, *J. Org. Chem.*, 2014, **79**, 5019–5027.

[176] F. Liu et al., *Polym. Chem.*, 2015, **6**, 2769–2776.

[177] L. Liu et al., *Adv. Funct. Mater.*, 2016, **26**, 1021–1027.

[178] A. H. Gröschel et al., *J. Am. Chem. Soc.*, 2012, **134**, 13850–13860.

[179] J. G. Kloosterboer, in *Electronic Applications*, Springer Berlin Heidelberg, 1988, vol. 84, pp. 1–61.

[180] J. V. Crivello and J. H. W. Lam, *J. Polym. Sci. Pol. Chem.*, 1999, **37**, 4241–4254.

[181] M. S. J. V. Crivello, *J. Polym. Sci. A Polym. Chem*, 2001, **39**, 343–356.

[182] R. G. W. Norrish and C. H. Bamford, *Nature*, 1937, **140**, 195–196.

[183] N. S. Allen, *Photopolymerisation and photoimaging science and technology*, Elsevier Applied Science, London, New York, 1989.

[184] R. G. W. Norrish and C. H. Bamford, *Nature*, 1936, **138**, 1016–1018.

[185] S. G. Cohen, A. Parola and G. H. Parsons, *Chem. Rev.*, 1973, **73**, 141–161.

[186] K. Dietliker et al., *Macromol. Symp.*, 2004, **217**, 77–98.

[187] B. M. Monroe and S. A. Weiner, *J. Am. Chem. Soc.*, 1969, **91**, 450–456.

[188] R. L. Bowen and H. Argentar, *J. Dent. Res.*, 1971, **50**, 923–928.

[189] D. M. Dulik, *J. Dent. Res.*, 1979, **58**, 1308–1316.

[190] R. L. Bowen, *J. Dent. Res.*, 1979, **58**, 1493–1503.

[191] J. Zhang et al., *Polym. Chem.*, 2014, **5**, 6019–6026.

[192] W. Cook and F. Chen, *Polym. Chem.*, 2015, **6**, 1325–1338.

[193] G. J. Sun and K. H. Chae, *Polymer*, 2000, **41**, 6205–6212.

[194] J. Zhang et al., *Macromolecules*, 2015, **48**, 2054–2063.

[195] N. Moszner et al., *Dent. Mater.*, 2008, **24**, 901–907.

[196] N. Moszner et al., *Macromol. Mater. Eng.*, 2009, **294**, 877–886.

[197] B. Ganster et al., *Macromolecules*, 2008, **41**, 2394–2400.

[198] A. K. O'Brien and C. N. Bowman, *Macromolecules*, 2006, **39**, 2501–2506.

[199] K. S. Anseth, S. M. Newman and C. N. Bowman, in *Biopolymers II*, ed. N. A. Peppas and R. S. Langer, Springer, Berlin, Heidelberg, 1995, pp. 177–217.

[200] R. Chartoff, *J. Therm. Anal. Calorim.*, 2006, **85**, 213–217.

[201] C. Decker, *Polym. Int.*, 1998, **45**, 133–141.

[202] V. V. Ivanov and C. Decker, *Polym. Int.*, 2001, **50**, 113–118.

[203] C. Decker et al., *Prog. Org. Coat.*, 2001, **42**, 253–266.

[204] J. V. Crivello, *Annu. Rev. Mater. Sci.*, 1983, **13**, 173–190.

[205] J. V. Crivello, US4138255 A, 1979.

[206] J. V. Crivello and J. H. W. Lam, *J. Polym. Sci. B Polym. Lett. Ed.*, 1978, **16**, 563–571.

[207] J. V. Crivello, *Adv. Polym. Sci.*, 1984, **62**, 1–48.

[208] C. Decker and K. Moussa, *J. Polym. Sci. A Polym. Chem.*, 1990, **28**, 3429–3443.

[209] N. S. Allen, *J. Photochem. Photobiol. A*, 1996, **100**, 101–107.

[210] J. V. Crivello and M. Sangermano, *J. Polym. Sci. A Polym. Chem.*, 2001, **39**, 343–356.

[211] H. J. Timpe et al., *Macromolecules*, 1993, **26**, 4560–4566.

[212] F. A. Ogliari et al., *J. Dent.*, 2007, **35**, 583–587.

[213] Q. Fang et al., *Polym. Chem.*, 2016, DOI: 10.1039/C6PY00788K.

[214] C. P. R. Nair, R. L. Bindu and V. C. Joseph, *J. Polym. Sci. A Polym. Chem.*, 1995, **33**, 621–627.

[215] C. Nair, *Prog. Polym. Sci.*, 2004, **29**, 401–498.

[216] C. E. Hoyle, T. Y. Lee and T. Roper, *J. Polym. Sci. A Polym. Chem.*, 2004, **42**, 5301–5338.

[217] G. Galli et al., *Macromol. Symp.*, 2001, **169**, 303–312.

3 Thesis Overview

This dissertation focuses on overcoming the main drawback of low reactivity of VCP monomers and resins obtained by RROP. Therefore, the overall objective was the development of a high reactive and low shrinking VCP system, which can compete on the basis of performance and variability with commonly used methacrylate systems. Finally, the potential of VCPs, to serve as low shrinking monomers and resins, was recognized more than 30 years ago. However, so far not a single VCP system could be utilized to a commercial application, since VCPs could not meet at all the main polymerization requirements, like reactivity and complete conversion. In this respect, two concepts were pursued: First, the mechanism of initiation and polymerization was investigated, using photo-polymerization techniques with different combinations of photo-initiators. In this regard also the potential of an enhanced thermodynamic control was uncovered. Second, an incorporation of selective intermolecular H-bonds was designed and studied. Thereby, a concept of partial self-assembly for VCP monomer units was explored.

Hence, curing experiments are based on photo-polymerization techniques, especially using the photo initiator system camphorquinone (CQ) and ethyl 4-(dimethylamino)-benzoate (EDMAB), respectively to initiate the polymerization by light exposure within the visible spectral range. In order to enhance the general reactivity and efficiency of VCP systems subsequent several mono-functional, as well as bi-functional monomer systems have been investigated. As a result, first highly reactive and low shrinking VCP systems were successfully prepared, being suitable for possible applications such as dental composites, electronics and microlithography.

The corresponding content of this work is presented within Section 4.1 – 4.3 as a compilation of three scientific publications, which are based on each other. The overview of each publication as well as the declaration of individual contribution to joint publications is given in the following.

3.1 Publication 1: Low volume shrinkage of polymers by photopolymerization of 1,1-bis(ethoxycarbonyl) 2-vinylcyclopropanes

Within a variety of academic and industrial applications such as microlithography, coatings, adhesives and dental materials, especially where the polymerization process has to be taken out on the spot, it is necessary to match final properties very precisely. But unfortunately, the originating volume change on polymerization is inevitable, due to the transition of intermolecular interactions for the monomers to covalent bonds for the polymers. Thus, there is a demand for vinyl monomers reducing the general volume shrinkage. For the radical polymerizations, for instance of conventional vinyl monomers like styrene (St) and methyl methacrylate (MMA), the volume shrinkage amounts to 16 and 21%, respectively. On the contrary cyclic monomers, which undergo a RROP, show a high potential applicability as low-shrinking monomer, reducing the volume change on polymerization by counteracting due to the ring-opening.

However, previous studies for thermally initiated mono-functional 2-vinylcyclopropane-1,1-dicarboxylate (VCP) derivatives exhibited very low reactivity and higher volume shrinkages as expected for RROP capable monomers. Therefore, we focused on the exploration of this phenomenon and pursued a photo-polymerization initiation for VCPs. Further, to compare the influence of methyl substitution on the photo-polymerization behavior, in particular in α- and β-position to the vinyl group, three different types of VCP derivatives were prepared (Scheme 13).

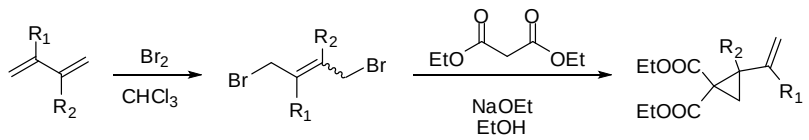

VCP: R_1 and R_2 = H
MeVCP: R_1 = CH_3 and R_2 = H or R_1 = H and R_2 = CH_3
DiMeVCP: R_1 and R_2 = CH_3

Scheme 13: Synthesis of substituted 1,1-bis(ethoxycarbonyl)-2-vinylcyclopropane (VCP) derivatives. According to the used 1,4-dibromo-2-butene derivative either VCP, *methyl* substituted VCP (MeVCP) or *dimethyl* substituted VCP (DiMeVCP) was achieved.

The successful monomer synthesis was proven by GC-MS as well as by 2D-NMR measurements, in which for the MeVCP derivative also the participation of a constitution isomer could be confirmed. Further, compared for instance to MMA, which will be

generally assigned in the following work as reference system, the RROP mechanism of VCPs is more complex (Scheme 14). It was shown, that a methyl substitution in α- and β-position to the vinyl group did influence the reactivity of the VCP system according to the sequence VCP > MeVCP >>DiMeVCP. Moreover the RROP polymerization mechanism of VCPs as well as its progression was studied also.

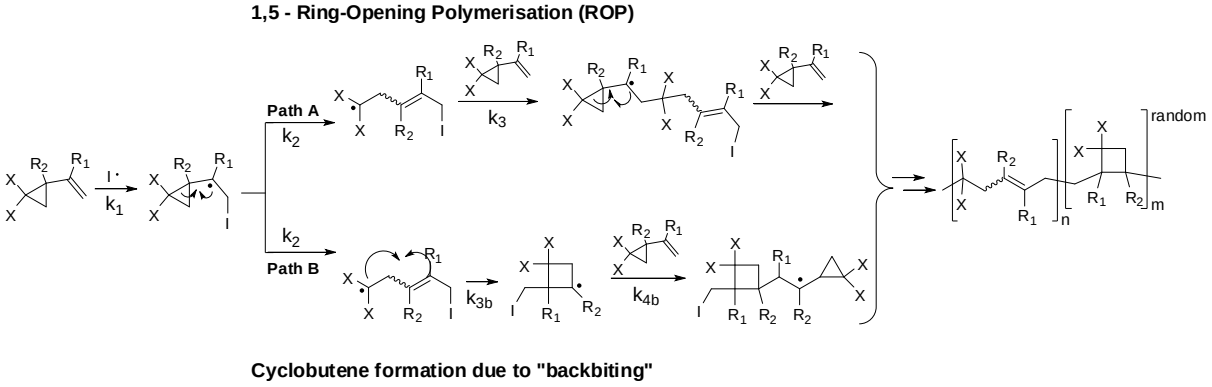

Scheme 14: Schematic description of the radical ring-opening polymerization (RROP) of VCP derivatives. Besides the 1,5 ring-opening (Path A) a cyclobutane formation (Path B) occurs as side-reaction.

Several polymerizations were conducted, in order to compare thermal initiation systems, like 2,2´-azobisisobutyronitrile (AIBN) and di-tert.-butyl-peroxide (DTBP) respectively for initiations at 70 and 120 °C, with binary and ternary photo-initiator systems respectively for initiations by light exposures at 25 °C. Thereby, applying a ternary photo-initiator system, with additional amounts of diphenyliodonium hexafluorphosphate (DPIHFP), enhanced the polymerization kinetic of VCPs, leading to higher polymerization rates within shorter exposure times. In comparison to previous studies a significant improvement in reactivity could be achieved.

Further, since a lower polymerization temperature was applied, an enhanced thermodynamic control occurred. In this regard, it could be shown that a significant higher amount of 1,5-ring-opened, and vice versa lower amount of cyclobutane-units, could be obtained during photo-polymerizations at 25 °C. Thereby, ^{1}H-NMR comparisons of different VCP polymers served as analytical proof, since the ratio of the obtained olefinic protons to the expected ones (for 100% ring-opening) distinguished directly the amount of the ring opened polymer units. Figure 12a illustrates this comparison. Based on the integral values of the olefinic protons 50% of ring-opening was obtained for the poly(VCP) polymerized by DTBP, whereas 79% of ring-opening was obtained for the photo-polymerized poly(VCP). Moreover, it was demonstrated that

the percentage of the ring-opening influenced the volume shrinkage, since the polymerization shrinkage of VCPs could be significantly reduced by reducing the content of cyclobutane units within the polymer. Thereby, Figure 12b illustrates this effect to the volume shrinkage for MMA, St, VCP and MeVCP. Whereas MMA and St showed hardly any effect, the temperature effect was pronounced for VCP and MeVCP.

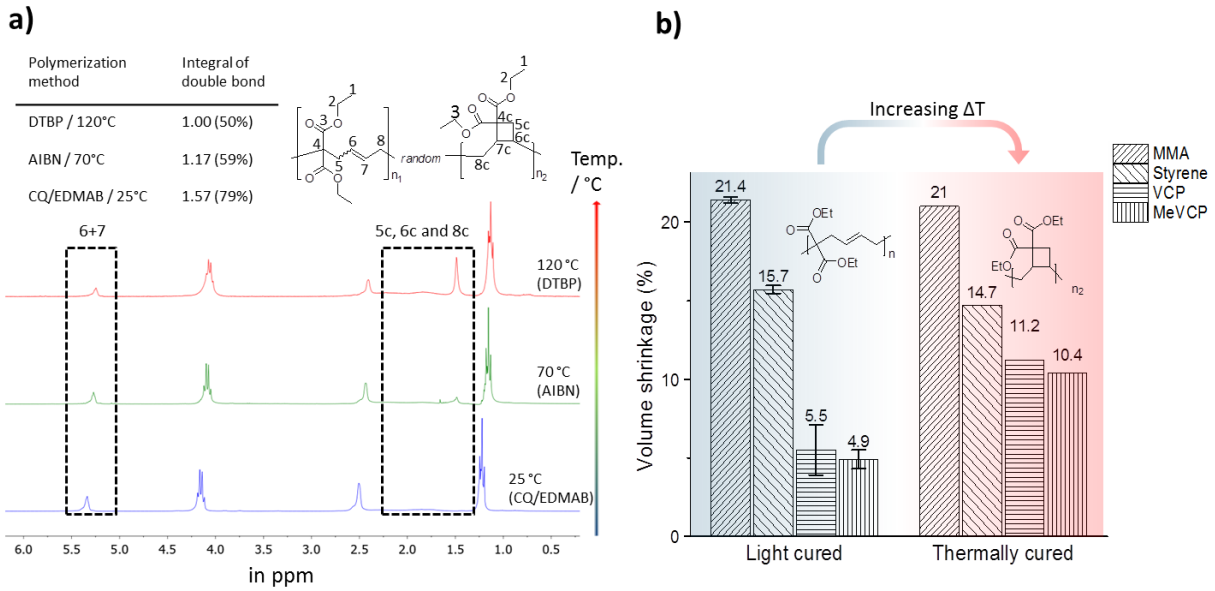

Figure 12: a) Overlay of three ^{1}H-NMRs of poly(VCP) ($CDCl_3$, 300 MHz) polymerized by photo-initiation at 25 °C, by thermal initiation at 70 °C and at 120 °C, respectively. A reduced cyclobutane formation by reducing the temperature to 25 °C for the photo-polymerization could be observed by comparing the integral values of the olefinic protons (signal 6+7). The bracketed values in percentage within the table illustrate the amount of ring-opened VCP units. b) Comparison of the effect on volume shrinkages for polymerization reaction of MMA, St, VCP and MeVCP dependent on the polymerization conditions (light cured at 25 °C & thermally cured at 70 °C).

In conclusion, this study on the photo-polymerization behavior of mono-functional VCPs can be seen as promising basis for further developments, in particular within photo-curable applications of bi-functional systems. In addition, the used VCP system offered an easy access to further modifications, due to the existence of the accessible ethoxycarbonyl side group, and was defined as model monomer for the onward work.

3.2 Publication 2: Renaissance for low shrinking resins: all-in-one solution by bi-functional vinylcyclopropane-amides

So far, not a single high reactive VCP resin could be obtained showing a polymerization efficiency in the range of the commercially used methacrylates. Thus, the interest for VCPs significantly decreased in academics as well as in industrial applications. Whereas a variety of mono- and bi-functional VCP resins was synthesized

and patented by several researches previously, none of the synthesized VCP resins took possession of selective H-bonds. In order to develop an all-in-one solution, providing high reactive and low volume shrinking of a bi-functional VCP resin, in the present study a novel approach was presented by introducing H-bond forming amide-groups.

Therefore, we investigated and compared two similar bi-functional VCP resins, whereby the novel VCP resin VCPMe$_3$hexAmid introduced intermolecular H-bonds into the VCP system. The second resin VCPhexEster served only as a representative of the previously explored bi-functional VCP resins. As illustrated in Scheme 15, the following two VCP systems were synthesized by peptide coupling reaction and by *Steglich* esterification, respectively.

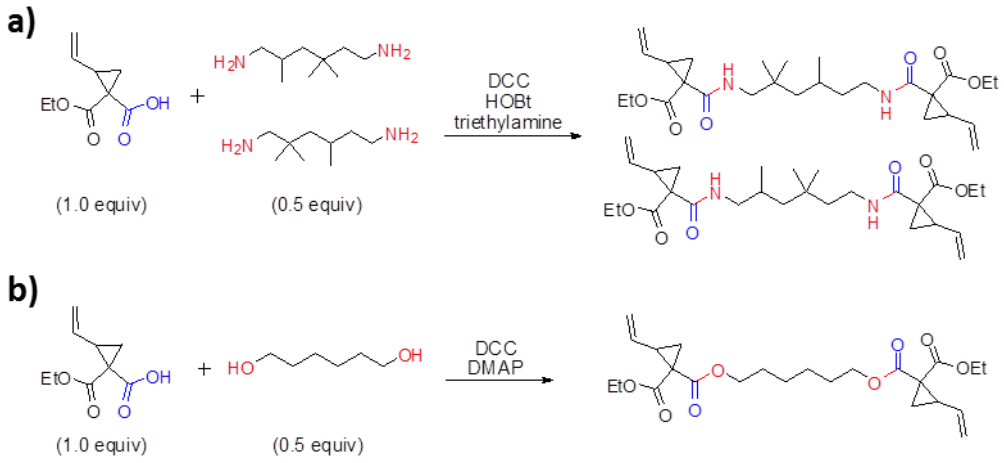

Scheme 15: Preparation of bi-functional VCPs, respectively for a) by peptide coupling reaction and b) by *Steglich* esterification. DCC = N,N'-dicyclohexyl-carbodiimide; DMAP = 4-dimethylaminopyridine; HOBt = benzotriazol-1-ol.

Thereby, a significant difference in reactivity between both VCP resins could be observed. While for the H-bond mediated VCPMe$_3$hexAmid a very fast curing kinetic was evident from high conversions of >80% after short exposure times, VCPhexEster did not reach a similar reactivity and high overall monomer conversions (Fig. 13). Hereby, the extensive difference in reactivity was explained by intermolecular H-bonding, leading to a partial preorganization of the monomer molecules.

To study the effect of H-bonds, various experiments by photo-DSC investigations and temperature dependent NMR measurements were performed. As a result, lower heat flow values and 37% lower rates of polymerization were reached respectively for adding 1 wt% of a KSCN solution as chaotropic additive. Furthermore, within the ^{1}H-NMR experiments a significant shift of the amide proton to higher fields with increasing temperature could be observed, confirming the participation of strong H-bonds.

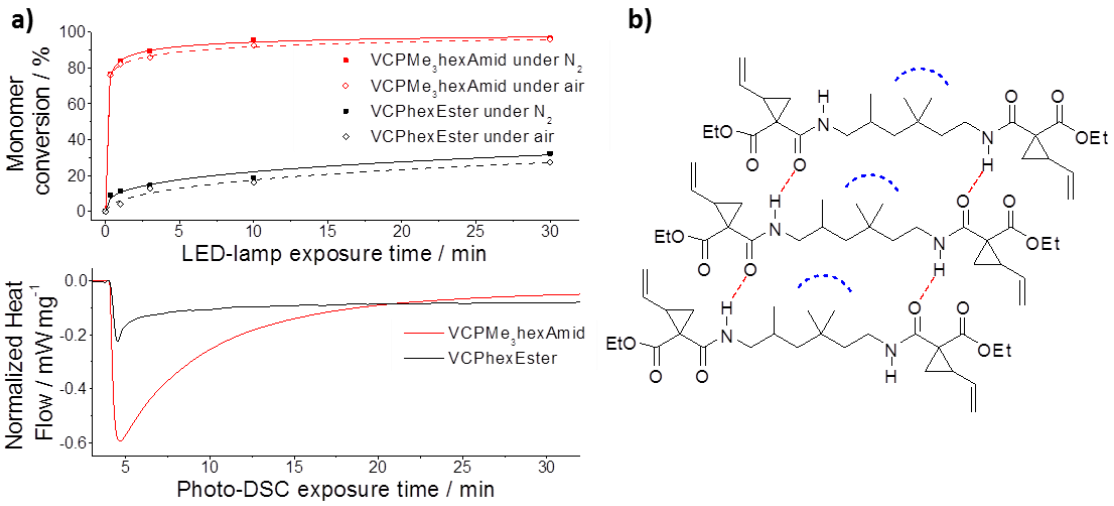

Figure 13: a) Photo-polymerization of VCPMe$_3$hexAmid and VCPhexEster. Upper graph: Time-dependent curing experiments using a commercial blue-light LED source, Lower graph: Illustration of heat flows (mW mg^{-1}) recorded during photo-DSC experiments for VCPMe$_3$hexAmid and VCPhexEster, respectively. b) Proposed concept of hydrogen bonding for VCPMe$_3$hexAmid, showing a partial preorganization of the monomer units (red dashed line). Thereby, the hydrogen bonding is also possible with the ester group, instead of the amide group. The blue dotted semi-circles illustrate the steric hindrance.

Using dielectric analysis, similar curing rates of VCPMe$_3$hexAmid and the well-known urethane dimethacrylate (UDMA) resin could be perceived, which represented the high efficiency and fast curing of this particular VCP resin. Especially with regard to dental applications any reduction of an excessive temperature rise reduces the hazard potential. Advantageously, only a low temperature increase (~4 °C) during the curing process of VCPMe$_3$hexAmid could be observed. In comparison UDMA showed a rise in temperature of 13 °C under identical conditions.

Further, by using a sterically-hindered and isomeric spacer element for VCPMe$_3$hexAmid any disproportionate increase within the resin viscosity could be prevented (2.4 Pa·s). Thus, VCPMe$_3$hexAmid showed due to RROP a reduction by 45% in volume shrinkage compared, for instance, to UDMA (Fig. 14a). Simultaneously, the low viscosity exhibited a vast potential for VCPMe$_3$hexAmid as dental composite. According to this, the cytotoxicity value (LD$_{50}$) of VCPMe$_3$hexAmid (0.067 ± 0.005 mM) was similar to UDMA (0.071 ± 0.009 mM), which in particular serves as standard resin with low cytoxicity. Moreover, the most valuable properties conversion, mechanical strength, viscosity, and optical refraction were all carefully balanced in optimum ranges. By comparing the refraction alteration a simple and accurate correlation (R^2 = 0.985) could be confirmed, presenting the effect of the volume shrinkage to the refraction (Fig. 14b).

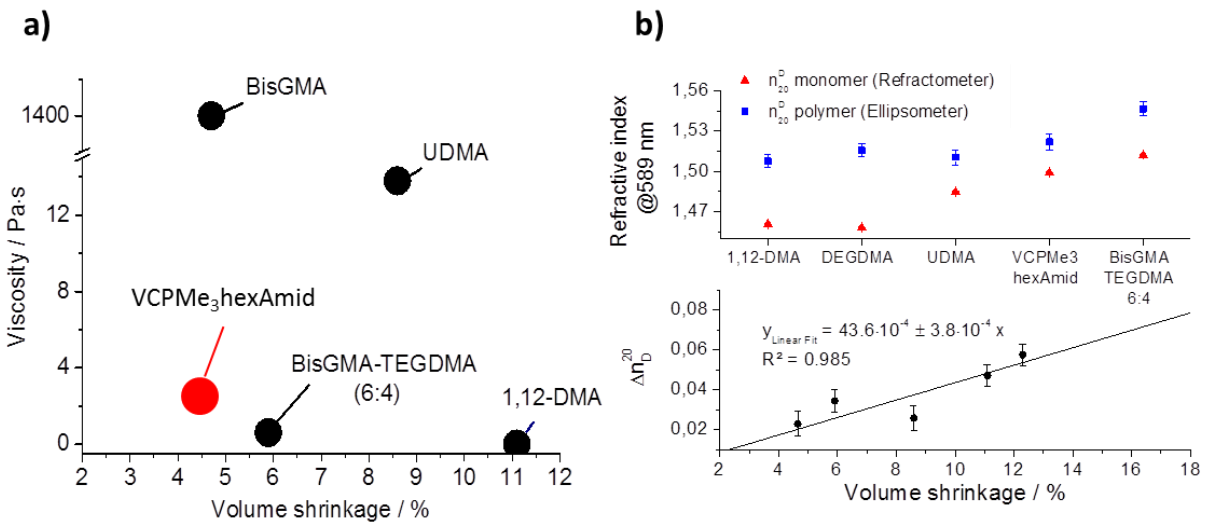

Figure 14: Classification of typical resin properties. a) Ashby plot of specific monomer viscosities in dependence to the volume shrinkage, highlighting the potential of VCPMe$_3$hexAmid. For further clarifications, also the resins bisphenol-A-glycidyl methacrylate (Bis-GMA) and dodecanediol-dimethacrylate (1.12-DMA) are noted, which set in terms of volume shrinkage and viscosity the standard. Thereby, the resin mixture BisGMA-TEGDMA(6:4) is one of the most widely used within dental materials. b) Upper graph: Refractive indices (@589 nm) respectively for the monomer and polymer networks. Lower graph: Graphical evaluation of the refractive index alteration Δn_D^{20} from the polymerization transition in dependence to the volume shrinkage of the respectively polymers showing a simple and accurate correlation between the volume shrinkage and the refraction alteration.

In summary, due to incorporation of intermolecular hydrogen bonds, for the first time a bi-functional VCP resin could be presented, showing similar reactivity in the range of commercially available UDMA. Moreover, the most valuable properties of the synthesized VCPMe$_3$hexAmid resin conversion, cross-linking density, cytoxicity, mechanical strength, viscosity, and optical refractive index were all carefully balanced in optimum ranges. Therefore, this novel VCP resin was especially recommended for dental- and biological-coating applications, where a low volume shrinking is required.

3.3 Publication 3: Photo-polymerizable, low shrinking modular construction kit with high efficiency based on vinylcyclopropanes

As mentioned within the previous section, intermolecular amide hydrogen bonds of the bi-functional VCPMe$_3$hexylAmid resin induced a very effective partial preorganization of the molecules. Yet, since a strong increase within the polymerization behavior and efficiency could be observed, the concept of the partial self-assembly was explored to a universal applicability. Thereby, uniformity within the intermolecular hydrogen bond strength provided an excellent control of constant high reactivity, nearly

regardless of the chosen spacer-unit, offering the system a possible application as modular construction kit for cross-linked networks. As illustrated in Figure 15, the universal concept of partial self-assembly based on the existence of selective intermolecular H-bonds exactly at the VCP-unit.

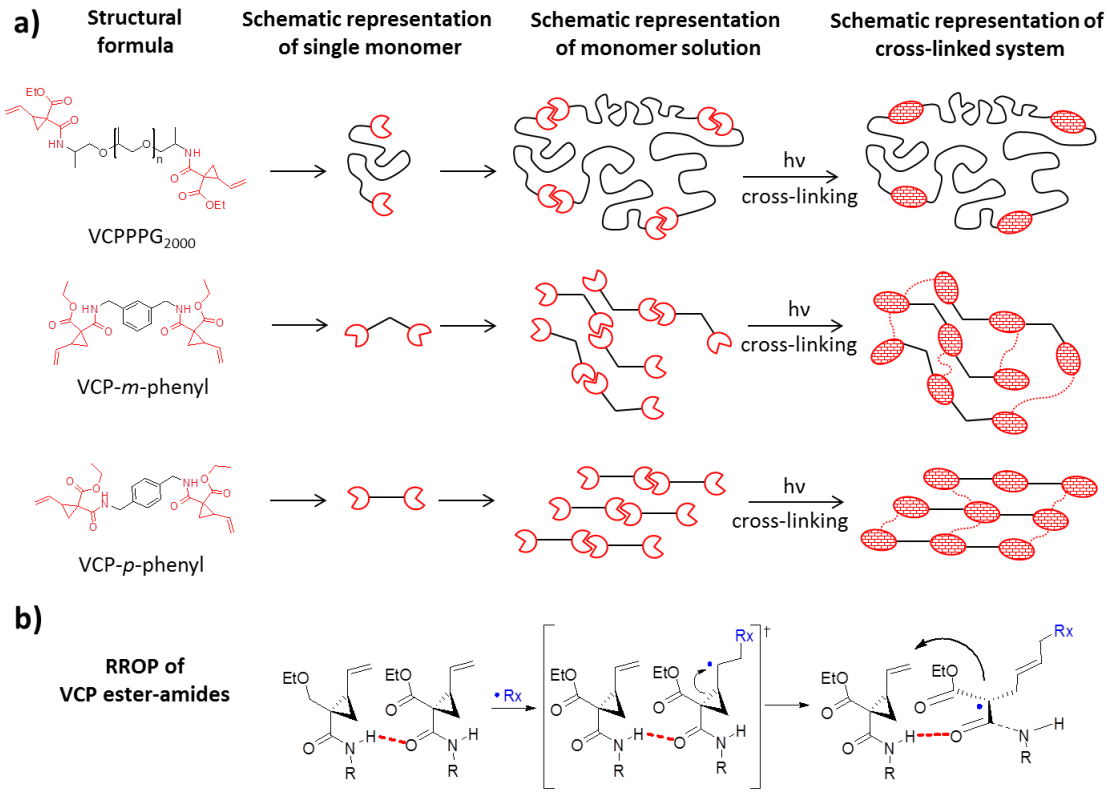

Figure 15: a) Schematic aspect of the H-bond mediated partial self-assembly of VCP ester-amide units. The alignment is primary taking place at the functional group and is independent to the chosen spacer. b) Proposed RROP mechanism of amide-based VCPs. Besides the partial self-assembly an enhanced orbital arrangement has to be taken into consideration.

The high reactivity of two entirely diversified VCP ester-amide systems proved the general efficiency of the system (Fig. 16a). Thereby, first a flexible and high molar mass macro-monomer VCPPPG$_{2000}$ (based on a oligo(propylene glycol) spacer), and secondly two low molar mass monomers VCP-*m*-phenyl and VCP-*m*-phenyl (based on a xylylenediamine spacer) have been synthesized and compared subsequently. Using a combination of temperature dependent NMR- and IR-measurements, the uniformity of the H-bond strength in solution as well as in bulk could be confirmed. Hence, it was assumed, that the spacer unit has a subordinate role to the reactivity, but is dominating the final network characteristics of the VCP ester-amide that, unlike to methacrylate systems, which show a high discrepancy in curing. Thus, methacrylate systems are not appropriate for modular construction kits.

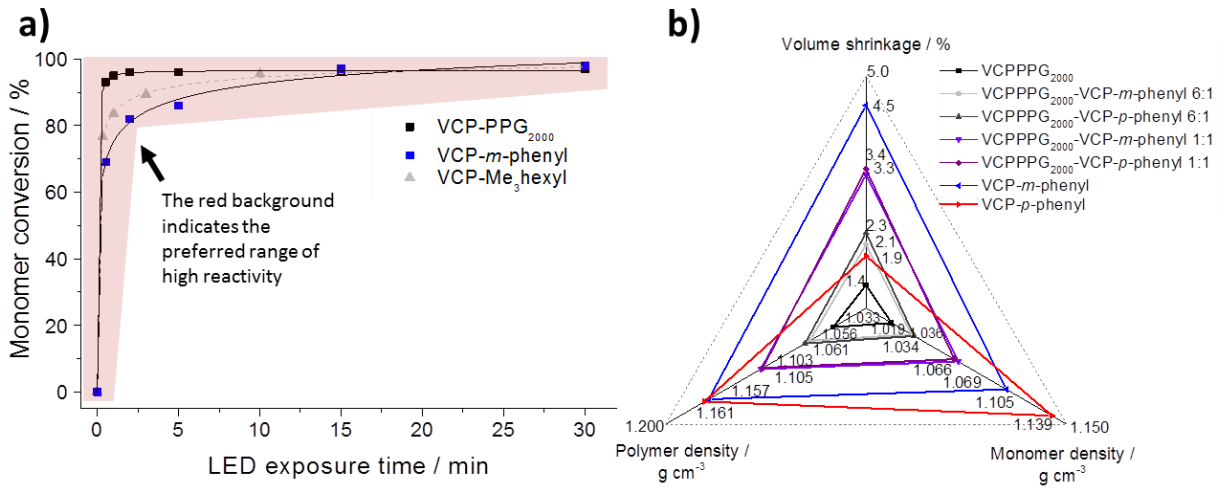

Figure 16: a) Determined monomer conversion for the photo-polymerization of $VCPPPG_{2000}$, VCP-*m*-phenyl and $VCPMe_3$hexyl, illustrating that entirely diversified VCP ester-amide systems show similar curing performances. b) Spider chart showing the dependency between the monomer- and polymer density to the volume shrinkage. For the partial-crystalline VCP-*p*-phenyl a disproportion within the correlation could be observed, based due to the denser partial-crystalline monomer structure (1.139 g·cm^{-3}).

Surprisingly, for $VCPPPG_{2000}$ an extremely low volume shrinkage of 1.4% during polymerization could be determined (Fig. 16b), because of its increased molecular weight as macro-monomer. The analog volume change of VCP-*m*-phenyl was 4.5%, which corresponds to reduction of 50% in volume shrinkage compared *e.g.* to UDMA of similar molecular weight. This reduction was remarkable, as ^{13}C-CP/MAS solid-state measurements confirmed an extraordinary high cross-linking density of the cured VCP systems, whereas methacrylate systems reach only cross-linking densities between 20 – 70%. Further, a significant difference between the cured isomers VCP-*m*-phenyl and VCP-*p*-phenyl occurred, as for VCP-*p*-phenyl only a volume shrinkage of 1.9% was observed. Hereby, VCP-*p*-phenyl combined a liquid phase with partial crystallinity, offering an intermediate and heterogeneous stage between both physical states. Thus, an increased density for the uncured VCP-*p*-phenyl was obvious, which additionally reduced the volume shrinkage. In fact, this characteristic was lost, when the crystalline phase was melted or diluted by any further phase, like it could be observed for the co-networks of VCP-*p*-phenyl. However, compared *e.g.* to other known volume example systems VCP-*p*-phenyl offered a more applicable method to reduce the volume shrinkage, especially as the wax-like structure was still easy to process.

Since the VCP ester-amide H-bonds were uniform, we could easily control the mechanical properties by varying the co-monomer content in co-networks. Therefore, the E-moduli of cured specimens were investigated by three point bending experiments.

With increasing content of the co-monomer VCP-*m/p*-phenyl, the moduli could be raised continuously from 0.19 MPa, respectively for $VCPPPG_{2000}$, up to 232.3 MPa, respectively for the cured VCP-*m*-phenyl. Thus, the moduli could be raised up to 1200 times to higher values. Thereby, cured VCP-*m*-phenyl could compete clearly with the commercially UDMA, which provided moduli of 224.1 MPa with significant higher volume shrinkages.

Thus, with an appropriate variation of the spacer-unit, selective characteristics, like *e.g*. optical properties or mechanical strength could be adjusted in a simple way, without obtaining any significant disadvantage for the curing behavior. Thereby, a uniformity of the VCP ester-amide H-bond strength was shown, providing a universal concept to apply VCP ester-amides as low-shrinking, high-performance resins. Owing to this, it was concluded that VCP ester-amides could be used as modular construction kit, enabling the system a vast number of combination possibilities and an outstanding application perspective.

3.4 Individual Contributions to Joint Publications

In the following, the individual contribution of each author and coauthor in particular to each paper is indicated in detail.

Publication 1: Low volume shrinkage of polymers by photopolymerization of 1,1-bis(ethoxycarbonyl) 2-vinylcyclopropanes

Published in *Polymer Chemistry*, **2015**, *6*, 2297–2304.

By Paul Pineda Contreras, Payal Tyagi and Seema Agarwal.

Dr. Payal Tyagi and I contributed equally to the experimental part of this work. Thereby, I prepared the monomer synthesis as well as the characterization of the precursors and polymers. This included the determination of the volume shrinkage and the characterization of the polymer structures, using NMR and GC-MS. Dr. Payal Tyagi developed the kinetic experiments and synthesized corresponding monomers herself. The manuscript was jointly written and developed by Dr. Payal Tyagi and myself. Prof. Seema Agarwal was involved in designing the concept, supervised the project, and revised the publication.

Parts of this work were established in my master thesis “Darstellung, Charakterisierung und ringöffnende Polymerisation von Vinylcyclopropan-Derivaten für eine Applikation in der Dentalindustrie” which has been published within my M. Sc. graduation at the Philipps-Universität Marburg in 2012. The overlap concerns parts of the experimental concept, which were reproduced and corrected within this publication.

Publication 2: Renaissance for low shrinking resins: all-in-one solution by bi-functional vinylcyclopropane-amides

Published in *Chemical Communications*, **2015**, *51*, 11899-11902.

By Paul Pineda Contreras, Christian Kuttner, Andreas Fery, Ullrich Stahlschmidt, Valérie Jérôme, Ruth Freitag and Seema Agarwal.

I performed and designed all monomer and polymer synthesis & characterizations, as well as all analytical experiments regarding curing kinetic experiments and hydrogen bond verifications. The ellipsometric measurements, including the calculation of the refractive index values, were performed by Dr. Christian Kuttner (under supervision of Prof. Andreas Fery). Ullrich Stahlschmidt performed the cytotoxicity measurements of

the uncured resins under the guidance of Dr. Valérie Jérôme and Prof. Ruth Freitag. The whole manuscript and the main part of the Supporting Information were written by me. Thereby, Dr. Christian Kuttner and Dr. Valérie Jérôme wrote the corresponding sections of the Supporting Information regarding spectroscopic ellipsometry and cytotoxicity determination. Prof. Seema Agarwal was responsible for supervision, development of ideas and corrected the publication.

Publication 3: Photo-polymerizable, low shrinking modular construction kit with high efficiency based on vinylcyclopropanes

Published in *Polymer Chemistry,* 2016, **7**, 3100–3106.

By Paul Pineda Contreras and Seema Agarwal

I developed and performed all synthetic and analytical experiments. Both, the manuscript and the Supporting Information were written by me. Prof. Seema Agarwal provided scientific input, supervised the work, and revised the manuscript.

4 Reprints of Publications

4.1 Low volume shrinkage of polymers by photopolymerization of 1,1-bis(ethoxycarbonyl) 2-vinylcyclopropanes

Paul Pineda Contreras, Payal Tyagi and Seema Agarwal*, *Polymer Chemistry*, **2015**, *6*, 2297–2304.

Makromolekulare Chemie II, Universität Bayreuth, Universitätsstraße 30, 95440 Bayreuth, Germany.

*Corresponding Author: E-mail: agarwal@uni-bayreuth.de; Fax: +49-921-553393.

Published by The Royal Society of Chemistry. (Open Access Article. Published on 16th January 2015. No permission required)

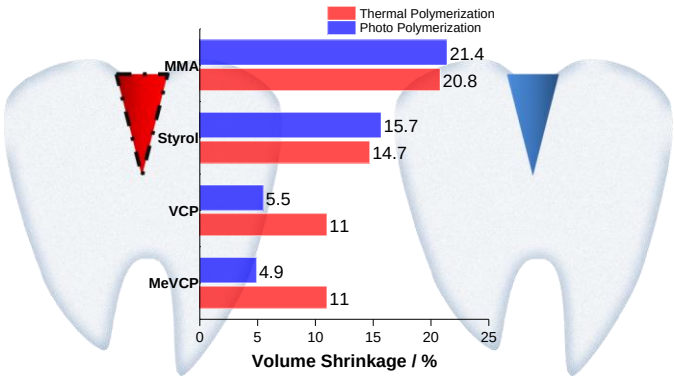

Polymer Chemistry

PAPER

View Article Online
View Journal | View Issue

Cite this: *Polym. Chem.*, 2015, **6**, 2297

Low volume shrinkage of polymers by photopolymerization of 1,1-bis(ethoxycarbonyl)-2-vinylcyclopropanes†

Paul Pineda Contreras,‡ Payal Tyagi‡ and Seema Agarwal*

Low volume shrinkage of polymers by photoring-opening polymerization of 1,1-bis(ethoxycarbonyl)-2-vinylcyclopropane (VCP) and its methyl substituted derivate 1,1-bis(ethoxycarbonyl)-2-(prop-1-en-2-yl)-cyclopropane (Me-VCP) is presented. The aim of this study was to evaluate the photopolymerization behavior and structure of the corresponding polymers from VCP and its methyl substituted derivates 1,1-bis(ethoxycarbonyl)-2-(prop-1-en-2-yl)-cyclopropane (Me-VCP) and 1,1-bis(ethoxycarbonyl)-2-methyl-2-(prop-1-en-2-yl)-cyclopropane (DiMeVCP). VCP monomers were polymerized using camphorquinone (CQ) as a photo-initiator either in a binary or ternary photo-initiator system. The binary systems were formulated with ethyl 4-dimethylaminobenzoate (EDMAB) in relation to the monomer and 1 mol% of CQ. The ternary system was a mixture of 1 mol% of CQ, 2 mol% of EDMAB and 2 mol% of DPIHFP. Ternary photo-initiator systems showed high polymerization rates leading to high conversion in a short photo-activation time. One of the important findings is the formation of higher amounts of 1,5-type ring-opened units and lower amounts of cyclobutane-containing units in photopolymerization, which can make VCP an attractive component of dental composites, as the volume shrinkage is proportional to the 1,5-ring opening. Earlier it was observed that thermal free radical polymerization of VCPs gives higher amounts of cyclobutane structures compared to 1,5-type ring-opened units in the corresponding polymers, causing VCP to be excluded from the list of promising dental composites, as the volume shrinkage was higher than expected.

Received 9th December 2014,
Accepted 16th January 2015

DOI: 10.1039/c4py01705f

www.rsc.org/polymers

1. Introduction

2-Vinylcyclopropane-1,1-dicarboxylates (VCPs) are attractive monomers as they display less polymerization shrinkage than other vinyl monomers, such as methacrylates.[1–3] This characteristic makes such cyclic monomers attractive as low-shrinking components in dental adhesives or filling composites, curing resins, molding and filling materials. As a consequence, VCPs have attracted considerable interest among researchers in publications and patents.[4–6] Many studies have been carried out to investigate the influence of the type and position of substituents on the rate, molecular weight, volume shrinkage and polymer structure of VCPs by thermal radical polymerization.[7] It has been reported that thermal radical polymerization provides a polymer consisting of a 1,5-ring opened unit along with a new unit, which is believed to have a cyclobutane structure (Scheme 1).[3]

By comparing the dependence between the shrinkage on polymerization and the reciprocal of the molecular weight of several VCP monomers, a higher shrinkage was observed than expected for ring-opening monomers. Furthermore the obtained volume shrinkage was in the range of vinyl monomers. This additional shrinkage was attributed to the formation of the cyclobutane containing unit during polymerization.[3] But since VCPs are possible ring-opening monomers, they are expected to be useful materials with lower shrinkage in volume, by reducing the formation of cyclobutane containing units during radical polymerization.

It is interesting to note that not many detailed studies in the open literature are provided for ring-opening photo-

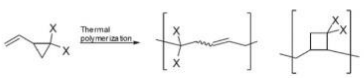

Scheme 1 Reported polymer structures of the radical ring-opening polymerization of VCPs.

University of Bayreuth, Macromolecular Chemistry II and Bayreuth Center for Colloids and Interfaces, Universitätsstraße 30, 95440 Bayreuth, Germany. E-mail: agarwal@uni-bayreuth.de; Fax: +49-921-553393; Tel: +49-921-553397

†Electronic supplementary information (ESI) available: NMR, GC, GC-MS and experimental notices of the synthesis and evaluation. See DOI: 10.1039/c4py01705f

‡Paul Pineda Contreras and Payal Tyagi have contributed equally to the experimental part.

polymerization of VCPs. Camphorquinone (CQ) and ethyl-4-dimethylamino-benzoate (EDMAB) and 2,4,6-trimethylbenzoyldiphenyl-phosphinoxide (Lucirin), a three component initiator system was used for photocopolymerization of bifunctional methacrylate monomers like bis-GMA and UDMA with a vinylcyclopropane derivate (1,3-bis[(1-ethoxycarbonyl-2-vinylcyclopropane-1-yl)carboxy)]benzene to form crosslinked networks.[8]

Till now, the practical application of VCPs has been restricted, as in comparison with standard methacrylate monomers they are less reactive.[3,9] However, the research group of N. Moszner *et al.* in particular, has synthesized and investigated with great effort a number of different 1,1-di-substituted VCPs to increase the reactivity during thermal radical polymerization; unfortunately the many different approaches resulted only in moderate improvements.[10] In order to enhance the polymerization reactivity of VCPs regardless, not by synthetic methods, but rather by a variation of the photopolymerization conditions, diaryliodonium salts were introduced to the photo-initiator system. Diaryliodonium salts are efficient photo-initiators for both radical and ionic (mostly cationic) polymerization.[11,12] When light is irradiated on the excited iodonium it decomposes to an aryliodo radical cation, a reactive aryl radical and an anion.[13] However, these salts do not absorb significantly above 300 nm, therefore UV light sources were used, which restrict their biological applications, where UV light is not recommended. However, it was reported that using dyes that absorb in the visible light region as sensitizers, would allow a reaction with the onium salts, promoting the decomposition.[14] In a similar way, onium salts can also act in radical polymerization.[15,16] Several kinds of visible light sensitizer dyes have been investigated, such as camphorquinone,[17] safranine,[18] acridine derivatives[16] and acetophenone dyes.[14] Camphorquinone, a dye widely used as a photo-initiator for radical polymerization, can act as a photo-sensitizer to diphenyliodonium hexafluorophosphate, which does not absorb light in the visible region, improving the reactivity of the photo-initiator system.[17]

The aim of the present work was to study the effect of the photoinitiated ring-opening polymerization of 2-vinylcyclopropane-1,1-dicarboxylate and the corresponding monomethyl substituted VCP on the polymer structure, kinetics and volume shrinkage. Camphorquinone was used as a photosensitizer with ethyl-4-dimethylaminobenzoate for binary, and together with diphenyliodonium hexafluorophosphate, for ternary initiation processes to evaluate the influence of an onium salt on the radical photopolymerization kinetics and polymer structure of VCPs.

2. Experimental section

2.1 Measurements

^{1}H- (300 MHz) and ^{13}C- (75 MHz) NMR spectra were recorded on a Bruker Ultrashield-300 spectrometer in $CDCl_3$, using tetramethylsilane (TMS) as an internal standard. GC measurements have been performed by a GC-FID system of the type QP-5050 from Shimadzu Company with nitrogen as carrier gas. GC-MS measurements have been performed with a system Agilent 5977A MSD with helium as carrier gas. Molecular weights and polydispersity index (PDI) of the polymers were determined by GPC with a Knauer system equipped with two columns, PSS-SDV (linear, 10 μl, 60 cm × 0.8 cm), and a differential refractive index (RI) detector. THF was used as an eluent at a flow rate of 0.8 ml min^{-1}. A polystyrene calibration was employed as a reference. A Mettler thermal analyzer of the type 821c DSC was used for the thermal characterization of polymers. DSC scans were recorded under a nitrogen atmosphere at a flow rate of 70 ml min^{-1} at heating rates of 10 K min^{-1}. Each sample weighed about 10 ± 2 mg for DSC analysis. The polymerization shrinkage was calculated from the difference in density of the monomer and the formed polymers (Archimedes principle). The densities of the monomers were measured by a 1 mL pycnometer, and the densities of the polymers, by water displacement of 400 mg cured samples. The polymer samples were prepared by inserting the monomer–initiator mixture into the bottom of a 10 mL standard test tube at light exclusion, flushing the tubes with an argon gas for 30 s and irradiating each sample for 48 h at room temperature. Afterwards the samples were cooled and bounced out of the glass tubes to a glass plate of similar density and weight, as the VCP polymers occurred as not totally solid but rather as viscous polymer melts. The polymerization shrinkage was determined separately for the three samples.

2.2 Materials

1,4-Dibromo-2-butene, diethyl malonate, sodium, isoprene, camphorquinone (CQ) and *tert*-butyl peroxide (DTBP) were supplied by Aldrich and used without further purification. Azobisisobutyronitrile (AIBN) was obtained from Bayer AG and recrystallized from methanol before use. Ethyl 4-dimethylaminobenzoate (EDMAB) (Fluka) and diphenyliodonium hexafluorophosphate (DPIHFP) (ABCR GmbH & Co. KG) were used without further purification. Tetrahydrofuran (BASF), ethanol (BASF), chloroform and pentane were distilled before use.

2.3 Monomer synthesis

1,1-Disubstituted 2-vinylcyclopropanes were obtained from diethyl malonate and the corresponding dibromo butane as per the published procedure.[3,19] 1,4-Dibromo-2-methyl-2-butene was prepared previously in a reaction between isoprene and bromine in chloroform (Scheme 2).[20]

The detailed reaction procedures, including purification and characterization, are given in the relevant ESI.† The structures were characterized by NMR and GC. In contrast to the

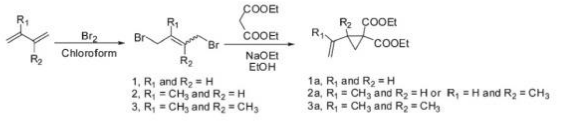

Scheme 2 Schematic pathway to synthesize monomers **1a–3a**.

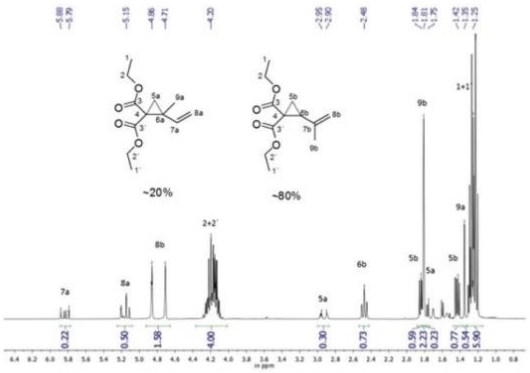

Fig. 1 ^{1}H-NMR of the monomer (**2a**), which consists of diethyl 2-(prop-1-en-2-yl)cyclopropane-1,1-dicarboxylate (~20%) and diethyl 2-methyl-2-vinylcyclopropane-1,1-dicarboxylate (~80%) ($CDCl_3$, 300 MHz).

reported literature, we observed for the synthesis of **2a** a constitution isomer of around 80 : 20 of diethyl 2-(prop-1-en-2-yl)-cyclopropane-1,1-dicarboxylate to diethyl 2-methyl-2-vinylcyclopropane-1,1-dicarboxylate, that could not be separated by distillation or column chromatography as shown in the NMR (Fig. 1). Therefore this mixture was used for polymerizations.

2.4 Polymerization

2.4.1 General procedure. The polymerization was carried out in a polymerization tube which was vacuum dried and degassed prior to use. The monomer was introduced into the polymerization tube along with a radical initiator. Different photoinitiator systems were investigated at various levels under stirring conditions: 1 mol% CQ and 2 mol% EDMAB; 1 mol% CQ + 2 mol% EDMAB and DPIHFP at different molar concentrations; 1 mol% CQ and 2 mol% DPIHFP. The light radiation source was a white-light LED lamp (details are given below). For comparison purposes thermal polymerizations were also carried out using 1 mol% DTBP and 1 mol% AIBN. The thermally induced polymerizations were carried out at 70 °C and 120 °C respectively for AIBN and DTBP initiators. The polymerizations were stopped after definite time intervals by freezing the mixture in liquid nitrogen. Afterwards the polymer melts were dissolved in THF and precipitated into cold pentane. The precipitated polymers were filtered and dried in a vacuum oven at room temperature till they achieved a constant weight. The degree of conversion was calculated by the mass difference of the polymer and the monomer. The data were plotted and curve fitting was performed by Hill three parameter non-linear regressions. Using these data, the polymerization rate R_p (min^{-1}) was calculated from the slope of the linear fit.

2.4.2 Radiation source. To perform the monomer photoactivation, a white light lamp of GSVITEC Company (Marathon MultiLED) was used. The lamp head consisted of 25 cells. The power of the lamp was 800 W halogen equivalents (data as per the lamp manual provided by GSVITEC). The emission spectrum of the white light LED lamp was recorded by a Shimadzu fluorescence spectrometer RF type 1502. The white-light LED lamp emits primarily at 442 and 540 nm wavelengths. The light emission between 400 and 480 nm (absorption range of CQ) corresponds to 43% of the total emission power of the emitted light of the lamp head.

3. Results and discussion

Thermal radical polymerization of VCPs such as 2-vinylcyclopropane-1,1-dicarboxylates and derivatives is well-studied in the literature.[1,3,7] The radical from the thermal initiator adds at the vinyl double bond of VCP followed by isomerization with ring-opening leading to the formation of a stable t-radical for further propagation. In the present work, photopolymerization of 2-vinylcyclopropane-1,1-dicarboxylate (**1a**) and the corresponding mono and di-α-methyl substituted VCPs (**2a** and **3a**) was studied using different photo-initiator systems in different ratios (camphorquinone (CQ) and ethyl 4-dimethylaminobenzoate (EDMAB) (1 : 2 mol%), and CQ and EDMAB (1 : 2 mol%) with different ratios of DPIHFP as the ternary initiator (1, 2 and 4 mol%)[17] (Scheme 3).

The reaction kinetics of the photo-polymerization with the binary initiator system (1 mol% CQ and 2 mol% EDMAB) is depicted in Fig. 2. White to light yellow colored polymers, which were soluble in common solvents were obtained from

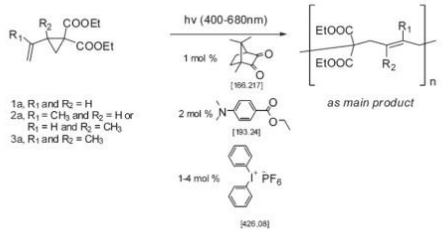

Scheme 3 Schematic polymerization equation of photosynthesized polymers.

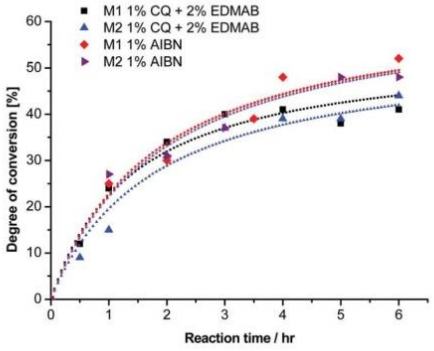

Fig. 2 Degree of conversion for the polymerization of monomers **1a** (M1) and **2a** (M2) with different initiators. Concentrations of 1 mol% CQ and 2 mol% EDMAB as well as 1 mol% AIBN were used.

1a and **2a**. However, **3a** the di-methyl substituted monomer did polymerize only in negligible yields, which confirms the reported literature for thermal polymerization of methyl substituted 1-ethoxycarbonyl-2-vinylcyclopropanes[21] and methyl-substituted 1,1-diethoxycarbonyl-2-vinylcyclopropanes.[19] This trend was explained with the assumption of the higher chain transfer reaction of the di-methyl substituted VCP.[19] Nevertheless it should be considered that the presence of two methyl substituents, one in the α-position and the other on the cyclopropane ring might provide the cause of hyperconjugation, a relative stable radical, whereby the rate of ring-opening is reduced to a range within the radical termination reaction, and becomes a byword of the propagation.

The rates of polymerization (R_p) of the photo-polymerization with the binary initiator system were 0.30 and 0.25% per min for **1a** and **2a**, respectively. As a matter of fact it seemed that by conventional radical polymerization, the radical ring opening process, independent of the radical initiator and α-substituent, was very slow. Therefore for providing a comparison we added in Fig. 2 the thermal polymerization kinetics of **1a** and **2a** in the presence of 1 mol% AIBN, a thermal initiator, where we observed almost identical R_p values of 0.29 and 0.28% per min. These R_p values were still slow, which is in line with the literature.[3,19]

However the ternary photoinitiator system with additional DPIHFP could provide faster vinylcyclopropane polymerizations. It is worth mentioning that the ternary photoinitiator systems are already known to provide enhanced rates of polymerizations to the conventional vinyl monomers owing to an increased concentration of initiating radicals or because of the concurrent cationic or radical initiating species.[16,17,22] The observed R_p values for ring-opening polymerization of VCPs were much higher with higher overall conversions (around 80%) compared to the conventional CQ-EDMAB system. Therefore for a detailed investigation we added DPIHFP as an initiator at different molar concentrations.

We observed for the degree of conversion as a function of the photo-activation time for the ternary initiator system with 2 mol% DPIHFP R_p values of 11.37 and 2.60% per min for **1a** and **2a**, respectively (Fig. 3). Thereby the R_p values, compared

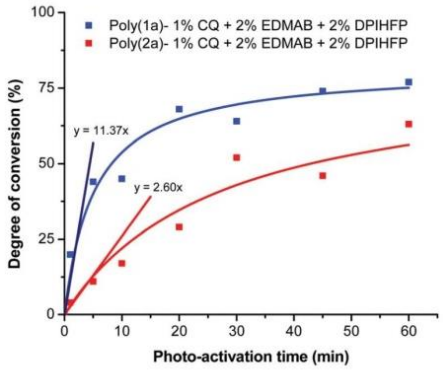

Fig. 3 Degree of conversion for the photo-polymerization of monomers **1a** and **2a** with 1 mol% CQ + 2 mol% EDMAB + 2 mol% DPIHFP as the ternary initiator.

to the conventional photopolymerization system CQ-EDMAB and to the thermal polymerization AIBN (Fig. 2), can be significantly improved by using a ternary system to the factor ~35 and ~10 for poly(**1a**) and by factor ~38 and ~9 for poly(**2a**). In general, an increase in the molar mass of polymers was also seen on using the ternary initiator system (Table 1).

Further the concentration level of DPIHFP within the ternary photo-initiator system showed a significant effect both on the rate of polymerization and the degree of monomer conversion (Fig. 4). Polymerization with a lower concentration of DPIHFP (below 2%) showed higher monomer conversions at low reaction times. 10 min of light radiation and just 0.5 mol% DPIHFP in the ternary initiator system was sufficient to polymerize almost 25% of the monomers. However, for further photo-activation, there was almost no further increment in the yield of polymerization. One of the possible reasons could be that the onium salt decomposes after a certain period of time. The highest conversion was obtained with 4% onium salt concentration (about 80% conversion in 15 minutes), although there were solubility problems with onium salts having a concentration of 2% or higher in 1,1-disubstituted 2-vinylcyclopropanes.

Table 1 Properties of binary and ternary photo- and thermal-polymerized monomers **1a** and **2a**[a]

Entry		Initiator[b]	Temp./ °C	Ring opened polymer structure[c]/%	Cyclo-butane polymer structure[c]/%	M_n[d]/ Da × 10^{-4}	D[d]	Yield/ %
1	Poly(**1a**)	CQ/EDMAB	25	78	22	0.8	1.5	62[e]
2	Poly(**2a**)	CQ/EDMAB	25	93	7	1.3	1.9	64[e]
3	Poly(**1a**)	AIBN	70	59	41	8.9	1.8	57[f]
4		DTBP	120	50	50	4.4	1.9	51[f]
5	Poly(**2a**)	AIBN	70	86	14	1.3	2.5	56[f]
6		DTBP	120	75	25	1.1	2.9	58[f]
7	Poly(**1a**)	CQ/EDMAB	25	86	14	5.5	2.9	24[g]
8		CQ/EDMAB/DPIHFP	25	80	20	2.0	2.1	77[g]
9	Poly(**2a**)	CQ/EDMAB	25	95	5	1.0	2.7	15[g]
10		CQ/EDMAB/DPIHFP	25	86	14	1.7	2.2	63[g]

[a] Monomer: 0.3 g. [b] 1 mol% CQ; 2 mol% EDMAB, 2 mol% DPIHFP. [c] Estimated by ^{1}H NMR in $CDCl_3$, polymer structure illustrated in Schemes 7 and 9 and Fig. 5 and S13–S17.† [d] Estimated by GPC; bimodal distribution of poly(**2a**). [e] Yield in 12 h. [f] Yield in 8 h. [g] Yield in 1 h.

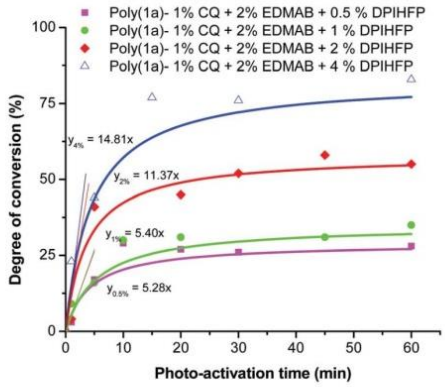

Fig. 4 Degree of conversion for the photo-polymerization of monomer **1a** with different concentrations of DPIHFP as the ternary initiator.

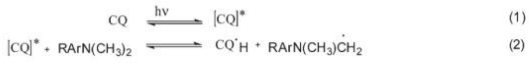

Scheme 4 Schematic simplified reaction scheme of CQ/EDMAB initiation.

The photo-initiator system CQ/EDMAB is frequently used for dentistry applications as the absorption maximum of CQ is around 470 nm, beyond the UV wavelength. Camphorquinone as a 1,2-diketone compound forms a reactive excited species (CQ*) during light absorption (eqn (1)).[23] These excited species interact with the EDMAB to form an exciplex, and within CQ* abstracts, with a hydrogen atom from the tertiary amine to give a ketyl radical and the α-amino-alkyl radicals (eqn (2)), which initiate the polymerization at the carbon double bond of the monomer (eqn (6)). Meanwhile the ketyl radical mainly dimerizes or disproportionates.[23] The simplified reaction mechanism of CQ/EDMAB is shown in Scheme 4.[23,24]

The reaction mechanism using a ternary photo-initiator system is more complex to understand, as Ogliari *et al.* and other authors have already described.[17,24] For consideration of our mechanism only the radical pathway has been described, as we observed that polymerization propagation was based only on radical species and not the cationic one (description further below). The amine radical generated from the exciplex state between CQ* and EDMAB (eqn (2)) could react with DPIHFP, irreversibly cleaving the C–I bond to generate a reactive phenyl radical (eqn (3)). This phenyl radical can either react with the remaining amine, abstracting a proton and generating a new amine free radical or simply start propagation (eqn (7)). It is also reported elsewhere that an exciplex between CQ* and DPIFHP is initially formed, which reacts further with the EDMAB, giving a radical amine species that initiates the polymerization and regenerates the DPIFHP (eqn (5)).[18] Beyond that the DPIFHP can be reduced by an electron transfer within the exciplex with CQ* to a diphenyliodine free radical, which is unstable and decomposes into a phenyliodine

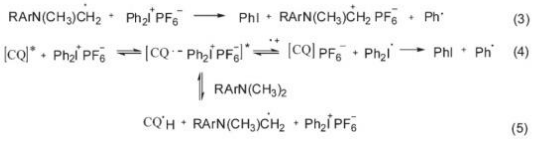

Scheme 5 Simplified scheme of the radical initiation reaction of the ternary photo-initiator system using DPIHFP as the onium salt.

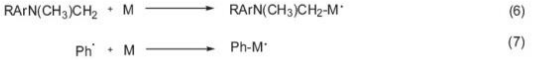

Scheme 6 Schematic propagation initiations during photo polymerization.

and again to a phenyl free radical (eqn (4)).[17,24] Photo-polymerization experiments with monomer **1a** were performed in the presence of the radical inhibitor, hydroquinone. It was observed that the polymerization of **1a** was completely inhibited in ternary systems (CQ/EDMAB/DPIHFP). This result indicated that the polymerization mechanism of the ternary initiation system (CQ/EDMAB/DPIHFP) was the only free radical mechanism for VCP polymerization, and not concurrently radical and cationic, as known for ternary initiator systems with onium salts (Schemes 5 and 6).[12]

Altogether, it can be concluded that the addition of the iodonium salt DPIHFP opens further pathways capable of generating radicals, whereby compared to the binary initiator system CQ/EDMAB, on the one hand the relative efficiency of the radical initiation is increased, while on the other hand an increased concentration of initiating radicals results simply by using DPIHFP as the ternary initiator.

3.1 Structure of the polymer

It has been described by Sanda *et al.* that a 1,5-type ring-opened polymer unit is primarily formed in the thermal polymerization of 1,1-disubstituted 2-vinylcyclopropanes with minor amounts of cyclobutane containing units (Scheme 7).[3,19]

The polymer structure of poly(**1a**) made by photo-polymerization was examined in detail by ^{1}H-NMR (Fig. 5), and compared with the structures formed using thermal radical polymerization. According to the reported literature a broad signal between 1.5 and 2.5 ppm in ^{1}H NMR is caused by the formation of a cyclobutane containing unit ($\mathbf{1a}_{II}$) for thermally polymerized samples.[3] This broad signal was not as clearly observed in poly(**1a**) obtained from photo-polymerization, as in the polymers obtained during thermal polymerization with AIBN or DTBP (Fig. 5).

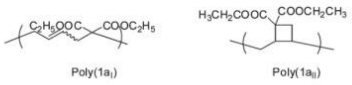

Scheme 7 Expected polymer structures for monomer (**1a**).

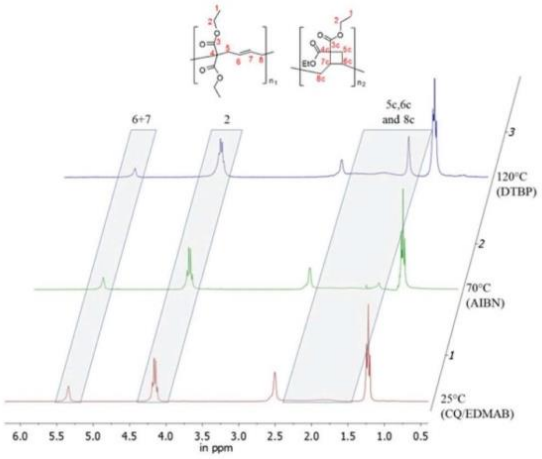

Fig. 5 Overlay of three ^{1}H-NMRs of poly(**1a**) (solvent $CDCl_3$, 300 MHz), polymerized by (1) 1 mol% CQ and 2 mol% EDMAB at 25 °C; (2) 1 mol% AIBN at 70 °C; (3) 1 mol% DTBP at 120 °C.

Nevertheless we could not observe a 92% percent ring opened structure (**1a**$_{\mathrm{I}}$) for poly(**1a**), polymerized thermally with AIBN at 70 °C,[3] rather we calculated only 59% of the ring opened structure (Table 1). To determine the amount of the ring opened structure for poly(**1a**) and poly(**2a**) equally, the ^{1}H-NMR integral values of the ethyl ester protons (proton signal 2 within Fig. 4) have been normalized to a value of four, as these exhibit an analogous chemical shift for the ring opened and the cyclobutane units. Thereby the total proton values were congruent to the expected one (16 protons for poly(**1a**) and 18 for poly(**2a**)). The ratio of the olefinic protons (signal 6 + 7 in Fig. 5) to the expected protons (for 100% ring opening) distinguished directly the amount of the ring opened structure.

A reduced amount of cyclobutane-containing units **1a**$_{\mathrm{II}}$ (Scheme 7) for poly(**1a**) and **2a**$_{\mathrm{III}}$ and **2a**$_{\mathrm{IV}}$ (Scheme 9) for poly (**2a**) could be observed, as the temperature for the polymerization was reduced to room temperature for photopolymerizations (Table 1). This is in accordance with the literature[3,4] in which the cyclobutane units increased as the polymerization temperature of the thermal polymerization increased.

From ^{1}H-NMR data, it was also evident that the presence of the onium salt DPIHFP and the reaction time did influence the ring opened structure of the polymers **1a** and **2a** (Table 1). Naturally with rising reaction time, viscosity as well as conversion increased leading to increased amounts of cyclobutane-containing units (entries 1 and 7; Table 1). The increase in cyclobutane units with increasing conversion, as a matter of increasing melt viscosity was also evident on addition of the onium salt DPIHFP (*i.e.* use of the ternary initiator system). Using a binary initiator system, the conversions of **1a** and **2a** were very low and unlike ternary initiator systems with DPIHFP, no glass-like state was observed by equivalent exposure times (please compare entries 7 with 8 and 9 with 10 in Table 1) giving less cyclobutane units. The cyclobutane units were formed by the addition of a newly formed radical during propagation to the double bond in the polymer main chain. It is a competitive reaction with the reaction of the ring-opened propagating radical with a new VCP monomer. With an increase in reaction viscosity and prolonged reaction time the addition of the ring-opened radical at the double bond of the same molecule giving cyclobutane units became more probable.

The effect of temperature on volume shrinkage has been mentioned in various publications,[25–27] usually as a matter of thermal curing effects and changes in the rates of polymerization. Nevertheless, by comparison of the volume shrinkages of poly(**1a**) and (**2a**) polymerized thermally by AIBN at 70 °C[3] with the volume shrinkages of those polymerized by photopolymerization, the effect of volume shrinkage could not be only explained by curing effects or changed rates in polymerization. Rather the polymerization behavior, and much more, the percentage of the ring opened polymer structure (Table 1) are relevant to the volume shrinkage, as the volume shrinkage of poly(**1a**) and poly(**2a**) is disproportionately reduced, compared to the effect of curing and changed rates of polymerizations for methylmethacrylate (MMA) and styrene (St) (Fig. 6).

As mentioned in the Experimental part the synthesized monomer **2a**, other than mentioned by Sanda *et al.*,[19] consists of a constitution isomer of around 80 : 20 (Fig. 1). Nevertheless, it was exhibited that the existence of the constitution isomer did not influence the polymer structure overall, as head and tail conjunctions results in nearly the same polymer structure (Scheme 8).

In addition the main structure of poly(**2a**) was concluded to be chiefly composed of 1,5-ring-opened units, with lower ratios of cyclobutane units compared to polymer **1a** (Table 1). Sanda *et al.*[19] examined intensely through ^{13}C-NMR spectroscopy, that within the polymer structure of poly(**2a**) a *cis* and a *trans* unit were assigned, which could be confirmed, as we observed within two-dimensional NOESY measurements

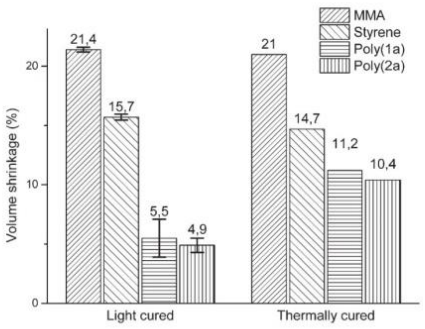

Fig. 6 Comparison of volume shrinkages of MMA, St, poly(**1a**) and poly-(**2a**) dependent on the polymerization method (light curing at 25 °C with CQ and EDMAB as initiators; thermal curing with AIBN at 70 °C.[3,19] The volume shrinkage of the light cured samples was adjusted to complete monomer conversion, by determination of the polymerization yield by ^{1}H-NMR (Fig. S18†).

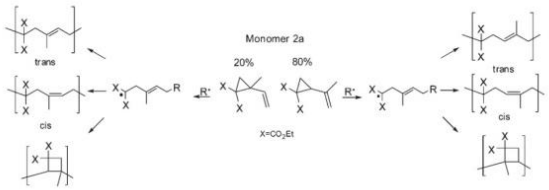

Scheme 8 Schematic description of the expected polymer structures for monomer (**2a**).

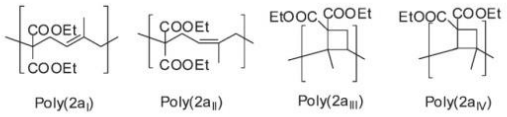

Scheme 9 Proved polymer structures for monomer (**2a**).

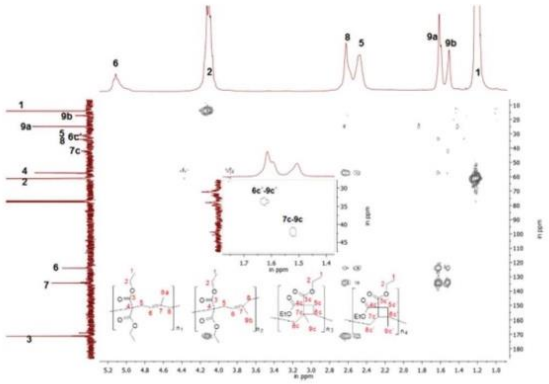

Fig. 7 2D-HMBC NMR of poly(**2a**) (solvent $CDCl_3$, 300 MHz), (polymerization conditions: 1 mol% CQ; 2 mol% EDMAB, 2 mol% DPIHFP), inclusive an expansion to verify the correlation between 6c′–9c′ and 7c-9c.

only cross peaks for 9a-5 (*trans* isomer), whereas the *cis* configuration was proved by the absence of an NOE correlation (Fig. S17†).

Furthermore the constitution isomer of the methyl substituted monomer (**2a**) seemed to be promising for the verification of the cyclobutane unit, as this unit could not be explicitly proved currently, because of the difficult characterization, as only a broad signal for poly(**1a**) was observed, that could not be assigned to any protons. Therefore previously the cyclobutane unit was assumed with the missing of the olefinic protons and the respectively higher volume shrinkage.[3,19] In contrast to the polymer structure of poly(**1a**) for poly(**2a**) further cross correlations for the methyl group (9a–c′) of the substructure $\mathbf{2a}_{III}$ and $\mathbf{2a}_{IV}$ (Scheme 9) should be verifiable during a two-dimensional HMBC measurement (Fig. 7). Thus a unique interpretation of the polymer signals has been iterated by ^{1}H-, ^{13}C-, HSQC-, NOESY (all shown in the ESI†), HMBC-NMR (Fig. 7) measurements.

Indeed from the HMBC spectra for poly(**2a**) further correlation signals of the methyl groups were present that are assumed to belong to the correlation signals of 6c′–9c′ ($\mathbf{2a}_{III}$) and 7c–9c ($\mathbf{2a}_{IV}$) of the cyclobutane unit, whereby to our knowledge, this cyclobutane unit has been detected directly for 1,1-bis(ethoxycarbonyl)-2-vinylcyclopropane for the first time.

4. Conclusions

In summary, 1,1-disubstituted 2-vinylcyclopropanes undergo radical photopolymerization with a reduced formation of cyclobutane units and increased 1,5-type ring-opening compared to thermally polymerized specimens. The reduced amount of cyclobutane units was proportional to the volume shrinkage. In addition, we varied the photopolymerization conditions to observe the impact on reaction kinetics. The addition of the onium salt DPIHFP as a ternary initiator to the radical initiator system drastically reduced the curing time for bulk polymerizations. This makes VCPs attractive as a monomer component in low shrinking dental adhesives or composites.

Acknowledgements

We thank the German Federal Ministry for Economic Affairs and Energy (BMWi) for financial support. Dr. A. Bublewitz and Dr. A. Theis are thanked for useful discussions during the work.

Notes and references

1 N. Moszner, T. Völkel and V. Rheinberger, *Macromol. Chem. Phys.*, 1996, **197**, 621–631.
2 N. Moszner, F. Zeuner, U. K. Fischer, V. Rheinberger, A. d. Meijere and V. Bagutski, *Macromol. Rapid Commun.*, 2003, **24**, 269–273.
3 F. Sanda, T. Takata and T. Endo, *Macromolecules*, 1993, **26**, 1818–1824.
4 N. Moszner and U. Salz, *Prog. Polym. Sci.*, 2001, **26**, 535–576.
5 T. E. F. Sanda, *J. Polym. Sci., Part A: Polym. Chem*, 2001, **39**, 265–276.
6 R. G. Fayter, *US*, 4321406, 1980.
7 N. Moszner, T. Völkel, U. K. Fischer and V. Rheinberger, *Macromol. Chem. Phys.*, 1999, **200**, 2173–2187.
8 J. Pavlinec and N. Moszner, *J. Appl. Polym. Sci.*, 2003, **89**, 579–588.
9 F. Sanda, T. Takata and T. Endo, *Macromolecules*, 1994, **27**, 3982–3985.
10 N. Moszner and U. Salz, *Macromol. Mater. Eng.*, 2007, **292**, 245–271.
11 J. H. W. L. J. V. Crivello, *J. Polym. Sci., Part A: Polym. Chem.*, 1999, **37**, 4241.
12 H.-J. Timpe, *Pure Appl. Chem.*, 1988, **60**, 1033.

13 J. V. Crivello and J. H. W. Lam, *Macromolecules*, 1977, **10**, 1307–1315.
14 M. S. J. V. Crivello, *J. Polym. Sci., Part A: Polym. Chem*, 2001, **39**, 343.
15 J. G. Kloosterboer and G. F. C. M. Lijten, *Polymer*, 1990, **31**, 95–101.
16 H. J. Timpe, S. Ulrich, C. Decker and J. P. Fouassier, *Macromolecules*, 1993, **26**, 4560–4566.
17 F. A. Ogliari, C. Ely, C. L. Petzhold, F. F. Demarco and E. Piva, *J. Dent.*, 2007, **35**, 583–587.
18 M. L. Gómez, V. Avila, H. A. Montejano and C. M. Previtali, *Polymer*, 2003, **44**, 2875–2881.
19 F. Sanda, T. Takata and T. Endo, *Macromolecules*, 1995, **28**, 1346–1355.
20 O. J. Sweeting and J. R. Johnson, *J. Am. Chem. Soc.*, 1946, **68**, 1057–1061.
21 T. Endo, M. Watanabe, K. Suga and T. Yokozawa, *J. Polym. Sci., Part A: Polym. Chem.*, 1987, **25**, 3039–3048.
22 K. Sirovatka Padon and A. B. Scranton, *J. Polym. Sci., Part A: Polym. Chem.*, 2000, **38**, 2057–2066.
23 W. D. Cook, *Polymer*, 1992, **33**, 600–609.
24 J. Pączkowski and D. C. Neckers, *Photoinduced Electron Transfer Initiating Systems for Free-Radical Polymerization, Electron Transfer in Chemistry* ed. V. Balzani, Wiley-VCH Verlag GmbH, Weinheim, Germany, 2001.
25 K. S. Anseth, C. N. Bowman and N. A. Peppas, *J. Polym. Sci., Part A: Polym. Chem.*, 1994, **32**, 139–147.
26 B. Lu, P. Xiao, M. Sun and J. Nie, *J. Appl. Polym. Sci.*, 2007, **104**, 1126–1130.
27 C.-M. Chung, J.-G. Kim, M.-S. Kim, K.-M. Kim and K.-N. Kim, *Dent. Mater.*, 2002, **18**, 174–178.

Supplementary Information

Low volume shrinkage polymers by photo Polymerization of 1,1-Bis(ethoxycarbonyl)-2-vinylcyclopropanes

Paul Pineda Contreras, Payal Tyagi ††, Seema Agarwal*

††Paul Pineda Contreras and Payal Tyagi have contributed equally to the experimental part.

P. Pineda Contreras, Dr. P. Tyagi, Prof. S. Agarwal
Makromolekulare Chemie II
Gebäude NWII, Universität Bayreuth
Universitätsstrasse 30
95440 Bayreuth
*E-mail: agarwal@uni-bayreuth.de

Monomer Synthesis

Scheme 1

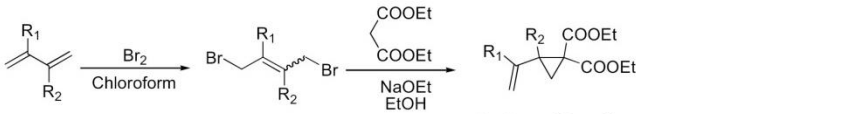

1, R_1 and R_2 = H
2, R_1 = CH_3 and R_2 = H
3, R_1 = CH_3 and R_2 = CH_3

1a, R_1 and R_2 = H
2a, R_1 = CH_3 and R_2 = H or R_1 = H and R_2 = CH_3
3a, R_1 = CH_3 and R_2 = CH_3

Synthesis of (*E*)-1,4-dibromo-2-methylbut-2-ene (2)

The reaction was carried out in a flame dried 250 mL round bottom flask, 35 mL (23.8 g, 349.3 mmol) of isoprene was added along with 150 mL of chloroform ($CHCl_3$). To this solution 17.9 mL (55.84g, 349.3 mmol) bromine dissolved in $CHCl_3$ was added drop wise through a dropping funnel at a temperature of -10 °C. After complete addition of bromine, reaction mixture was stirred overnight. After the reaction, the solvent was evaporated by rotary evaporator and the crude product was recovered in a vacuum fractionating column which was distilled at a pressure of 0.04 mbar and 60 °C. The synthesized *cis-trans* isomer was represented by a 30:70 distribution, confirmed by ^{1}H-NMR and GC-FID.

Yield 39 g (49%): ^{1}H-NMR (300 MHz, $CDCl_3$, δ): 5.90 (t, ^{3}J = 8.4 Hz, *trans*-CH_{sp2}, 1H (70 %)), 5.71 (t, ^{3}J = 8.4 Hz, *cis*-CH_{sp2}, 1H (30 %)), 4.10-3.95 (m, CH_2, 4H), 1.92 (s, cis-CH_3, 3H (30 %)), 1.87 (s, trans-CH_3, 3H (70 %)). ^{13}C-NMR (75 MHz, $CDCl_3$, δ): 138.30 (C_{sp2}, *cis*-C), 138.25 (C_{sp2}, *trans*-C), 125.97 (C_{sp2}, *cis*-C), 125.71 (C_{sp2}, *trans*-C), 39.18 (CH_2, *trans*-C), 29.30 (CH_2, *cis*-C), 27.50 (CH_2, *trans*-C) 26.53 (CH_2, *cis*-C), 22.07 (CH_3, *cis*-C), 14.65 (CH_3, *trans*-C).

Synthesis of trans-1,4-dibrom-*2,3*-dimethyl-but-2-en (3)

18.88 g (0.23 mol) of 2,3-dimethylbutadiene was dissolved in 100 mL $CHCl_3$ and the mixture was cooled to -20 °C using ice-salt mixture. 11.77 mL of bromine (36.73 g, 0.23 mol) was dissolved in 50 mL $CHCl_3$ and dropped into the flask over a period of 2 hour with vigorous stirring in a counter current of argon. After complete addition of the bromine, the solution was stirred for an additional 1 hr. at -10 °C and 0.5h at 0 °C. The solvent was removed by vacuum. Residual liquid was kept in the refrigerator overnight. Lower temperature induced crystallization of the product and the crystals were filtered and washed with cold hexane. Residual filtrate was again concentrated and kept in the refrigerator. The step was repeated till no further crystals were observed on cooling. Yield 28g (50%): ^{1}H-NMR (300 MHz, $CDCl_3$, δ): 3.99 (s, 4H, CH_2), 1.88 (s, 6H, CH_3). ^{13}C-NMR (75 MHz, $CDCl_3$, δ): 131.92 (C_{sp2}), 35.01 (CH_2), 17.19 (CH_3).

Diethyl 2-vinylcyclopropane-1,1-dicarboxylate (1a)

A sodium ethoxide solution was prepared by dissolving sodium in dry ethanol. The sodium was purified prior by melting it up in kerosene. 2.2 eq. of a the sodium ethoxide solution were added drop wise at 0°C to a solution of 1.0 eq. of 1,4-dibromo-2-butene and 1.0 eq. of diethyl malonate in a counter current of argon. After the addition, the reaction mixture was stirred overnight and then heated for 1 h at 65 °C. The resulting mass was filtered and the filtrate was charged to a rotary evaporator to remove the solvent. The residue was extracted with diethyl ether and water. The organic layer was washed with brine and dried over magnesium sulphate. The raw product was distilled under reduced pressure. bp 60-64 °C/0.04 bar; yield (82%):

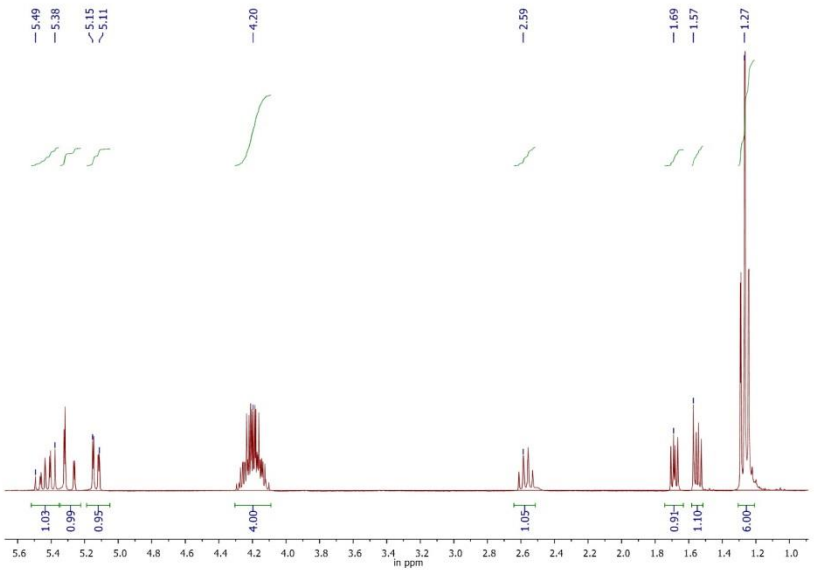

Figure S1: ^{1}H NMR of diethyl 2-vinylcyclopropane-1,1-dicarboxylate (1a) ($CDCl_3$, 300 MHz).

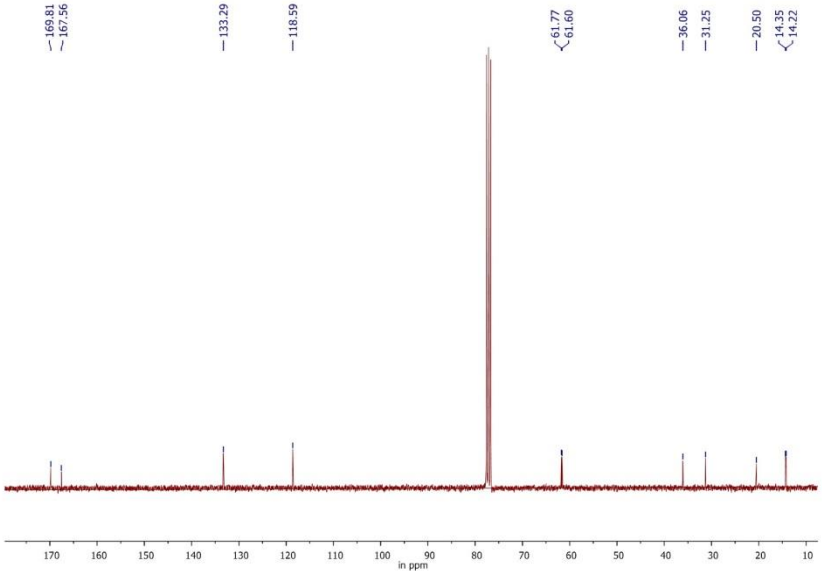

Figure S2: ^{13}C NMR of diethyl 2-vinylcyclopropane-1,1-dicarboxylate (1a) ($CDCl_3$, 75 MHz).

^{1}H-NMR (300 MHz, $CDCl_3$, δ): 5.43-5.23 (m, 1 H), 5.29-5.23 (dd, *J* = 9.45 Hz, 1.95 Hz, 1H), 5.09-5.03 (dd, *J* = 5.85 Hz, 2.1 Hz, 1H), 4.29-4.08 (m, 4H), 2.59-2.51 (q, *J* = 8.7 Hz, 1H), 1.68-1.64 (dd, *J* = 6.3 Hz, 5.1 Hz, 1H), 1.53-1.48 (dd, *J* = 6.9 Hz, 4.8 Hz, 1 H), 1.28-1.21 (m, 6 H, CH_3, H1). ^{13}C-NMR (75 MHz, $CDCl_3$, δ): 169.52 (C=O), 167.27 (C=O), 133.08 (C_{sp2}), 118.27 (C_{sp2}), 61.47 (OCH_2), 61.30 (OCH_2), 35.83 ($C_{quart.}$) 30.94 (CH,), 20.20 (CH_2), 14.08 (CH_3), 13.96 (CH_3).

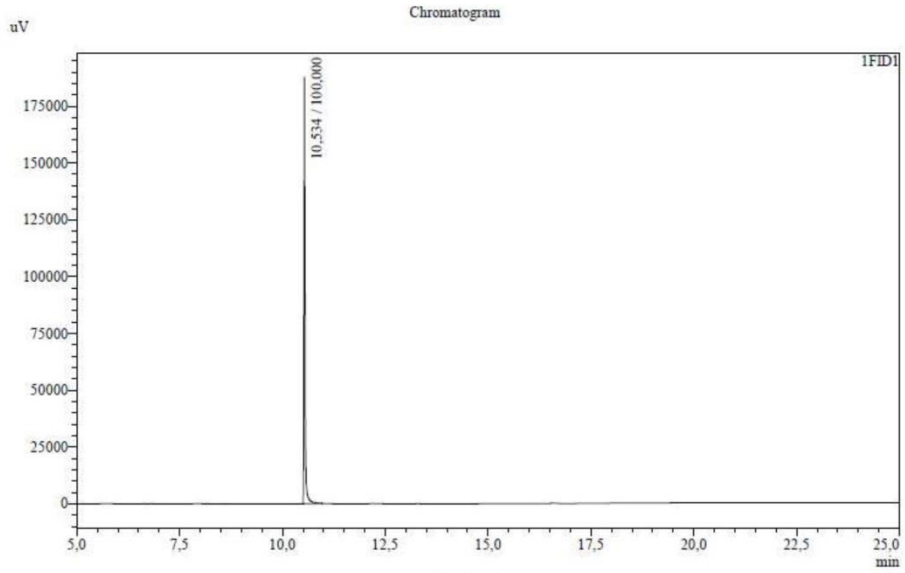

Peak Table

FID1

Peak#	Ret. Time	Area%	Area	Height
1	10.534	100.000	362940	187874
Total		100.000	362940	187874

Figure S3: GC-FID chromatogram of diethyl 2-vinylcyclopropane-1,1-dicarboxylate (1a) (0.5 µg/mL in acetone, injection volume 1.0 µl, N_2 as carrier gas, split ratio 50, initial temperature 50 °C (hold for 2min) and temperature gradient of 15 C/min up to 300 °C).

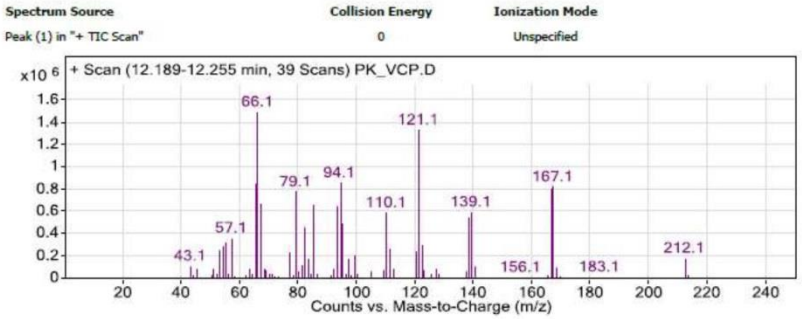

Figure S4: Mass spectrum (Quadropol MS **Agilent 5977A MSD:** EI with 1000 eV) of GC-MS detected diethyl 2-vinylcyclopropane-1,1-dicarboxylate (1a).

Diethyl 2-(prop-1-en-2-yl)cyclopropane-1,1-dicarboxylate and diethyl 2-methyl-2-vinylcyclopropane-1,1-dicarboxylate (2a)

The procedure is analog to monomer (1a) with the difference of using 1,4-dibromo-2-methylbut-2-ene (2) instead of 1,4-dibromo-2-butene. bp 75 °C/0.04 bar; yield (42%).

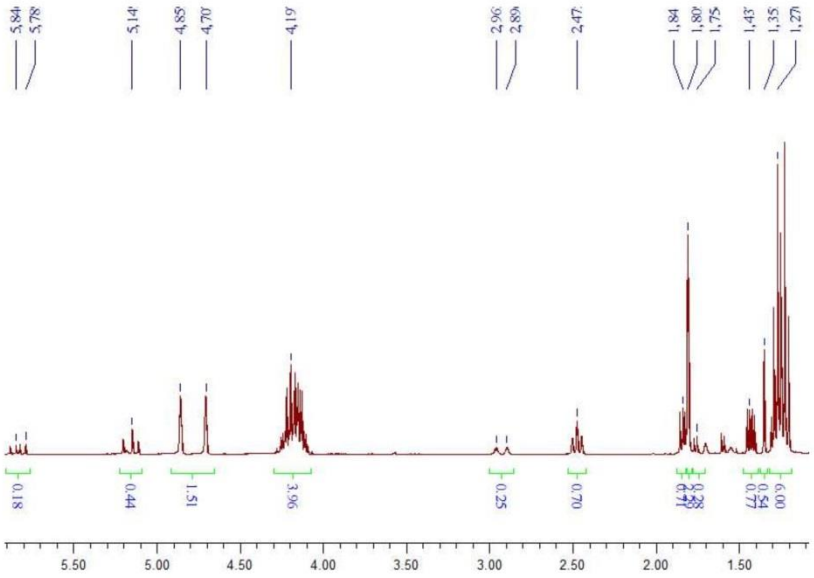

Figure S5: ^{1}H NMR of diethyl 2-(prop-1-en-2-yl)cyclopropane-1,1-dicarboxylate and diethyl 2-methyl-2-vinylcyclopropane-1,1-dicarboxylate (2a) ($CDCl_3$, 300 MHz).

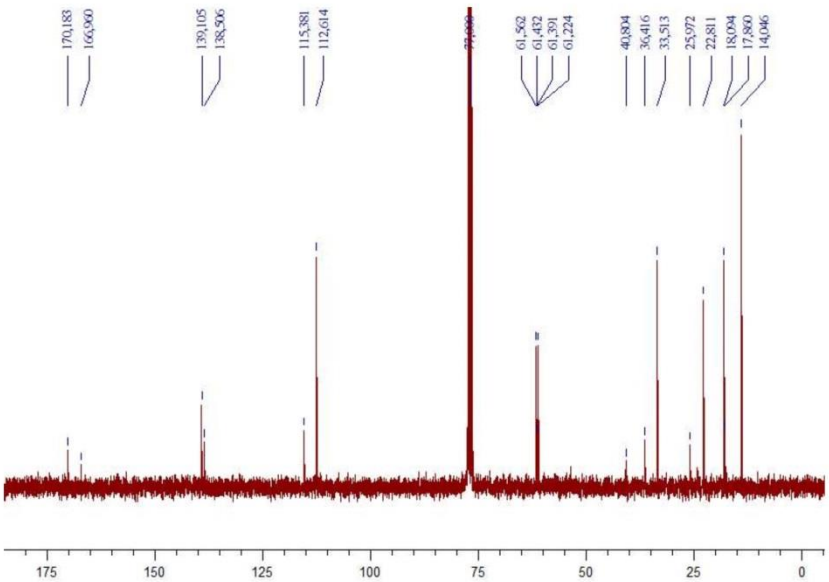

Figure S6: ^{13}C-NMR of diethyl 2-(prop-1-en-2-yl)cyclopropane-1,1-dicarboxylate and diethyl 2-methyl-2-vinylcyclopropane-1,1-dicarboxylate (2a) ($CDCl_3$, 75 MHz).

^{1}H-NMR (300 MHz, $CDCl_3$, δ): 5.85-5.77 (dd, J = 13.8 Hz, 10.8 Hz, 1H (25 %)), 5.116 (m, 2H (25 %)), 4.7-4.83 (d, 2H (75 %)), 4.06-4.25 (m, 4H,), 2.86-2.94 (m, 1H), 2.42-2.47 (t, J = 8.4 Hz, 1H), 1.83-1.80 (m, 1H (75 %)), 1.78 (s, 3H (75 %)), 1.75 (m, 1 H (25 %)), 1.34-1.42 (dd, J = 7.05 Hz, 5.01 Hz, 1 H (75 %)), 1.32 (s, 3H (25 %)), 1.17-1.27 (m, 6H). ^{13}C-NMR (75 MHz, $CDCl_3$, δ): 170.18 (C=O, (75 %)), 16.96 (C=O, (25 %)), 139.11 (C_{sp2}), 138.51 (C_{sp2}), 115.38 (C_{sp2}), 112.61 (C_{sp2}), 61.56 (OCH_2, (75 %)), 61.43 (OCH_2, (25 %)), 61.39 (OCH_2, (25 %), 61.22 (OCH_2, (75 %), 40.81 ($C_{quart.}$, (25 %)), 36.42 ($C_{quart.}$, (75 %)), 33.51 (CH), 25.97 (CHH), 22.81 (CH_3), 18.09 (CHH), 17.86 (CH_3), 14.05 (CH_3).

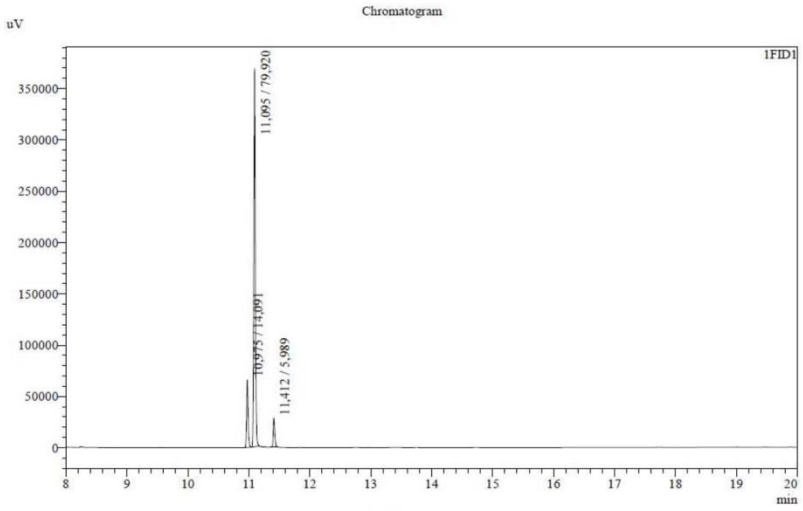

Peak Table

FID1

Peak#	Ret. Time	Area%	Area	Height
1	10,975	14,091	113551	65967
2	11,095	79,920	644005	368496
3	11,412	5,989	48257	27379
Total		100,000	805813	461841

Figure S7: GC-FID chromatogram of diethyl 2-(prop-1-en-2-yl)cyclopropane-1,1-dicarboxylate and diethyl 2-methyl-2-vinylcyclopropane-1,1-dicarboxylate (2a) (0.5 µg/mL in acetone, injection volume 1.0 µl, N_2 as carrier gas, split ratio 50, initial temperature 50 °C (hold for 2min) and temperature gradient of 15 C/min up to 300 °C). The appearance of three chromatogram peaks relies on the stereo isomeric separation of the diethyl 2-methyl-2-vinylcyclopropane-1,1-dicarboxylate.

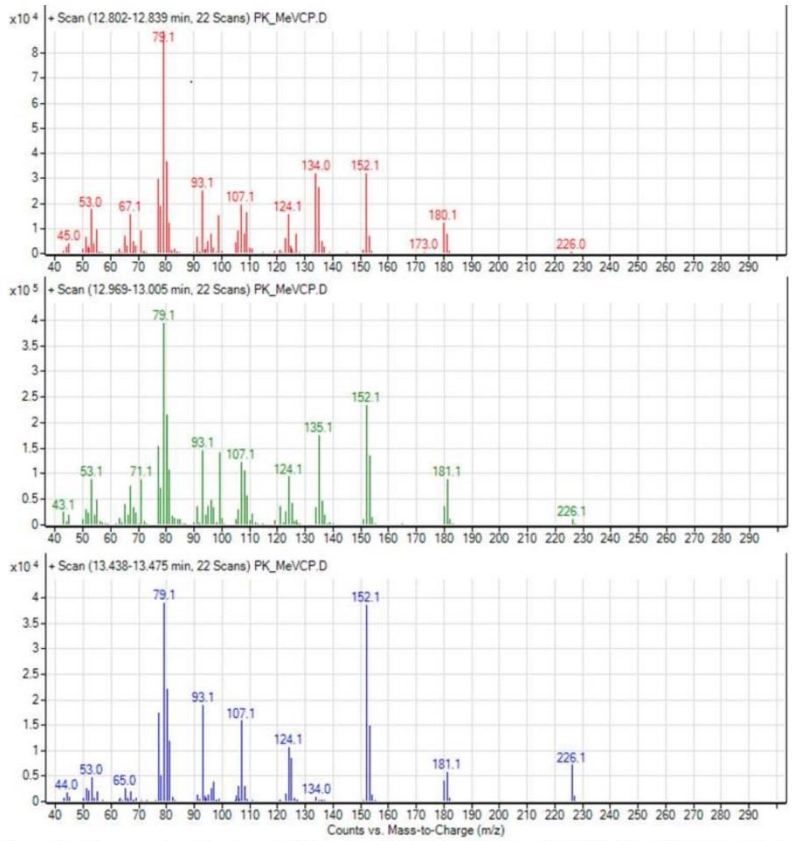

Figure S8: Mass spectra (Quadropol MS **Agilent 5977A MSD:** EI with 1000 eV) of GC-MS detected diethyl 2-(prop-1-en-2-yl)cyclopropane-1,1-dicarboxylate and diethyl 2-methyl-2-vinylcyclopropane-1,1-dicarboxylate (2a). The appearance of the three chromatogram peaks within the GC-FID and GC-MS relies on the stereo isomeric separation of the diethyl 2-methyl-2-vinylcyclopropane-1,1-dicarboxylate, as all three mass spectra are almost identical. .

Diethyl 2-methyl-2-(prop-1-en-2-yl)cyclopropane-1,1-dicarboxylate (3a)

The procedure is analog to monomer (1a) with the difference of using *trans*-1,4-dibrom-*2,3*-dimethyl-but-2-en (3) instead of 1,4-dibromo-2-butene. bp 75 °C/0.04 bar; yield (41%)

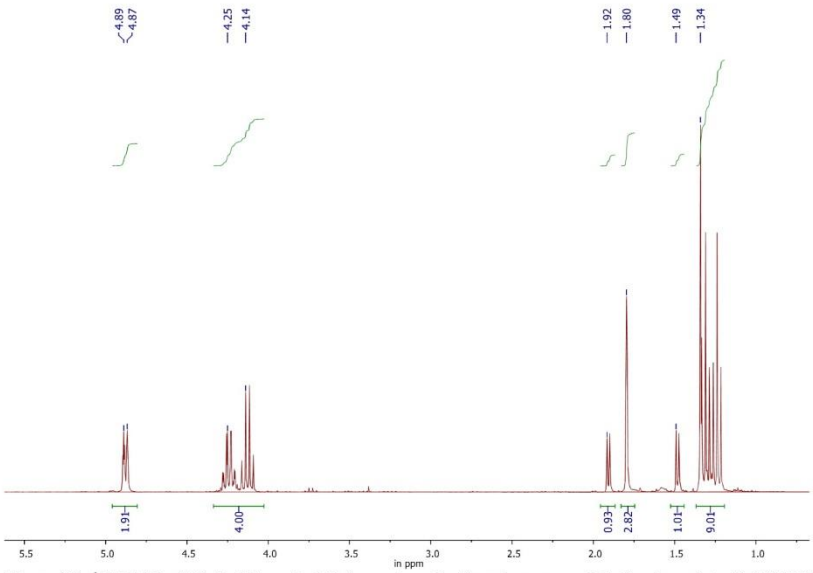

Figure S9: ^{1}H NMR of diethyl 2-methyl-2-(prop-1-en-2-yl)cyclopropane-1,1-dicarboxylate (3a) ($CDCl_3$, 300 MHz).

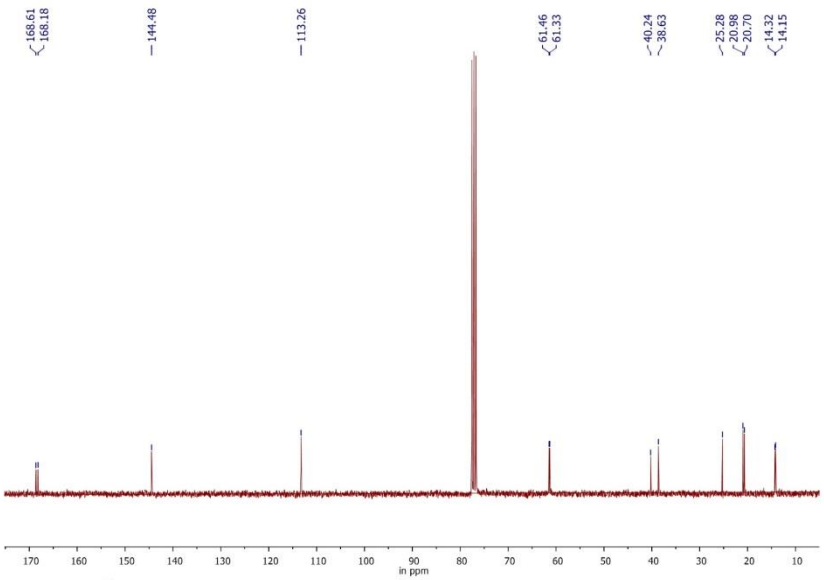

Figure S10: ^{13}C-NMR of diethyl 2-methyl-2-(prop-1-en-2-yl)cyclopropane-1,1-dicarboxylate (3a) ($CDCl_3$, 75 MHz).

^{1}H-NMR (300 MHz, $CDCl_3$, δ): 4.87 (d, 2J = 5.4 Hz, 2H), 4.25-4.05 (m, 4H), 1.88 (d, 2J = 5.0 Hz,1H), 1.77 (s, 3 H), 1.45 (d, 2J = 5.0Hz, 1H), 1.32 (s, 3H), 1.31-1.20 (m, 6H). ^{13}C-NMR (75 MHz, $CDCl_3$, δ): 168.45 (C=O), 168.01(C=O), 144.38 (C_{sp2}), 113.10 (C_{sp2}), 61.72 (OCH_2), 61.15 (OCH_2), 40.15 ($C_{quart.}$), 38.46 ($C_{quart.}$), 25.10 (CHH), 20.86 (CH_3), 20.51 (CH_3), 14.15 (CH_3), 13.98 (CH_3).

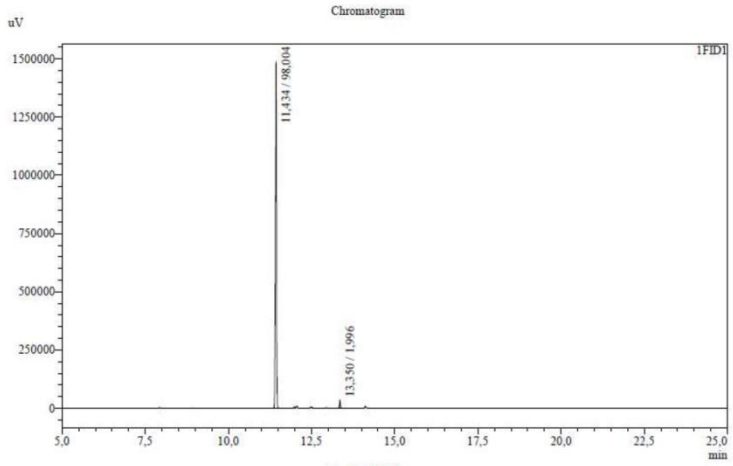

Peak Table

FID1

Peak#	Ret. Time	Area%	Area	Height
1	11.434	98.004	3300365	1480692
2	13.350	1.996	67210	34840
Total		100.000	3367576	1515532

Figure S11: GC-FID chromatogram of diethyl 2-methyl-2-(prop-1-en-2-yl)cyclopropane-1,1-dicarboxylate (3a) (0.5 µg/mL in acetone, injection volume 1.0 µl, N2 as carrier gas, split ratio 50, initial temperature 50 °C (hold for 2min) and temperature gradient of 15 C/min up to 300 °C).

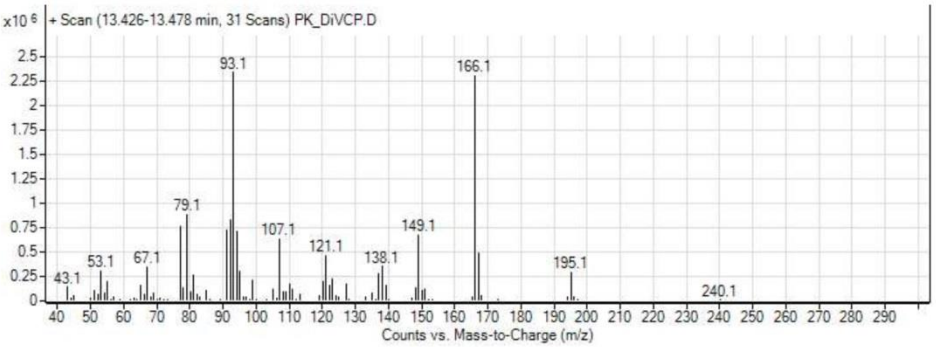

Figure S12: Mass spectrum (Quadropol MS **Agilent 5977A MSD:** EI with 1000 eV) of GC-MS detected diethyl 2-methyl-2-(prop-1-en-2-yl)cyclopropane-1,1-dicarboxylate (3a).

Structure of Polymer 1a

It has been described by Sanda that a 1,5-type ring-opened polymer unit is primarily formed in the polymerization of 1,l-disubstituted 2-vinylcyclopropanes (1).[3;29] The structure of the polymers (poly(1a) and poly(2a)) was examined by ^{1}H-NMR. In the ^{1}H-NMR spectrum of poly(1a) (Figure S7), there was a smooth signal at 1.5-2.5 ppm. According to the reported literature that signal is caused by the formation of a cyclobutane containing unit ($1a_{II}$) which has no olefinic protons. According to this the ratio of olefinic proton is smaller than that for polymers which consists only of a 1,5-type ring-opened unit($1a_I$).

Scheme 2

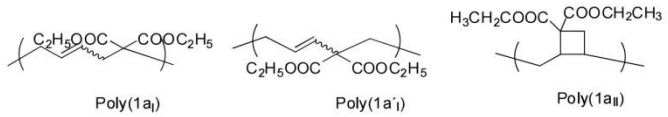

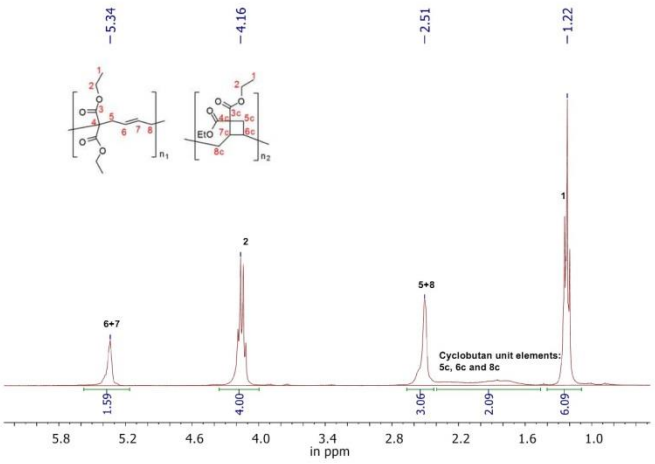

Figure S13: ^{1}H NMR of Poly(1a) (solvent $CDCl_3$, 300 MHz), (Polymerization conditions: 1 mol % CQ; 2 mol % EDMAB, 2 mol % DPIHFP).

Structure of Polymer 2a

As mentioned in the experimental part the synthesized monomer 2a consists of a constitution isomer of around 80:20 (Figure S5-S8). Nevertheless the existence of the constitution isomer did not influence the polymer structure overall, as head and tail conjunctions results in nearly the same polymer structure (Scheme S3).

Scheme S3: Schematic description of the expected polymer structures for monomer (2a).

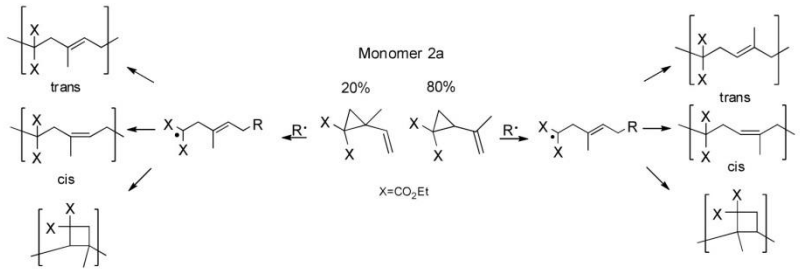

Within the polymer structure of poly(2a) a cis and trans unit appears, which could be confirmed within the two-dimensional NOESY measurement, as only cross peaks for 9a-5 (trans isomer) could be detected, whereas the cis configuration was proved by the absence of an NOE correlation (Figure S17).

Scheme S4: Proved polymer structures for monomer(2a).

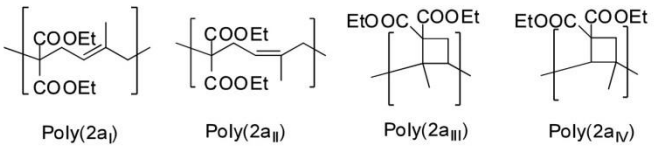

Furthermore the polymer structure was verified by a unique interpretation of the polymer signals by ^{1}H-, ^{13}C-, HSQC-, NOESY, HMBC-NMR measurements (Figures S14-S17).

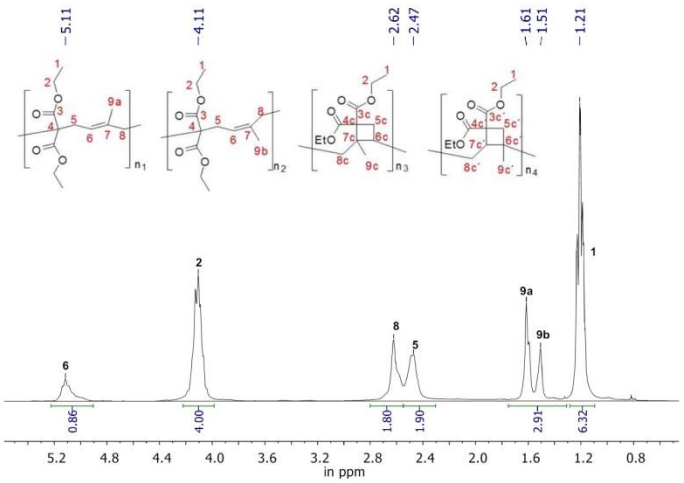

Figure S14: ^{1}H NMR of Poly(2a) (solvent $CDCl_3$, 300 MHz), (polymerization conditions: 1 mol % CQ; 2 mol % EDMAB, 2 mol % DPIHFP).

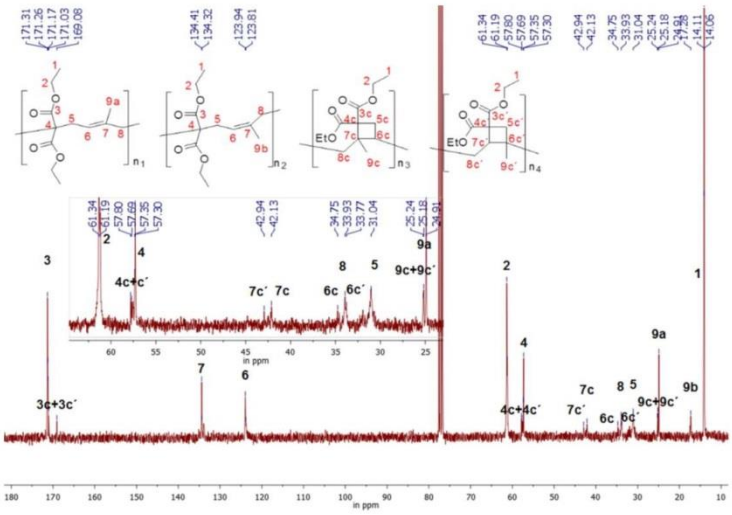

Figure S15: ^{13}C NMR of Poly(2a) (solvent $CDCl_3$, 300 MHz), (polymerization conditions: 1 mol % CQ; 2 mol % EDMAB, 2 mol % DPIHFP), inclusive an expansion from ^{13}C NMR between 70-20 ppm.

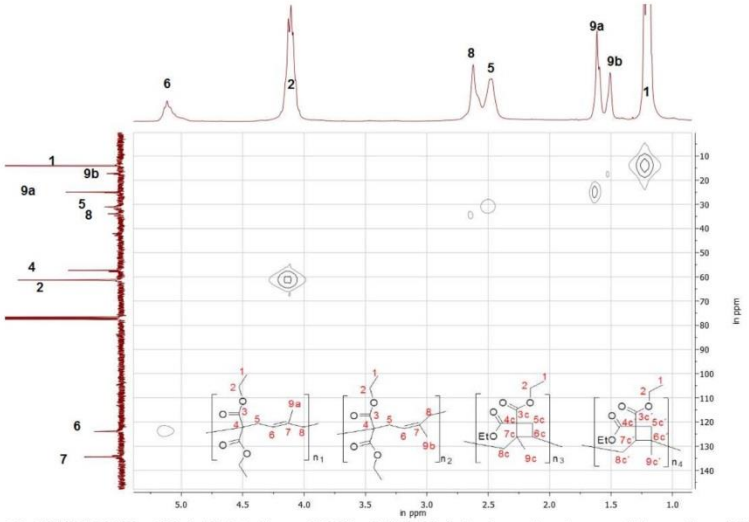

Figure S16: 2D-HSQC NMR of Poly(2a) (solvent $CDCl_3$, 300 MHz), (polymerization conditions: 1 mol % CQ; 2 mol % EDMAB, 2 mol % DPIHFP).

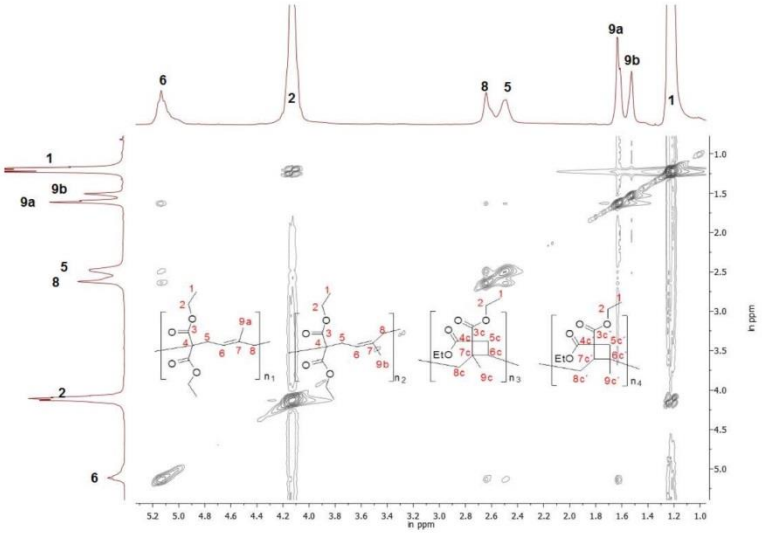

Figure S17: 2D-NOESY NMR of Poly(2a) (solvent $CDCl_3$, 300 MHz), (polymerization conditions: 1 mol % CQ; 2 mol % EDMAB, 2 mol % DPIHFP).

Adjustments of the volume shrinkage values

The polymerization shrinkage was calculated from the difference in density of the monomer to the formed polymers. The densities of the monomers were measured by a 1mL pycnometer, the densities of the polymers by water displacement of 400mg cured samples. The volume shrinkage of the light cured samples was adjusted to a complete monomer conversion by determination the polymerization yield by ^{1}H-NMR. To determine the conversion the ^{1}H-NMR integral values of the ethyl ester protons of the monomer and polymer (H2 Figure S18) have been normalized to a value of four, as these exhibit for the monomer and polymer in an analog chemical shift. The content of monomer was calculated by the ratio of the monomer signals H5, H5´ and H8 (Figure S18) to their theoretical once. The measured volume shrinkage was then devided by the yield of polymerization, to obtain the adjusted value.

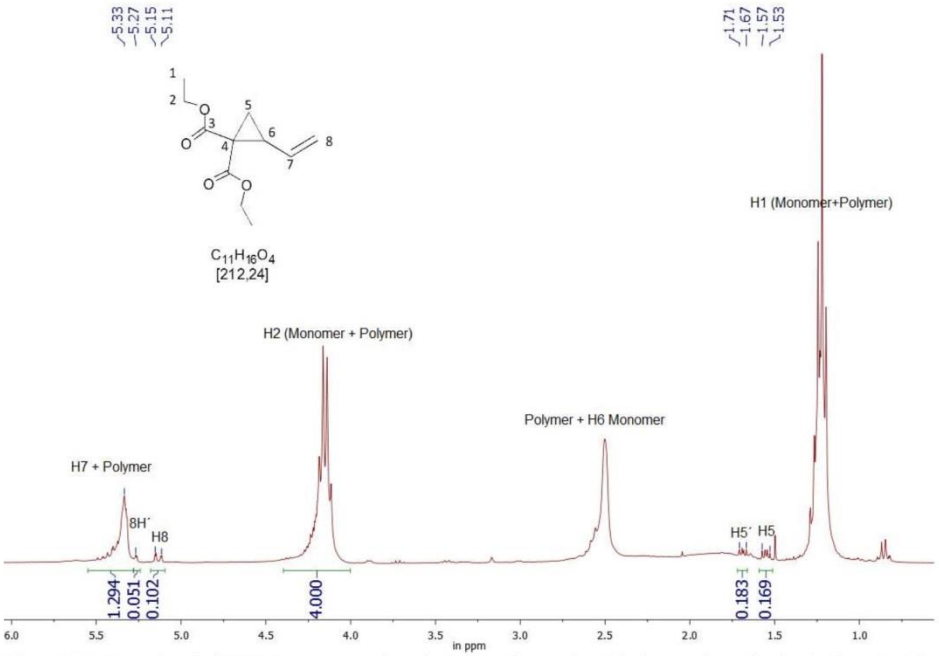

Figure S18: Example of a ^{1}H NMR spectrum of a poly(1a) specimen after 48h photo polymerization (solvent $CDCl_3$, 300 MHz), without precipitating the polymer to calculate the monomer conversion for adjustment of the volume shrinkage value.

4.2 Renaissance for low shrinking resins: all-in-one solution by bi-functional vinylcyclopropane-amides

Paul Pineda Contreras,[a] Christian Kuttner,[b] Andreas Fery,[b] Ullrich Stahlschmidt,[c] Valérie Jérôme,[c] Ruth Freitag[c] and Seema Agarwal*[a], *Chemical Communications*, **2015**, *51*, 11899-11902.

[a]Makromolekulare Chemie II, Universität Bayreuth, Universitätsstraße 30, 95440 Bayreuth, Germany.

[b]Physical Chemistry II, Universität Bayreuth, Universitätsstrasse 30, 95440 Bayreuth, Germany.

[c]Process Biotechnology, Universität Bayreuth, Universitätsstrasse 30, 95440 Bayreuth, Germany.

*Corresponding Author: E-mail: agarwal@uni-bayreuth.de; Fax: +49-921-553393.

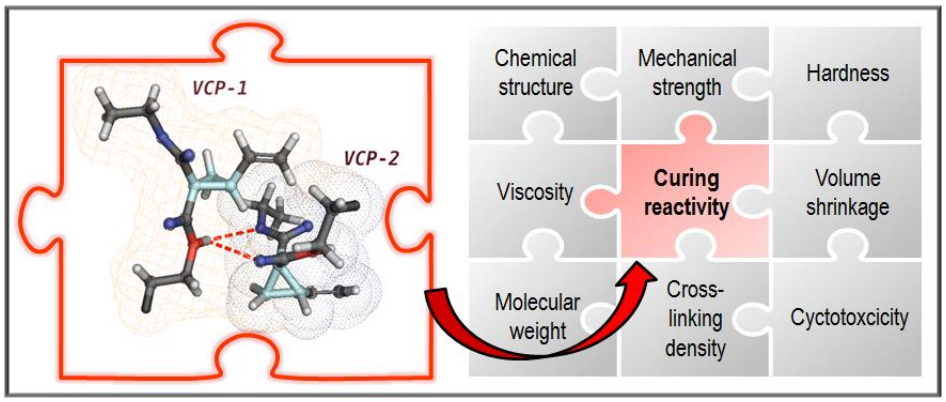

ChemComm

COMMUNICATION

View Article Online
View Journal | View Issue

Renaissance for low shrinking resins: all-in-one solution by bi-functional vinylcyclopropane-amides†

Paul Pineda Contreras,[a] Christian Kuttner,[b] Andreas Fery,[b] Ullrich Stahlschmidt,[c] Valérie Jérôme,[c] Ruth Freitag[c] and Seema Agarwal*[a]

Cite this: *Chem. Commun.*, 2015, **51**, 11899

Received 11th May 2015,
Accepted 16th June 2015

DOI: 10.1039/c5cc03901k

www.rsc.org/chemcomm

A low volume shrinking vinylcyclopropane (VCP) monomer, showing both a high reactivity and a low viscosity, was obtained by applying a sterically hindered and isomeric spacer element, incorporating intermolecular amide hydrogen bonds. The resulting properties locate this VCP system in a pronounced range that so far no other efficient and radical polymerizable resin could enter.

Photo-polymerizable resins with a low volume shrinkage are fundamental for coatings,[1] electronics,[2] microlithography,[3] holographic data storages,[4] advanced composites,[5] and dental applications.[6] In these applications, the final properties of the cross-linked network have to match precise specifications adapted for the final end-use. In general, this precision is achieved by the selection of highly specified resin systems.[7] Thereby, in many cases the fast and selective curing, the solvent-free formulation and the targeted control of curing over a wide temperature, time, and radiation range made in particular the photo-polymerization technique overwhelming.[8] Thus, especially acrylate and methacrylate monomers are favoured in nearly all radically polymerizable resins due to their synthetic ease of access, processability, and chemical variability.[9]

However, the observed volume shrinkage is pronounced and inevitable due to the transition of the intermolecular interactions from van der Waals spheres for monomers to covalent bonds in the cured resins.[10] As a result, a high shrinkage can lead to the reduction in adhesion between the coating layer and the substrate in coating applications, or may cause the formation of contraction gaps between filling and cavity in dental resins, whereby recurrent caries might be the consequence.[11]

So far, many ongoing developments in dimethacrylate monomers could not adequately resolve the remaining issue of high volume shrinkage.[12] Therefore, universally applied resins like bisphenol-A-glycidyl methacrylate (BisGMA) have so far played a pivotal role, as they provided a low volume shrinkage,[13] rapid curing, and superior mechanical properties after curing.[14] Nevertheless, the core of BisGMA resins is based on bisphenol-A (BPA), which has raised health concerns recently in the food packaging industry, consumer plastics, as well in dental materials about its widespread use, thus the exposure limits for BPA are reduced continuously.[15]

A promising resin system that sets a great promise on low volume shrinkage consists of vinylcyclopropane (VCP) derivatives, as the radical photo-polymerization results mainly in 1,5-ring-opened polymer units, whereby the volume shrinkage can significantly be reduced compared to methacrylate resins.[16] However, so far not a single VCP resin could be successfully introduced to any real-world industrial application. Furthermore, due to the low curing kinetics and efficiency, VCPs have lost interest in academics as well.[17]

Herein, the first VCP-amide resin ($VCPMe_3hexAmid$) (Scheme 1) with very fast photo-radical polymerization kinetic, a high monomer conversion in less than 2 min in air, low volume shrinkage, low viscosity, an effective refractive index, and good mechanical properties is reported. We studied in detail the preparation of the

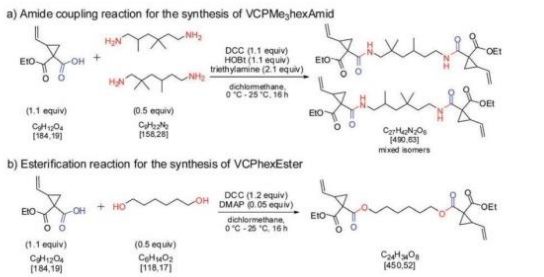

Scheme 1 Preparation of bi-functional VCPs. DCC = *N*,*N*′-dicyclohexylcarbodiimide; DMAP = 4-dimethylaminopyridine; HOBt = benzotriazol-1-ol.

[a] *Macromolecular Chemistry II and Bayreuth Center for Colloids and Interfaces, Universität Bayreuth, Universitätsstrasse 30, 95440 Bayreuth, Germany. E-mail: agarwal@uni-bayreuth.de; Tel: +49-921-553397*
[b] *Physical Chemistry II, Universität Bayreuth, Universitätsstrasse 30, 95440 Bayreuth, Germany*
[c] *Process Biotechnology, Universität Bayreuth, Universitätsstrasse 30, 95440 Bayreuth, Germany*

† Electronic supplementary information (ESI) available: Materials, methods, synthesis, and supplementary characterization. See DOI: 10.1039/c5cc03901k

VCP resin, its enhanced curing behaviour by photo-differential scanning calorimetry (photo-DSC) and dielectric analysis (DEA), its volume shrinkage, viscosity, and cytotoxicity. Furthermore, the change in the optical refractive index during curing by spectroscopic ellipsometry (SE), as well as the mechanical properties and the network structure of the cross-linked network by ^{13}C-CP/MAS (cross polarization/magic angle spinning) solid state NMR spectroscopy were studied to provide a detailed overview of the most relevant resin features.

In order to optimize the reactivity by hydrogen bonding and to prevent any disproportional increase in viscosity a sterically hindered and isomeric amide spacer was used (VCPMe$_3$hexAmid). A VCP-amide monomer, based on a linear C-6 spacer using simple hexamethylenediamine, provided slow crystallization and made itself unsuitable for any comparable detailed bulk polymerization study.

The VCPMe$_3$hexAmid was synthesized in high purity and yield according to Scheme 1, the structural characterization using NMR spectroscopy showed the formation of an isomeric mixture due to the stereo- and constitution specificity of the VCP- and spacer-molecules. A more complete description of the VCP resin is presented in the ESI† in Fig. S1–S7.

The VCPMe$_3$hexAmid was exposed to a commercial light-emitting diode (LED) source for studying the photo-curing kinetics and the absolute monomer conversion, which was determined by time-dependent extraction of the resulting material using deuterated chloroform. A mixture of camphorquinone (CQ) and ethyl 4-(dimethylamino)-benzoate (EDMAB) in a molar ratio of 1 : 2 was used for photo-polymerization at 35 °C. The very fast curing kinetics of VCPMe$_3$hexAmid was evident from a conversion of ~80% within 30 s and very high overall conversions of around 96% (Fig. 1a). The experiments were carried out both in inert gas as well as in air. The very fast curing-kinetics was retained even in air.

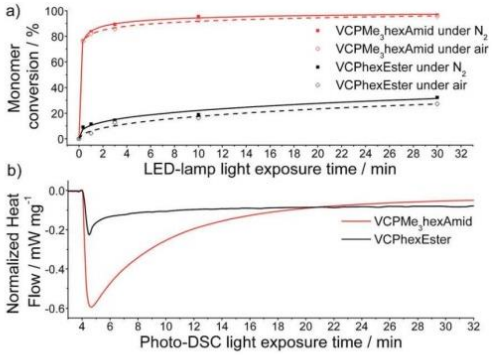

Fig. 1 Photo-polymerization of VCPMe$_3$hexAmid and VCPhexEster (1 mol% photo-initiator CQ : EDMAB in a molar ratio of 1 : 2). (a) Time-dependent curing experiments under a controlled atmosphere of nitrogen and air using a commercial blue-light LED source (2.013 mW cm^{-2} for 465 nm). The determination of residual monomer has been carried out by GC for VCPhexEster and by ^{1}H-NMR for VCPMe$_3$hexAmid. (b) Typical heat flows (mW mg^{-1}) recorded during photo-DSC experiments (6.93 mW cm^{-2} for the whole xenon spectrum).

These results were compared with that of the bi-functional VCP-ester derivative (VCPhexEster) (Scheme 1b, Fig. 1a). VCPhexEster yielded monomer conversions of ~30% after 30 min of curing, while VCPMe$_3$hexAmid reached the same conversion in less than 20 s. Furthermore, VCPhexEster could not reach a high overall monomer conversion even after prolonged curing times up to several hours (the maximum conversion in nitrogen was 42% in 12 h). Therefore VCPhexEster is several orders of magnitude less reactive than the VCPMe$_3$hexAmid. Furthermore, the polymerization heat flow during the curing process was monitored by carrying out photo-polymerization in a DSC-cell for both VCPhexEster and VCPMe$_3$hexAmid (Fig. 1b). Recording the relatively low heat flow changes during the curing of VCPhexEster also illustrated the general low reactivity of ester-based VCP resin.

The difference in reactivity of VCPMe$_3$hexAmid and VCPhexEster could be due to the molecular structure of VCPMe$_3$hexAmid allowing intermolecular hydrogen bonding *via* amide units, leading to a partial preorganization of monomer molecules (Fig. 2a). This could also lead to a profitable orientation of the singly occupied molecular orbital (SOMO) of the ring-opened VCP-structure to further monomer units or rather their π-orbitals, which enhances the curing process (Fig. 2b). The shift of the amide protons of VCPMe$_3$hexAmid to higher fields with increasing temperature in ^{1}H-NMR experiments (see Fig. S8 and S9 in the ESI†) and the meaningful difference in the monomer viscosities, VCPMe$_3$hexAmid was significantly more viscous (2.4 Pa s) than VCPhexEster (0.08 Pa s), verified the H-bonding. Furthermore, photo-DSC curing experiments, with an additional amount of potassium thiocyanate (KSCN) as a chaotropic agent, have been carried out to underline the hydrogen bonding effect (Fig. 2c). Thereby, chaotropic agents can disrupt the H-bonding forces.[18] An unambiguous effect toward increasing KSCN amounts to the curing behavior was observed, yielding 19% lower heat flow values (ΔH_{max}) and 37% lower rates of polymerization (R_P), respectively, for 1 wt% of a KSCN solution (392 mg mL^{-1} in DMSO) and 1 wt% pure DMSO (R_P values were determined from the slope of the linear fit after reaching H_{max}). The enhanced R_P for acrylate monomers capable of having H-bonding is documented in the literature,[19] however this effect appears to be not so pronounced as for VCPs.

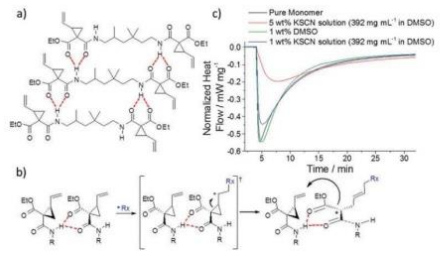

Fig. 2 Effect of hydrogen bonding on curing of VCPMe$_3$hexAmid. (a) Proposed scheme showing partial preorganized monomer units. (b) Proposed mechanism for amide-based VCP polymerization in which the propagation rate is enhanced because of profitable orbital arrangements. (c) Photo-DSC measurements independent of KSCN as a chaotropic additive, proving the effect of hydrogen bonding for VCPMe$_3$hexAmid.

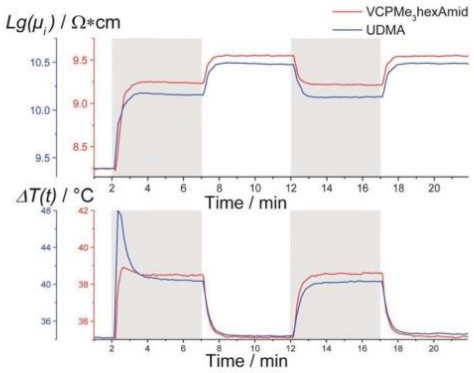

Fig. 3 Recorded changes in ion-viscosity (μ_i) in DEA measurements monitored for a constant frequency of 1 Hz (upper graph) and polymerization temperature (lower graph) for the curing of $VCPMe_3hexAmid$ and UDMA (1 mol% initiator CQ : EDMAB in a molar ratio of 1 : 2). The grey background indicates the light exposure.

Due to the fact that with time curing reactions are exothermic and could lead to undesirable local heating and an increase in temperature, additional experiments were carried out to monitor temperature changes during polymerization of $VCPMe_3hexAmid$ by the DEA technique. Advantageously, the temperature increase ΔT during curing was very low (slightly above 4 °C) for $VCPMe_3hexAmid$ (Fig. 3). Furthermore, for $VCPMe_3hexAmid$ the curing began immediately with an increase in the ion-viscosity (μ_i) reaching the top of a plateau in about 1–2 min, whereas the continued exposure did not further affect μ_i. Thus, the curing was practically completed within the first 2 min. The slight increase in μ_i upon switching off the light source was due to a decrease in temperature from 39 °C (the maximum attained during curing) to around 35 °C (start temperature). No attempts were made to carry out similar experiments with VCPhexEster due to its very slow and incomplete polymerization as shown above. In contrast to $VCPMe_3hexAmid$, the well-known photo-cross-linkable resin urethane-dimethacrylate (UDMA) showed during curing a rise in temperature of 13 °C to about 48 °C under similar reaction conditions. Especially with regard to biological coatings and dental applications any reduction in an excessive exothermic temperature rise reduces the hazard potential significantly.[20]

The volume shrinkage as measured by Archimedes's method amounted to 4.9% for pure $VCPMe_3hexAmid$. The same measurement for VCPhexEster unfortunately could not be done due to incomplete conversions. Therefore, a comparison of our synthesized $VCPMe_3hexAmid$ to widely used methacrylate resins, like UDMA, dodecanediol-dimethacrylate (1,12-DMA), and a mixture of BisGMA and triethylene-glycol-dimethacrylate (TEGDMA), was made.

$VCPMe_3hexAmid$ showed a reduction by 45% in volume shrinkage to UDMA, 17% to a 6 : 4 mixture of BisGMA : TEGDMA and similar to BisGMA. Furthermore, upon comparing the resin viscosity in dependence of volume shrinkage (Fig. 4a), a unique advantage of $VCPMe_3hexAmid$ could be observed. Both BisGMA with 1200 Pa s[21] and UDMA with 13.8 Pa s are too viscous to be used on their own. In contrast, $VCPMe_3hexAmid$ exhibits

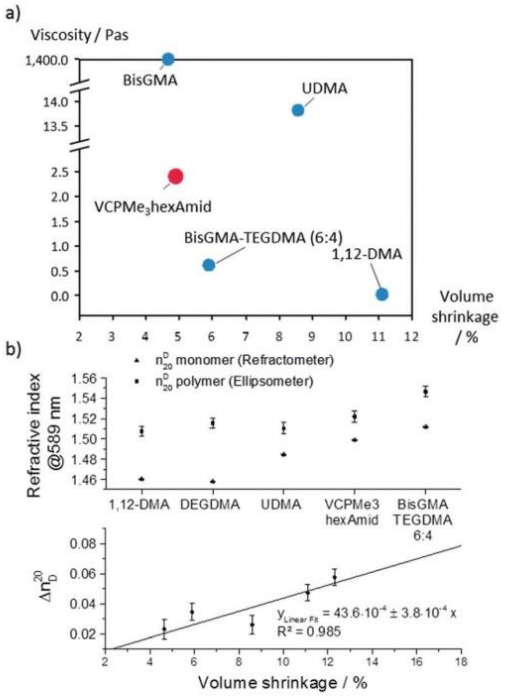

Fig. 4 Classification of resin properties in comparison to commercially available methacrylate resins. (a) Ashby plot of specific monomer viscosities as a function of the volume shrinkage. (b) Upper graph: refractive indices (@589 nm), respectively, for the monomer and polymer networks. Lower graph: graphical evaluation of the refractive index alteration Δn_D^{20} from the volume shrinkage of the respectively polymers. Please find in the ESI† and Table S1 a summary of the properties of the materials shown here.

with 2.4 Pa s a clearly lower viscosity and simultaneously low volume shrinkage. The optical refractive index n of the cured $VCPMe_3hexAmid$ averaged to 1.522 as measured by SE and lies in the range of other existing systems, *e.g.* UDMA with 1.508 (Fig. 4b). The regression line for the changes in the refractive indices Δn_D^{20} in dependence of the volume shrinkage ΔV showed a simple and accurate correlation (R^2 = 0.985) that the effect of the volume shrinkage mainly induced the refraction alteration.

Furthermore, $VCPMe_3hexAmid$ showed similar LD_{50} values (0.067 ± 0.005 mM) to those of UDMA (0.071 ± 0.009 mM) in case it has to be recommended for dental applications (see the ESI† for cytotoxicity determination, Fig. S15 and S16).

As the polymer network structure could influence the overall properties, high-resolution solid state ^{13}C-CP/MAS NMR was used for studying the network structure by comparing the participation of double bonds in the cross-linking process. Almost all vinyl double bonds participated in the cross-linking reaction as evidenced by the presence of a very significant peak at 129.3 ppm originating from the carbon signal of the C=C double bond of the ring-opened VCP-unit. Only a very small shoulder at 119.7 ppm (dedicated to unreacted vinyl double bonds) was identified, implying an extraordinary high cross-linking density of the cured $VCPMe_3hexAmid$. A closer examination of the network structure is presented in

the ESI† and Scheme S4 and Fig. S10; with respect to the polymerization mechanism of VCPs the formation of cyclobutane structures besides the 1,5-ring-opened units should also be taken into consideration, but unfortunately it could not be analyzed using present techniques.[16]

Cured VCPMe$_3$hexAmid specimens showed E-moduli of 130.9 ± 0.7 MPa which increased to 181.9 ± 0.5 MPa after additional storage at 100 °C (the complete evaluation is provided in the ESI† and Fig. S12) and Vickers hardness (HV) values of 1.52 ± 0.02 HV. These values are in the range of commercially available and cured UDMA.

In summary, after ~10 years of silence in academics and patent registrations the first highly reactive and low volume shrinking VCP resin was obtained, which can serve as a model monomer for further resin systems. The introduction of H-bond forming amide groups into the monomer structure induced partial preorganization, leading to high propagation efficiency during curing. Any disproportionate increase in resin viscosity could be prevented by using a sterically hindered, isomeric spacer element. The resulting VCPMe$_3$hexAmid represents for the first time a highly efficient and fast curing VCP resin. Moreover, the most valuable properties conversion, mechanical strength, viscosity, and optical refractive index were all carefully balanced in optimum ranges. Since radical polymerizable, low-shrinking resins remain a challenge for several applications, this novel resin could be of immense interest, offering a real and sustainable alternative to the currently used dimethacrylate resins. So far, the outstanding possibilities offered by VCP resins have not yet been exploited. Therefore a broad application range for both industry and academia may be imagined.

This work was supported by the German Federal Ministry for Economic Affairs and Energy (BMWi) (www.zim-bmwi.de). We thank Dr A. Bublewitz, Dr A. Theis and the Kettenbach GmbH for providing further resources and support. The authors are indebted to Prof. P. Strohriegel and Dr R. Giesa for providing access to photo-DSC and DMTA, to Prof. J. Senker and Dr R. Siegel for solid-state NMR measurements, and further to NETZSCH company and Dr S. Schmölzer for DEA measurements. We also thank C. Goldhahn and P. Schmode for their experimental support as research students.

Notes and references

1 (*a*) Y. Jian, Y. He, L. Zhao, A. Kowalczyk, W. Yang and J. Nie, *Adv. Polym. Technol.*, 2013, **32**, 21331; (*b*) E. Andrzejewska, *Prog. Polym. Sci.*, 2001, **26**, 605.
2 (*a*) J. G. Kloosterboer, *Adv. Polym. Sci.*, Springer, Berlin Heidelberg, 1988, vol. 84, pp. 1–61; (*b*) Y. Fuchs, O. Soppera and K. Haupt, *Anal. Chim. Acta*, 2012, **717**, 7.
3 C. Decker, *Macromol. Rapid Commun.*, 2002, **23**, 1067.
4 J. Guo, M. R. Gleeson and J. T. Sheridan, *Phys. Res. Int.*, 2012, **2012**, 1.
5 J. Lange, S. Toll, J.-A. E. Månson and A. Hult, *Polymer*, 1997, **38**, 809.
6 (*a*) N. Moszner and T. Hirt, *J. Polym. Sci., Part A: Polym. Chem.*, 2012, **50**, 4369; (*b*) K. L. van Landuyt, J. Snauwaert, J. de Munck, M. Peumans, Y. Yoshida, A. Poitevin, E. Coutinho, K. Suzuki, P. Lambrechts and B. van Meerbeek, *Biomaterials*, 2007, **28**, 3757.
7 K. S. Anseth, C. N. Bowman and N. A. Peppas, *J. Polym. Sci., Part A: Polym. Chem.*, 1994, **32**, 139.
8 (*a*) A. Lendlein, H. Jiang, O. Jünger and R. Langer, *Nature*, 2005, **434**, 879; (*b*) C. Fo Tsang, *Microelectron. Int.*, 2000, **17**, 27.
9 (*a*) C. Decker, *Prog. Polym. Sci.*, 1996, **21**, 593; (*b*) K. L. van Landuyt, J. Snauwaert, J. de Munck, M. Peumans, Y. Yoshida, A. Poitevin, E. Coutinho, K. Suzuki, P. Lambrechts and B. van Meerbeek, *Biomaterials*, 2007, **28**, 3757.
10 F. Rueggeberg and K. Tamareselvy, *Dent. Mater.*, 1995, **11**, 265.
11 B. Lu, P. Xiao, M. Sun and J. Nie, *J. Appl. Polym. Sci.*, 2007, **104**, 1126.
12 J. W. Stansbury, M. Trujillo-Lemon, H. Lu, X. Ding, Y. Lin and J. Ge, *Dent. Mater.*, 2005, **21**, 56.
13 R. L. Bowen, US 3066112, 1959.
14 (*a*) R. L. Bowen, *J. Am. Dent. Assoc., JADA*, 1963, **66**, 57; (*b*) A. Peutzfeldt, *Eur. J. Oral Sci.*, 1997, **105**, 97.
15 (*a*) C. Liao and K. Kannan, *Environ. Sci. Technol.*, 2011, **45**, 9372; (*b*) L. Chen and B. Suh, *JSM Dent*, 2013, **1**, 1004; (*c*) C. Bolognesi, L. Castle, J.-P. Cravedi, K.-H. Engel, P. Fowler, R. Franz, K. Grob, R. Gürtler, T. Husøy, W. Mennes, M. R. Milana, A. Penninks, F. Roland, V. Silano, A. Smith, M. de Fátima Tavares Poças, C. Tlustos, F. Toldrá, D. Wölfle and H. Zorn, *EFSA J.*, 2015, **13**, 3978.
16 P. Pineda Contreras, P. Tyagi and S. Agarwal, *Polym. Chem.*, 2015, **6**, 2297.
17 N. Moszner, *Macromol. Symp.*, 2004, **217**, 63.
18 F. Liu, J. Seuring and S. Agarwal, *J. Polym. Sci., Part A: Polym. Chem.*, 2012, **50**, 4920.
19 (*a*) J. F. G. A. Jansen, A. A. Dias, M. Dorschu and B. Coussens, *Macromolecules*, 2003, **36**, 3861; (*b*) S. H. Dickens, J. W. Stansbury, K. M. Choi and C. J. E. Floyd, *Macromolecules*, 2003, **36**, 6043; (*c*) I. Sideridou, V. Tserki and G. Papanastasiou, *Biomaterials*, 2002, **23**, 1819.
20 (*a*) A. C. Shortall and E. Harrington, *J. Oral Rehabil.*, 1998, **25**, 908–913; (*b*) Z. Czech and R. Milker, *J. Appl. Polym. Sci.*, 2003, **87**, 182.
21 S. G. Pereira, T. G. Nunes and S. Kalachandra, *Biomaterials*, 2002, **23**, 3799.

Renaissance for Low Shrinking Resins: *all-in-one* Solution by Bi-Functional Vinylcyclopropane-Amides**

Paul Pined Contreras,[a] *Christian Kuttner,*[b] *Andreas Fery,*[b] *Ullrich Stahlschmidt,*[c] *Valérie Jérôme,*[c] *Ruth Freitag,*[c] *and Seema Agarwal*[a]*

[a.] *Macromolecular Chemistry II, Universität Bayreuth, Universitätsstrasse 30, 95440 Bayreuth, Germany, E-mail: agarwal@uni-bayreuth.de; Tel: +49-921-553397*
[b.] *Physical Chemistry II, Universität Bayreuth, Universitätsstrasse 30, 95440 Bayreuth, Germany*
[c.] *Process Biotechnology, Universität Bayreuth, Universitätsstrasse 30, 95440 Bayreuth, Germany*

Content

Materials ... 3
Methods ... 3
Monomer Synthesis ... 8
Synthesis of diethyl 2-vinylcyclopropane-1,1-dicarboxylate (1) and 1-(ethoxycarbonyl)-2-vinylcyclopropanecarboxylic acid (1a) ... 8
Complexness of isomerization for VCP derivatives ... 8
Synthesis of 1,2-bis[(1-ethoxycarbonyl-2-vinylcyclopropan--1yl)carbonyloxy]hexane (VCPhexEster) ... 9
Synthesis of diethyl-1,1'-(2,4,4-trimethylhexane-1,6-diyl)bis(azanediyl)bis-(oxomethylene)bis(2-vinylcyclopropanecarboxylate) (VCPMe$_3$hexAmid) ... 13
Supplementary Analytical Data ... 16
Temperature variable 1H-NMR experiment to confirm the hydrogen bonding effect of the VCP-amide resin (VCPMe$_3$hexAmid) ... 16
Photo-polymerization mechanism of bi-functional VCP derivatives ... 17
High resolution solid state ^{13}C-NMR spectroscopy of cured VCPMe$_3$hexAmid ... 18
Spectroscopic Ellipsometry: Refractive index measurements ... 19
Determination of mechanical properties (E-Modulus) ... 20
Determination of residual monomer amount of cross-linked samples by extraction experiments ... 20
Compilation of characteristic resin features ... 23
Determination of Cytotoxicity: ... 23
References ... 25

Materials

Trans-1,4-dibromo-2-butene (99 %), potassium hydroxide (KOH, >85 %), diethyl malonate (99 %), N,N´-dicyclohexylcarbodiimide (DCC, 99 %), 4-(dimethylamino)pyridine (DMAP, >98 %), 2,2,4(2,4,4)-trimethyl-1,6-hexandiamine (99 %), hexamethylenediamine (HMDA, 98 %), 1,6-hexandiol (99 %), triethylamine (99 %), ethyl 4-(dimethylamino)benzoate (EDMAB, 99 %), 1,3,5-trimethylbenzen (mesitylene, >99.8 %), camphorquinone (CQ, 97 %) and dichloromethane (>99.5 %) were supplied by Sigma Aldrich and used without further purification. 1-hydroxybenzotriazole (HOBt anhydrous) (Omnilab Life Science / OLS) and ethanol absolute (EtOH, >99 %) (VWR) were used as received. Sodium (cubes, delivered in mineral oil) (Aldrich, 99 %) was purified by melting in dry xylole prior to use. Urethane-dimethacrylate (UDMA), dodecanediol-dimethacrylate (1,12-DMA) and a 6:4 mixture of bisphenol-A-glycidyl methacrylate (BisGMA) and triethylene-glycol-dimethacrylate (TEGDMA) have been gratefully provided by the Kettenbach GmbH (Eschenburg, Germany) and were used as received.

Methods

Nuclear magnetic resonance (NMR) spectroscopy: Both ^{1}H- (300 MHz) and ^{13}C- (75 MHz) NMR spectra were recorded on a Bruker Ultrashied-300 spectrometer at 20 °C in $CDCl_3$. The spectra were calibrated on the solvent signal ($\delta(^{1}H)$ = 7.26 ppm; $\delta(^{13}C)$ = 77.16 ppm). High-resolution solid state ^{13}C CP/MAS (cross polarization/magic angle spinning) NMR Spectra were measured by a Bruker spectrometer operating at 100.6 MHz, using a pulse experiment with a 30 s pulse delay for 2048 scans. The ^{13}C signals of the olefinic groups in uncured and cured VCPMe$_3$hexAmid resin are observed at about 133 and 119 ppm for the uncured and at about 129 ppm for the cured VCPMe$_3$hexAmid resin, respectively. In order to evaluate the spectra, MestReNova (Mestrelab Research, version 6.1) was used.

Gas chromatography (GC): GC measurements have been done by a GC-FID system (QP-5050) from Shimadzu company, using nitrogen as carrier gas. The injector temperature was 300 °C. The reaction mixtures were dissolved in acetone (2 µL mL^{-1}), 1 µL was injected in a split ratio of 1:50 and measured from 50 °C (2 min hold) up to 300 °C with a heating rate of 15 K min^{-1}. Software: LabSolutions (Shimadzu, version 5.54 SP2).

Gas chromatography-mass spectrometry (GC-MS):

GC-MS measurements were carried out on a Agilent system (5977A MSD), using helium as carrier gas. The injector temperature was 300 °C. The reaction mixtures were dissolved in acetone (2 µL mL^{-1}), 1 µL was injected in a split ratio of 1:50 and measured from 50 °C (2 min hold) up to Maestro 1 GCMSD/EnhancedMassHunter (Gerstel, version 1.4.23.11) (Shimadzu, version 5.54 SP2).

Medium Pressure Silica gel Chromatography (MPLC):

MPLC purifications were performed with a GRACE Reveleris X2 system operating with an integrated UV-VIS and ELSD detector for fraction detection. Commercial grade solvents were distilled before use.

Photo-Differential Scanning Calorimetry (Photo-DSC):

Photo-DSC measurements were carried out on a Perkin-Elmer Photo-DSC instrument (DSC 7) at isothermal conditions of 35 °C in a nitrogen atmosphere (flow rate = 50 mL/min) with 20 ± 5 mg of sample amount. Before irradiation, each sample has been purged with nitrogen for 4 minutes to avoid oxygen inhibition. The instrumental setup consists of a 450 W xenon lamp as light source, whose light beam was passed through an IR absorbing water filter and a grey filter to reduce the light total intensity to 10 %. An optical splitter was used to part the light beam into a sample and a reference beam, which were focused to the polymerizable samples and an empty reference pan respectively. The light intensity accounted to 6.93 mW cm^{-2}. The heat flow of polymerization reaction was recorded as a function of time. The polymerizable samples were prepared by dissolving the photo initiators in the respective monomer mixture in a brown glass vial at 25 °C in a shaking device for an appropriate time.

Dielectric Analysis (DEA):

Photo-curing experiments have been monitored by dielectric analysis on a DEA Epsilon 288 from NETZSCH company at 35 °C isothermal conditions, using IDEX 115/40 sensor types with frequencies of 1, 10, 100, and 1000 Hz and an OmniCure S2000 UV lamp as radiation source, whose light emission was filtered by an optical filter to a spectrum of 400-500 nm.

Spectroscopic Ellipsometry (SE): Refractive index measurements

SE was done in polarizer-compensator-sample-analyzer (PCSA) configuration (SE800, Sentech) with a xenon lamp as white-light source. The ellipsimetric ratio ρ was measured from 380 to

680 nm at angles of incidence of $\phi = 60°$, 65°, and 70° at 3 different positions of the sample. Each incidence angle was evaluated using Eq. 1. After averaging over ϕ, the respective standard deviation was calculated from the Gaussian error propagation on basis of the variation of $\rho(\lambda,\phi)$. For a simple two-media interface, the complex optical properties of the bottom layer can be directly evaluated by the pseudo-dielectric function:[1]

$$n_{bottom}^2 = n_{top}^2 \sin^2\phi \left[1+\tan^2\phi \, (1-\rho)^2/(1+\rho)^2\right] \quad \text{with} \quad \rho(\lambda,\phi) = r_p / r_s \qquad \text{Eq. 1}$$

For light incident from an ambient medium n_{top} of known refractive index ($n_{air} = 1$), the optical properties of the reflecting bottom medium n_{bottom} can be determined directly from the measured ellipsometric ratio ρ and the angle of incidence ϕ. From the resulting wavelength-dependent dispersion, the refractive index at 589 nm was calculated. The change in refractive index Δn was calculated from the bulk index of polymer in reference to the monomer index.

Dynamic Mechanical Thermal Analysis (DMTA): E-Modulus determination

A dynamic-mechanical analyzer (DMTA IV) from Rheometric Scientific has been used to determine the E-moduli by three-point bending tests, using specimens of the dimension 25x3x1 mm^3. The experiments were conducted within the linear-elastic range, a span width of 20 mm, strain rates of 2 mm/min and at room temperature (20 °C with a relative humidity of 70 %). For the computer-based evaluation, equation (2) was used to calculate the E-modulus

$$E_{B3} = \frac{l_v * h * F_2 - F_1}{8 * J * 0{,}002} \text{N mm}^{-2} \qquad \text{Eq. 2}$$

where F are the used forces (in N); l_v is the test span (in mm), J is the area moment of inertia, and h is the thickness of the respective specimen (in mm). The E-modulus was determined by the linear slope of the graphical analysis of the flexural stress against the sample strain.

Vickers Hardness:

A MHT-10 cap in combination with an optical microscope from Leica was used to perform Vickers hardness measurements in dependence of the used load. The loading time differs between 15-30 s. Five samples for each polymer with forces between 20-200 mN were used to define the Vickers hardness.

Rheometric Measurements:

Viscosity testing was carried out with a cone-plate rotation viscometer PK 100, coupled with a RV 20-M5 Rotavisco analyzer and a RC 20 controller from Haake. The viscosity has been

measured in dependence of the shearing rate at 25 ± 0.5 °C with ~0.5 mL of sample amount respectively. Rheowin software was used for acquisition. All values represent the average of five measurements and refer to a shearing rate of 100 s^{-1}.

Preparation of Polymer Networks:

To perform the monomer photo-activation a homemade photo reactor in the dimension 450x450x300 mm^3 including 22 Cree XM-L LEDs (dominant wavelength emission of blue-light LED 450-465 nm) was used as radiation source. The radiant flux of the photo reactor (scattered light) was determined to 2.013 mW cm^{-2} by a NEWPORT Multi-Function Optical Meter (1835-C) respectively for 465 nm. The preparation of the polymer specimens were carried out in dependence of the instrumental experiment. The specimens for the DMTA measurements were produced by filling a stainless steel profile with five equal milled edges with a dimension of 25x3x1 mm^3 with the current monomer/initiator mixture. The profile was enclosed and fixed both on top and on the bottom with a 100 µm thick Hostophan sheet. Finally, the profile was irradiated for 2 h within the photo reactor. The cured polymer was pressed out carefully and has been stored for 24 h at room temperature prior testing. To avoid measurement deviations cause of volume shrinkage the final specimen dimension of ca. 25x3x1 mm^3 was verified exactly by using a digital measuring slide. The specimens for the Vickers hardness measurements have been prepared by coating 400 µm thick monomer/initiator mixtures with a doctor knife on a glass slide. The glass slide has been infiltrated to a desiccator, flushed constantly with argon as protection gas. Finally, the desiccator has been irradiated for 2 h within the photo reactor. The homogenous and cured polymer samples were stored for 24 h at room temperature prior testing. The preparation of the specimens for the ellipsometric measurements occurred analog to the samples assigned for the Vickers hardness besides the samples were cured on silicon wafers.

Determination of Residual Monomer Amount:

While the quantification of the residual VCPhexEster monomer from the cured samples was performed by GC, the residual amount of the $VCPMe_3$hexAmid was performed by ^{1}H-NMR measurements, as this monomer was due to its higher molar mass and polarity within GC measurements not detectable. According to the VCPhexEster monomer conversion within the Photo-DSC experiments, the weighted and cured samples have been immediately immersed after radiation to 5.0 mL of chloroform (as extraction fluid) in 10 mL bottles with snap-on caps for 24 h respectively. The residual monomer amounts have been calculated by comparison the

integration areas of the samples with the previous established calibration curve. According to the $VCPMe_3hexAmid$ monomer, the weighted and cured samples have been immediately immersed after radiation to 1.0 mL of $CDCl_3$ (as extraction fluid) in 2 mL bottles with snap-on caps for 24 h respectively. The residual monomer amounts have been calculated by comparison the integration areas of the respective ^{1}H-NMR proton signals (amide-, vinyl and cyclopropane-protons) to the proton signals of mesitylene, which has been added to the $CDCl_3$ as internal standard in 2.8216 mg mL^{-1} amount. The concentration range of the previous established calibration curve of the $VCPMe_3hexAmid$ amounted between 5 mg mL^{-1} and 0.01 mg mL^{-1}. For each ^{1}H-NMR a number of scans of 2048 has been chosen to achieve an appropriate signal to noise resolution.

Determination of Volume Shrinkage:

The polymerization shrinkage was calculated from the difference in density of the monomer to the formed polymers by using Archimedes's principle. Applying a 1 mL pycnometer at room temperature the densities of the monomers were measured by taring the density. For the cured samples the densities have been calculated by its water displacement, respectively for ~400 mg cured specimens. The shrinkage of polymerization was determined separately for three samples and adjusted to the confirmed monomer conversion respectively.

Determination of Cytotoxicity:

The cytotoxicity of the $VCPMe_3hexAmid$, VCPhexEster and UDMA was tested using L929 murine fibroblasts (CCL-1, ATCC) according to the norm ISO 10993-5 using 1 mg mL^{-1} MTT-stock solution. The L929 cells were maintained in MEM cell culture medium supplemented with 10 % fetal calf serum (FCS), 100 mg mL^{-1} streptomycin, 100 IU mL^{-1} penicillin, and 4 mM of L-glutamine. The cells were cultivated at 37 °C in a humidified 5 % CO_2 atmosphere. The uncured monomer resins were tested in a concentration range from 0 to 5 mM (UDMA and $VCPMe_3hexAmid$). This concentration range corresponds to up to 2 vol.% DMSO per well, i.e., a concentration already slightly toxic for the cells. The VCPhexEster resin was tested at concentrations up to 20 mM corresponding to up to 8.9 vol.% DMSO per well, i.e., a concentration highly toxic for the cells (Fig. S15). The cells were seeded at a density of 1 x 10^4 cells per well, in 96-well plate, 24 h prior to the experiment. As 100 % viability control, untreated cells were used. For each dilution step, eight replicates were used. After dissolving the metabolically formed formazan crystals in isopropanol, the absorbance was measured using a plate reader (Genios Pro, Tecan) at a wavelength of 580 nm. For data evaluation the software

SigmaPlot 11.0 from the Systat Software GmbH was used, the x-scale was plotted logarithmically, and a nonlinear fit was run to obtain the lethal dose 50 (LD_{50}) values. Group data are reported as mean ± standard deviation. Statistical significance was defined as having $p < 0.001$.

Monomer Synthesis

Synthesis of diethyl 2-vinylcyclopropane-1,1-dicarboxylate (1) and 1-(ethoxycarbonyl)-2-vinylcyclopropanecarboxylic acid (1a)

Diethyl 2-vinylcyclopropane-1,1-dicarboxylate was obtained as mono-functional VCP, using diethyl malonate and the corresponding dibromo butane as per published procedure.[2,3] The chemical hydrolysis of 1 to the 1-(ethoxycarbonyl)-2-vinylcyclopropanecarboxylic acid was obtained with 1.10 eq. of potassium hydroxide as per published procedure.[4]

Complexness of isomerization for VCP derivatives

The hydrolysis of the racemic 2-vinylcyclopropane-1,1-dicarboxylate (1) results in a racemic mixture of diastereoisomers in a ratio of about 90:10.[4] With continuing process of synthesis, and using isomeric spacer elements like for $VCPMe_3hexAmid$, the isomeric complexity increase further. Therefore, to avoid losing a general overview over the basic monomer structure, only the most probable isomeric structure was presented within the main part of the manuscript and following figures and schemes. An exemplary structural description of a VCP derivative is presented in Scheme S1.

Scheme S1. Exemplary structural description of the stereo centers and the isomerization complexity of VCP derivatives.

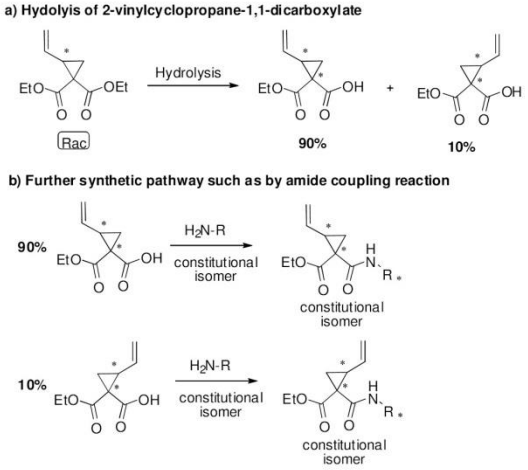

Synthesis of 1,2-bis[(1-ethoxycarbonyl-2-vinylcyclopropan--1yl)carbonyloxy]hexane (VCPhexEster)

Scheme S2. Synthesis of bi-functional vinylcylopropane ester (VCPhexEster).

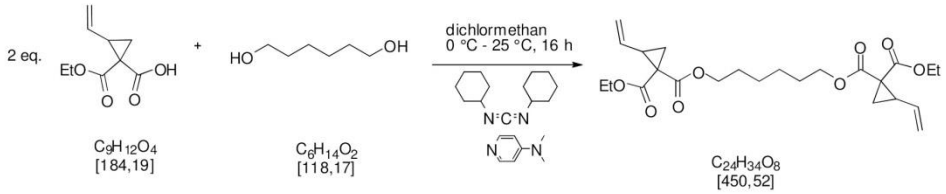

A flame-dried and with argon purged flask was charged with 200 mL of anhydrous DCM. 24.18 g (1.20 eq., 0.117 mol) of DCC were introduced and dissolved by stirring. This solution was transferred to a flame-dried funnel, which was connected to a flame dried 500 mL three-necked reaction flask. This three-necked reaction flask was charged with 100 mL of anhydrous DCM, 21.59 g (1.20 eq., 0.117 mol) of 1a, 0.596 g (0.05 eq., 4.9×10^{-3} mol) of DMAP and 5.771 g (0.50 eq., 0.049 mol) of anhydrous 1,6-hexanediol and stirred for 15 min at room temperature. Subsequently, the reaction solution was cooled to 0 °C and the DCC solution with a drip rate of about 60 mL h^{-1} was added drop wise. The reaction solution was stirred for 16 h at room

temperature. Subsequently the reaction mixture was filtered through a Büchner funnel, thereby resulting urea derivatives have been filtered off. The pale yellow solution was washed with 1 molar NaOH solution (1 x 100 mL), 1 molar HCl solution (1 x 100 mL) and with neutral water (3 x 50 mL). After drying over anhydrous magnesium sulfate, the solution was deposed on 32 g silica gel and purified by flash chromatography (medium pressure liquid chromatography MPLC-system), using hexane and ethyl acetate as eluent. The purified phase of 1,2-bis[(1-ethoxycarbonyl-2-vinylcyclopropan-1yl)carbonyloxy]hexane (VCPhexEster) was annexed with 150 ppm BHT and dried in vacuo; yield: 75 %, colorless liquid. ^{1}H-NMR (300 MHz, $CDCl_3$): δ = 5.47-5.35 (m, 2 H, CH=CH_2), 5.30-5.27 (m, 2 H, CH=CHH), 5.14-5.10 (m, 2 H, CH=CHH), 4.23-4.02 (m, 8 H, O-CH2), 2.59-2.51 (m, 2 H, CH-CH), 1.72-1.60 (dd, $^{3}J_{HH}$ = 9.0, $^{2}J_{HH}$ 4.9 Hz, 2 H, CHH-CH; m, 4 H, -CH_2-), 1.55-1.50 (dd, $^{3}J_{HH}$ = 9.0, $^{2}J_{HH}$ = 4.9 Hz, 2 H, CHH-CH), 1.40-1.31 (m, 4 H, CH_2-CH_2), 1.24 (t, $^{3}J_{HH}$ = 7.1, 6 H, CH_3); ^{13}C-NMR (75 MHz, $CDCl_3$) δ = 169.8 (O-C=O), 167.4 (O-C=O), 133.2 (CH=CH_2), 118.6 (CH=CHH), 65.6 (O-CH_2), 61.6 (O-CH_2), 36.0 (C4), 31.3 (-CHH), 28.5 (-CH_2), 25.6 (-CH_2), 20.5 (CH-CH), 14.3 (-CH_3); FT-IR (attenuated total reflectance (ATR)): ν = 3085 (w), 2980 (w), 2938 (w), 2862 (w), 1722 (s), 1639 (w), 1465 (w), 1443 (w), 1370 (m), 1317 (m), 1266 (s), 1195 (s), 1129 (s), 1032 (m), 990 (w), 958 (w), 915 (m), 862 (w), 778 (w), 748 (w), 707 (w), 665 cm^{-1} (w).

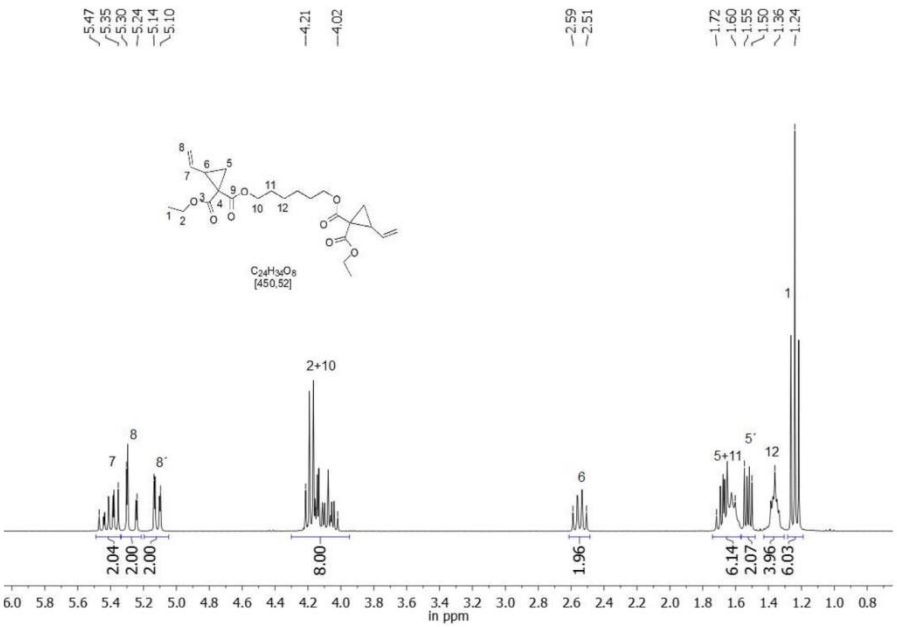

Figure S1. ^{1}H NMR of VCPhexEster ($CDCl_3$, 300 MHz).

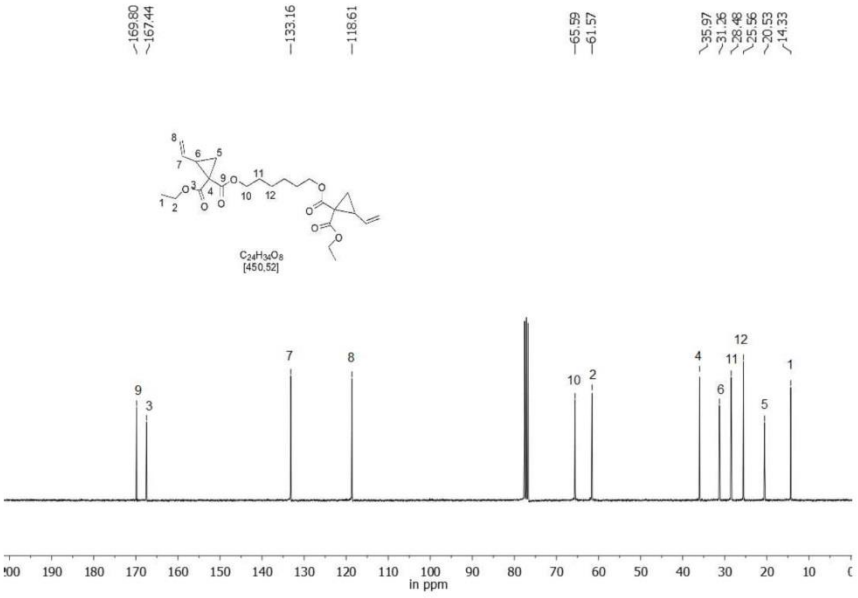

Figure S2. ^{13}C NMR of VCPhexEster ($CDCl_3$, 75 MHz).

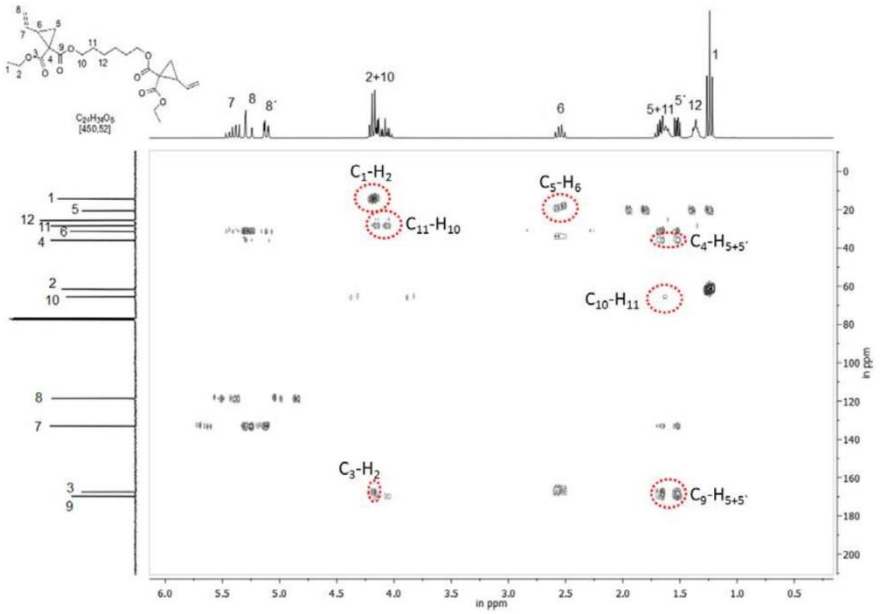

Figure S3. 2D-HMBC NMR of VCPhexEster ($CDCl_3$, 300 MHz).

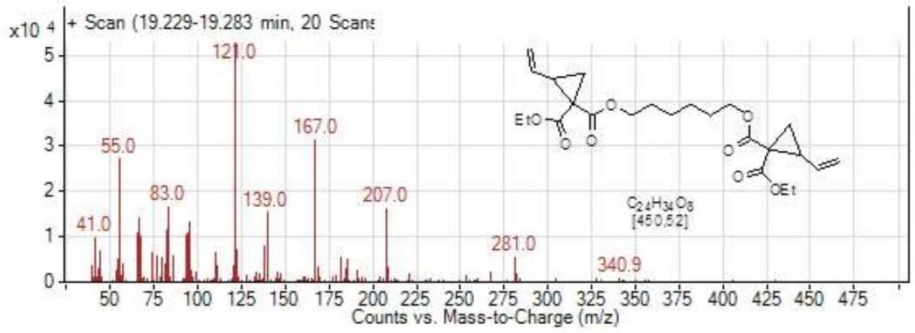

Figure S4. Mass spectra (Quadropol MS Agilent 5977A MSD: EI with 1000 eV) of GC-MS detected VCPhexEster. The VCPhexEster mass peak with ~450 m/z is due the low intensity and the fragmentation within this image section not visible.

Synthesis of diethyl-1,1'-(2,4,4-trimethylhexane-1,6-diyl)bis(azanediyl)bis-(oxomethylene)bis(2-vinylcyclopropanecarboxylate) (VCPMe$_3$hexAmid)

Scheme S3: Synthesis of bi-functional vinylcylopropane amide (VCPMe$_3$hexAmid).

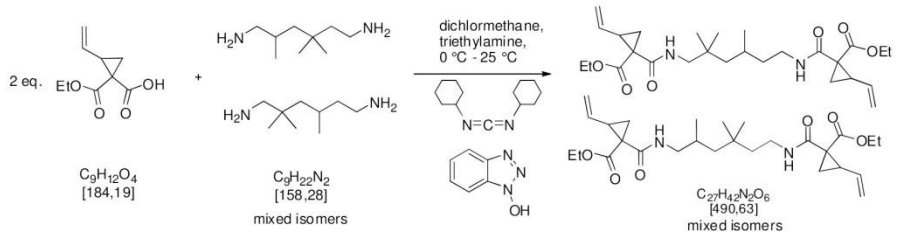

A flame-dried and with argon purged flask was charged with 15.28 g (0.50 eq., 0.051 mol) of 2,2,4(2,4,4)-trimethyl-1,6-hexandiamine and diluted with 200 mL of anhydrous DCM. This solution was transferred to a flame-dried funnel, which was connected to a flame dried 1000 mL three-necked reaction flask. This three-necked reaction flask was charged with 200 mL of anhydrous DCM, 20.65 g (1.10 eq., 0.112 mol) of 1a, 23.13 g (1.1 eq., 0.112 mol) of DCC and stirred for 15 min at room temperature, then cooled to 0 °C and charged with 29.66 mL (2.1 eq., 0.214 mol) of triethylamine. Subsequently, the diamine solution with a drip rate of about 40 mL h^{-1} was added drop wise. The reaction solution was stirred for 16 h at room temperature. Subsequently the reaction mixture was filtered through suction filter. The pale yellow solution was washed with water (2 x 100 mL), 1 molar HCl solution (1 x 100 mL) and with neutral water (3 x 50 mL). After drying over anhydrous magnesium sulfate, the solution was deposed on 35 g silica gel and purified by flash chromatography (MPLC-system), using hexane and ethyl acetate as eluent. The purified phase of diethyl-1,1'-(2,4,4-trimethylhexane-1,6-diyl)bis(azanediyl)bis-(oxomethylene)bis(2-vinylcyclopropane-carboxylate) (VCPMe$_3$hexAmid) was annexed with 800 ppm BHT and dried in vacuo; yield: 81 %, colorless liquid. ^{1}H-NMR (300 MHz, $CDCl_3$): δ = 8.49-8.09 (m, 2 H, NH), 5.74-5.52 (m, 2 H, CH=CH_2), 5.28-5.18 (m, 2 H, CH=CHH), 5.09-5.02 (m, 2 H, CH=CHH), 4.21-4.00 (m, 4 H, O-CH_2), 3.30-2.89 (m, 4 H, NH-CH_2), 2.49-2.27 (m, 2H, CH-CH), 2.01-1.93 (m, 2H, -CHH), 1.80-1.75 (m, 2H, -CHH), 1.73-1.65 (m, -CH) 1.56-1.30 (m, -CH; m, -CH_2), 1.24-1.16 (m, CH_3; -CH_2), 1.01 (m, -CH_2, CH), 0.92-0.88 (m, 3H, -CH_3), 0.86 (s, 6H, -CH_3); ^{13}C-NMR (75 MHz, $CDCl_3$) δ = 171.6-171.5 (NH-C=O), 168.1-167.8 (NH-C=O), 133.5 (CH=CH_2), 119.6 (CH=CHH), 61.6-61.5 (O-CH_2), 47.7-47.6 (NH-CH_2), 47.0 - 46.8

(CH2), 42.0, 41.9-38.2 (-CH_2), 37.1-36.3 (CH-CH), 35.0-34.4 (C_4), 33.20-25.5 (-CH_3), 29.2+29.1 (C4), 21.4-21.0 (-CHH), 14.3 (-CH_3); FT-IR (attenuated total reflectance (ATR)): ν = 3360 (m, broad), 3085 (w), 2960 (m), 2933 (m), 2872 (w), 1705 (s), 1654 (s), 1533 (s), 1469 (m), 1446 (m), 1392 (w), 1371 (m), 1337 (w), 1314 (s), 1265 (m), 1198 (m), 1140 (s), 1020 (m), 992 (m), 960 (w), 914 (m), 865 (m), 835 (w), 773 (w), 740 cm^{-1} (w).

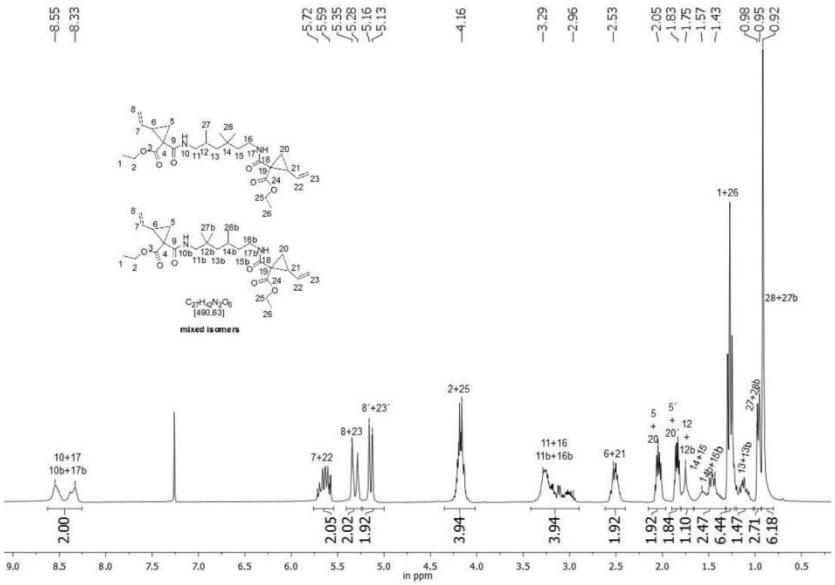

Figure S5. ^1H NMR of VCPMe$_3$hexAmid ($CDCl_3$, 300 MHz).

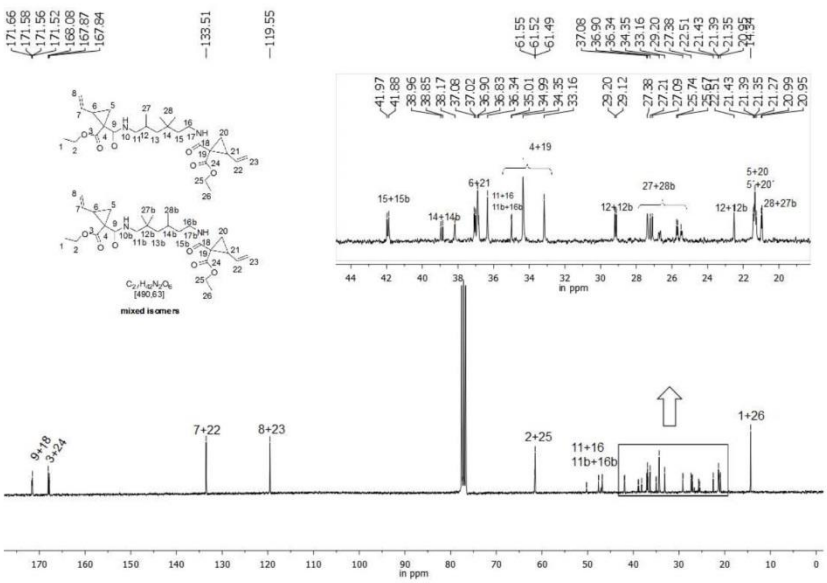

Figure S6. ^{13}C NMR of VCPMe$_3$hexAmid ($CDCl_3$, 75 MHz), inclusive an expansion from ^{13}C NMR between 45-18 ppm.

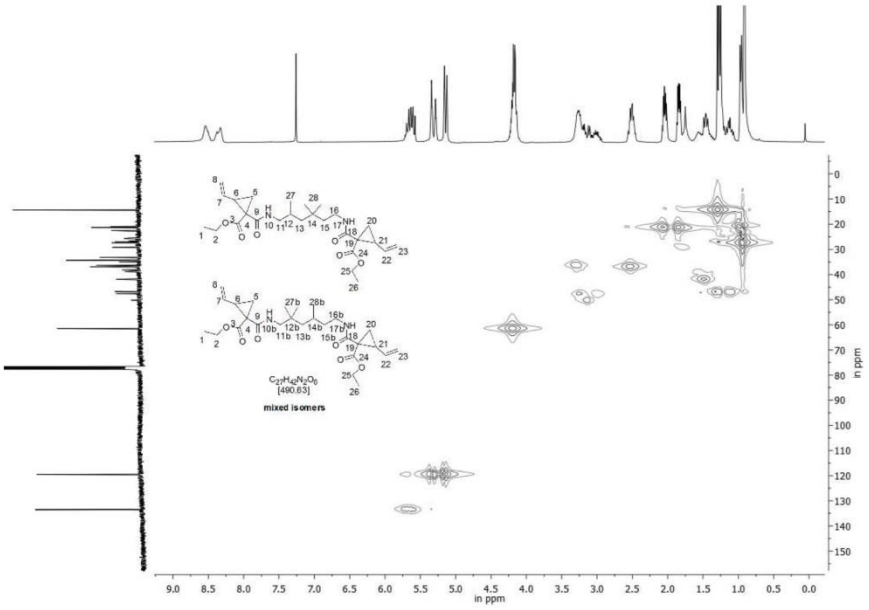

Figure S7. 2D-HSQC NMR of VCPMe$_3$hexAmid ($CDCl_3$, 300 MHz).

Supplementary Analytical Data

Temperature variable 1H-NMR experiment to confirm the hydrogen bonding effect of the VCP-amide resin (VCPMe$_3$hexAmid)

The temperature dependence of the amide protons or rather their chemical shift with temperature is well known in the literature.[5] The main reason of this effect is associated to the presence of H-bonds.[6] Generally, at higher temperature amide protons become shifted to the high field (Figure S8), as with increased temperatures a decreased deshielding effect is anticipated. For non-hydrogen bonded protons firstly the effect of temperature is generally weaker, and on the other hand often inversely proportional, as these protons become slightly shifted to the low field. Within the identical temperature range of the ^{1}H-NMR experiment for the corresponding VCP-ester derivative (VCPhexEster) no similar characteristic hydrogen-bonding shifts could be observed. Only the weaker and common temperature effect of the non-hydrogen bonded protons could be monitored. A graphical plot of the chemical shift during the variable ^{1}H-NMR temperature experiments is provided within Figure S9.

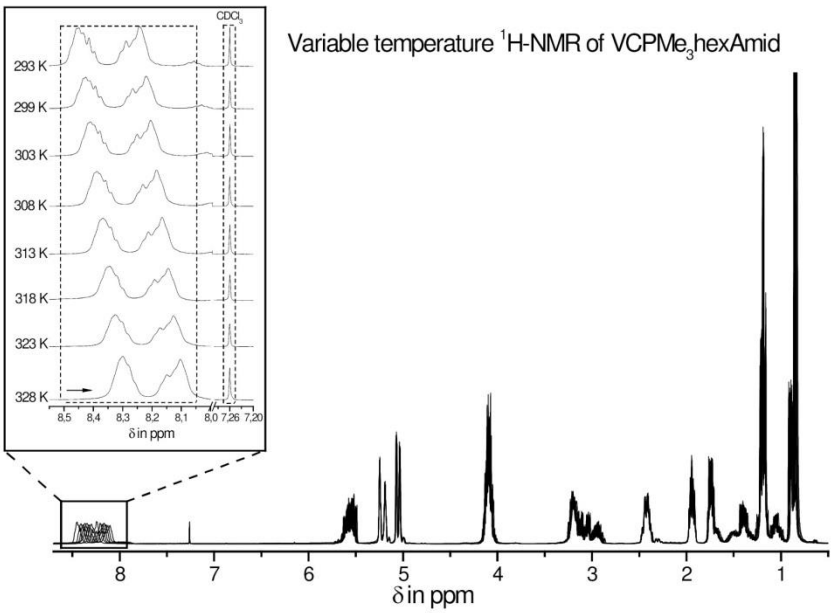

Figure S8: Variable temperature 1H-NMR of VCPMe$_3$hexAmid (0.5 mM in $CDCl_3$, 300 MHz) between a temperature range of 293 – 328K. The temperature dependence of the amide protons indicates the presence of intermolecular hydrogen bonding effects. All spectra were calibrated to the $CDCl_3$ signal at 7.26 ppm.

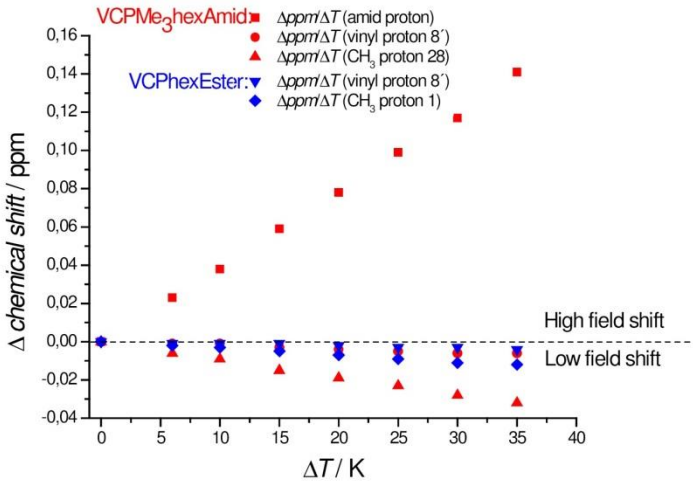

Figure S9: Graphical plot of the some selected proton shifts during variable ^{1}H-NMR temperature experiments. Only the amide proton signal of the VCPMe$_3$hexAmid shows a characteristic shift to higher magnetic fields, which proved the presence of hydrogen bonding for this monomer.

Photo-polymerization mechanism of bi-functional VCP derivatives

The radical photo-polymerization of substituted VCPs results mainly in 1,5-ring-opend polymers units,[3] however, the competitive cyclization reaction predominately to cyclobutane containing units can minimize the benefit of the ring cleavage.[2,3] Therefore several independent polymer units for the cross-linking of VCPs are likely (Scheme S4). The relation of these units depends upon polymerization temperature, viscosity and conversion.[3] So far an unambiguous structural elucidation of cured VCP networks is by the current spectroscopic state of the art techniques difficult, as no technique can resolute and quantify clearly between the cyclobutane-units (B-I and B-II) and the ring-opened units (A-I and A-II) as shown in Scheme S4. Nevertheless, residual monomer because of incomplete conversion can be quantified with extraction experiments (included in the main part of the manuscript). Further, the concentration of partially polymerized VCP units (A-II) seemed to be very low for VCPMe$_3$hexAmid as described in the main part of the manuscript, based on the results of the solid state NMR.

Scheme S4. Schematic radical induced photo polymerization mechanism of bi-functional VCP derivatives.

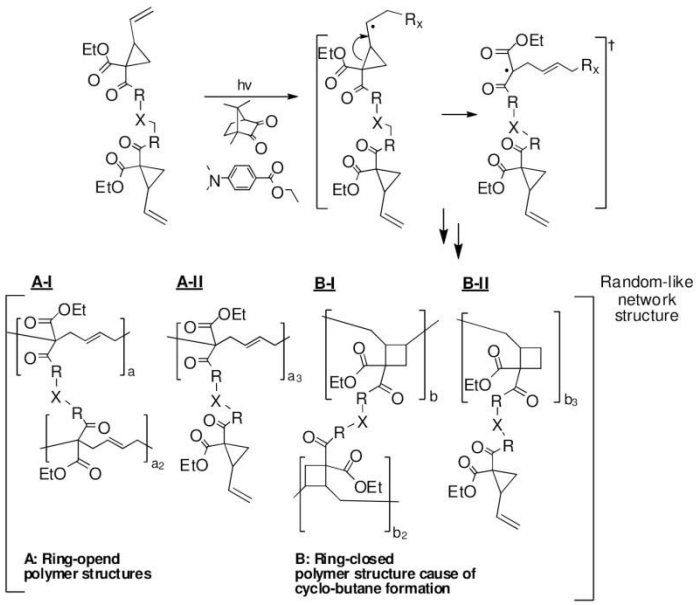

High resolution solid state ^{13}C-NMR spectroscopy of cured VCPMe$_3$hexAmid

High-resolution solid state ^{13}C-CP/MAS (cross polarization/magic angle spinning) NMR Spectra of cured VCPMe$_3$hexAmid were measured by a Bruker spectrometer operating at 100.6 MHz. Within the ^{13}C-CP/MAS spectrum of the cured VCPMe$_3$hexAmid (directly after curing) the peak at 119.7 ppm defines clearly the vinyl-carbon atom 8 + 23 of the VCPMe$_3$hexAmid (Figure S6). In contrast the peak at 129.3 ppm defines the carbon signal of the C=C double bond of the ring-opened VCP-unit.[3] After extraction of residual monomer the peak at 119.7 ppm has gone, only a light shoulder remained, indicating an incomplete but extraordinary high cross-linking (dedicated to the structures of A-II and B-II of Scheme S4). Unfortunately an explicit quantification was not possible as the signal intensity was outside the current detection limit for this method. Further, as mentioned in the main part of the manuscript the formation of cyclobutane-units should be taken into consideration also. As mentioned above an unambiguous structural elucidation of cured VCP networks is unfortunately by the current state of the art techniques difficult, as no technique can resolute clearly between the cyclobutane-units and the ring-opened units as shown in Scheme S4.

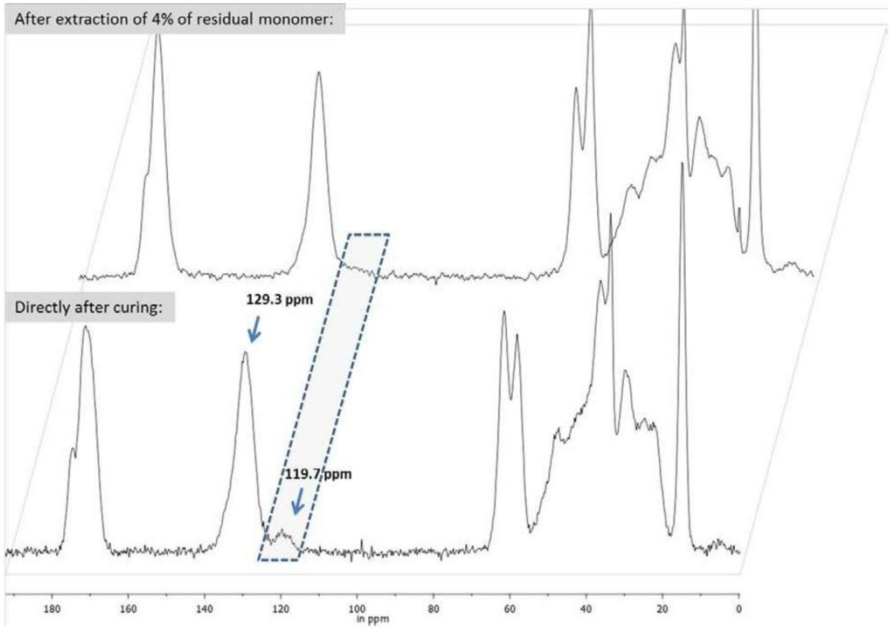

Figure S10: ^{13}C-CP/MAS NMR spectra (100MHz) of cured VCPMe$_3$hexAmid. The lower spectrum shows a cured VCPMe$_3$hexAmid sample directly after curing. The upper graph shows the analogue sample after extraction of 4% of residual monomer. The peak at 129.3 ppm defines the carbon signal of the C=C double bond of the ring-opened VCP-unit. The peak at 119.7 ppm defines clearly the vinyl-carbon atom 8+23 of the VCPMe$_3$hexAmid (Figure S6).

Spectroscopic Ellipsometry: Refractive index measurements

Illustration of the wavelength-dependent dispersion of the refractive index. The refractive index at 589 nm was calculated by averaging over the five values of each sample at 589 nm.

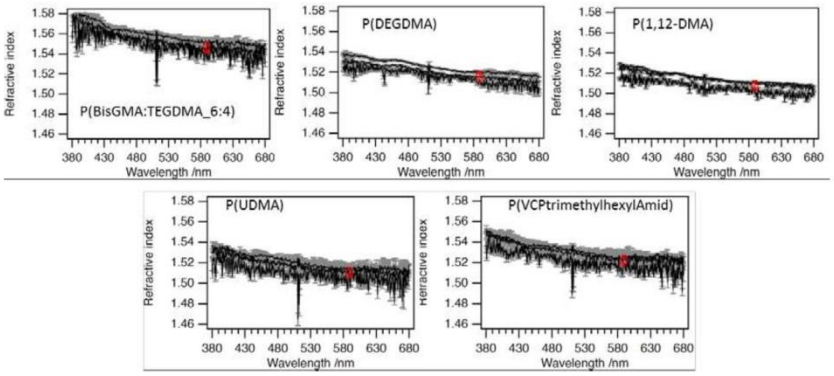

Figure S11. Within SE-determined refractive indices. The graphic display shows the refractive index in dependence of the wavelength. The average value of each specimen at 589 nm has been used for evaluation within the main part

of the manuscript.

Determination of mechanical properties (E-Modulus)

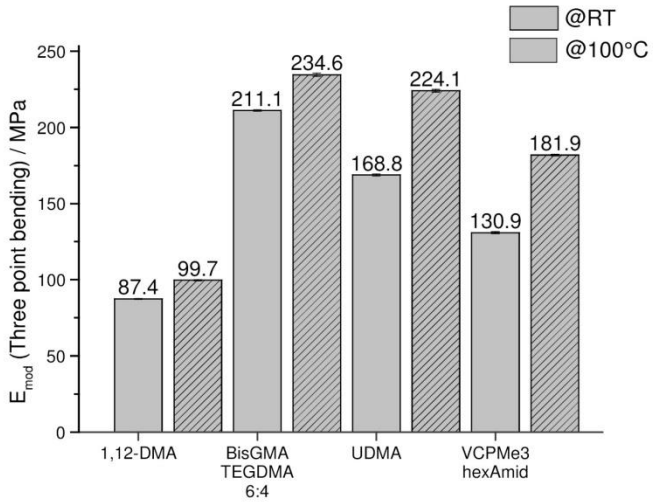

Figure S12. E-modules values of three point bending experiments for cured specimens with sizes of 25x3x1 mm^3. The examinations of the specimens have been carried out once directly after curing and secondly after 12 h storage at 100 °C in vacuo to determine additionally the potential modulus after partial relaxation of internal network tensions.

Determination of residual monomer amount of cross-linked samples by extraction experiments

GC calibration for VCPhexEster:

The GC measurements have been done by a GC-FID system as described within the experimental section for methods. The calibration ranged between ~7 mg mL^{-1} up to 14 µg mL^{-1} (Figure S13).

Concentration / mg/mL	GC area of peak / a.u.
6,951	2176856
1,3902	436798
0,6951	210644
0,13902	31675
0,06951	13245
0,013902	1160

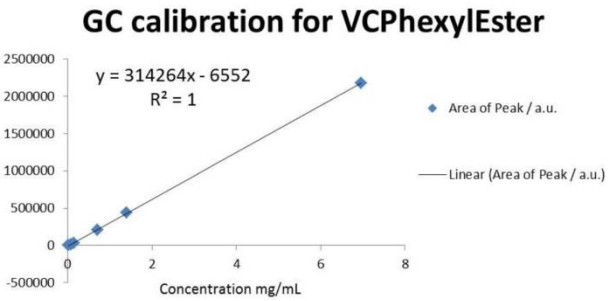

Figure S13. GC calibration for VCPhexEster in a range between ~7 mg mL^{-1} up to 14 µg mL^{-1}.

NMR calibration for VCPMe$_3$hexAmid:

For VCPMe$_3$hexAmid no GC measurements could be performed, as this monomer cannot enter into the gas phase due its higher molar mass and polarity. Therefore, a NMR calibration of VCPMe$_3$hexAmid has been carried out. By comparison the integration areas of the respective ^{1}H-NMR proton signals (amide-, vinyl and cyclopropane-protons) to the proton signals of mesitylene, which has been added to the $CDCl_3$ as internal standard in 2.8216 mg mL^{-1} amount. The concentration range of the established calibration curve of the VCPMe$_3$hexAmid amounted between 5 mg mL^{-1} up to 10 µg mL^{-1}. For each ^{1}H-NMR a number of scans of 2048 has been chosen to achieve an appropriate signal to noise resolution.

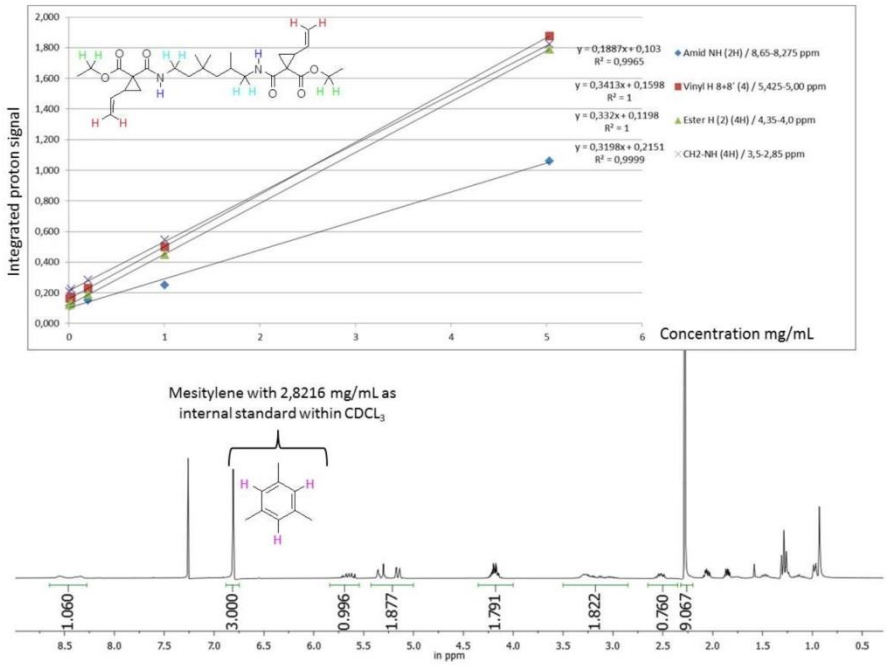

Figure S14. ^{1}H-NMR calibration of VCPMe$_3$hexAmid, inclusive an exemplary proton NMR of a sample with a concentration of 5.03 mg mL^{-1}.

With these calibration curves, the residual monomer amount was determined by extraction experiments. For VCPhexEster the cured and weighted samples have been immediately immersed after radiation to 5.0 mL of chloroform (as extraction fluid) in 10 mL bottles with snap-on caps for 24 h respectively. The bottles have been shacked slightly within a Heidolph Multi Reax shaking system (~500 rpm). Afterwards the supernatant solution has been directly transferred, without any further process, to a GC vial to be measured. According to VCPMe$_3$hexAmid, the weighted and samples have been immediately immersed after radiation to the $CDCl_3$ solution (inclusive the mesitylene standard) for 24 h, respectively. Analog to VCPhexEster the bottles have been shacked slightly within a Heidolph Multi Reax shaking system (~500 rpm). Afterwards 0.7 mL of the supernatant solution has been directly transferred to a NMR vial to be measured.

Compilation of characteristic resin features

Within the main part of the manuscript, several resin features have been mentioned without further specifications. In order to classify all mentioned resins in detail by numerical values within Table S1 relevant data was summarized.

Table S1. Compilation of relevant resin properties, registered with their numerical values.

	1,12-DMA	UDMA	BisGMA	BisGMA-TEGDMA_ 6:4	VCPhex Ester	VCPMe$_3$hex Amid
Molecular weight / g mol^{-1}	338.48	470.56	512.59	422.08	450.52	490.63
Viscosity[a] / Pa s	<0.01	13.8	~1400[7]	0.61	0.08	2.38
Volume shrinkage[b] / %	11.1	8.9	4.7[8]	5.9	-	4.9
E_{mod}[c] / MPa	87.4	168.8	-	211.1	-	130.9
Refractive index[d] (uncured) @589 nm	1.461	1.485	1.549[9]	1.512	1.478	1.499
Refractive index[e] (cured) @589 nm	1.511	1.508	-	1.547	-	1.522
Vickers hardness[f]	0.81	1.80	-	2.18	-	1.55
LD_{50}[g] / mM	>5.00[10]	0.071 ± 0.009	0.08 ± 0.03[8]	-	6.3 ± 2.3	0.067 ± 0.005

[a] Determined at 25 ± 0.5 °C with shearing rate of 100 s^{-1}; [b] determined by the Archimedes's principle; [c] for specimens of the dimension 25x3x1 mm^3, respectively; [d] n_D^{20} value determined by Abbe refractometer; [e] determined by SE; [f] average value of five specimens for measuring forces between 20, 40, 80, 120 and 200 mN; [g] according to the norm ISO 10993-5.

Determination of Cytotoxicity:

The influence of VCPMe$_3$hexAmid and VCPhexEster resins on the metabolic activity of mammalian cells was tested by MTT assay and compared with UDMA used as reference. Therefore, the L929 cells were exposed to UDMA, VCPMe$_3$hexAmid and VCPhexEster for 24h.

The addition of the resins in the concentration range 0 to 20 mM affects the cellular metabolic activity in a concentration-dependent manner (Figure S15 and S16). Under these conditions, the LD_{50} were 0.067 ± 0.005 mM and 6.3 ± 2.3 mM for cells treated with $VCPMe_3hexAmid$ and VCPhexEster, respectively. For VCPhexEster, the cytotoxicities measured at concentrations ≥ 50 mM are similar to the ones detected with the solvent (i.e., DMSO) only (Fig. S16). Whereas, $VCPMe_3hexAmid$ shows cytotoxicity comparable to UDMA (0.071 ± 0.009 mM), the VCPhexEster resin has an 88-fold higher LD_{50} and is therefore less cytotoxic.

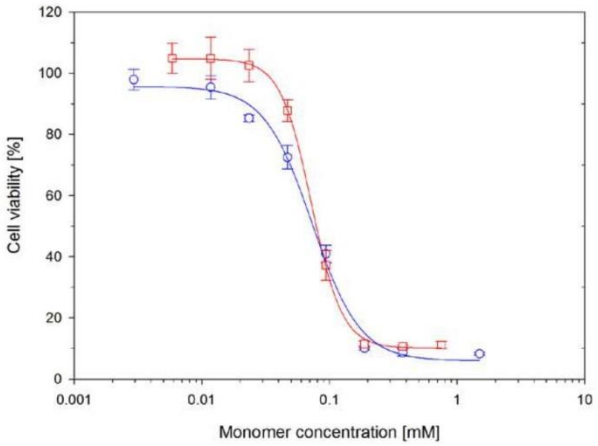

Figure S15. Cytotoxicity of the monomers in L929 cells. (a) Incubation period was 24 hours and cell seeding density 1 $x10^4$ cells per well: (O) UDMA (used as a reference) and (□)$VCPMe_3hexAmid$. The data represent mean ± standard deviation from three independent experiments. There is no significant difference between the curves ($p \leq 0.001$; t-test).

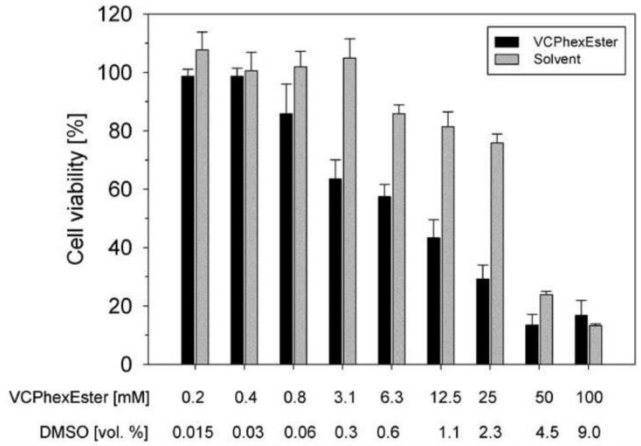

Figure S16. Cytotoxicity of the monomers in L929 cells. (a) Incubation period was 24 hours and cell seeding density 1 x10^4 cells per well in 96-well plate. The data represent mean ± standard deviation from three independent experiments.

References

[1] T. W. H. Oates, H. Wormeester, H. Arwin, *Progress in Surface Science* **2011**, *86*, 328–376.

[2] F. Sanda, T. Takata, T. Endo, *Macromolecules* **1993**, *26*, 1818–1824.

[3] P. Pineda Contreras, P. Tyagi, S. Agarwal, *Polym. Chem.* **2015**, *6*, 2297–2304.

[4] a) V. Alupei, H. Ritter, *Macromol. Rapid Commun.* **2001**, *22*, 1349–1353. b) N. Moszner, F. Zeuner, T. Völkel, U. K. Fischer, V. Rheinberger, *Journal of Applied Polymer Science* **1999**, *72*, 1775–1782.

[5] a) D.K. Kopple, M. Ohnishi, A. Go, *J. Am. Chem. Soc.*, **1969**, *91*, 4264–4272. b) K. H. Scheit, Angew. Chem., **1967**, *79*, 190.

[6] G. Wagner, A. Pardi, K. Wuthrich, *J. Am. Chem. Soc.*, **1983**, *105*, 5948–5949.

[7] S. G. Pereira, T. G. Nunes, S. Kalachandra, *Biomaterials* **2002**, *23*, 3799–3806.

[8] C.-M. Chung, J.-G. Kim, M.-S. Kim, K.-M. Kim, K.-N. Kim, *Dental Materials* **2002**, *18*, 174–178.

[9] C. A. Khatri, J. W. Stansbury, C. R. Schultheisz, J. M. Antonucci, *Dental Materials* **2003**, *19*, 584–588.

[10] W. Geurtsen, F. Lehmann, W. Spahl, G. Leyhausen, *J. Biomed. Mater. Res.* **1998**, *41*, 474–480.

4.3 Publication 3: Photo-polymerizable, low shrinking modular construction kit with high efficiency based on vinylcyclopropanes

Paul Pineda Contreras and Seema Agarwal*, *Polymer Chemistry,* 2016, **7**, 3100–3106.

Makromolekulare Chemie II, Universität Bayreuth, Universitätsstraße 30, 95440 Bayreuth, Germany.

*Corresponding Author: E-mail: agarwal@uni-bayreuth.de; Fax: +49-921-553393.

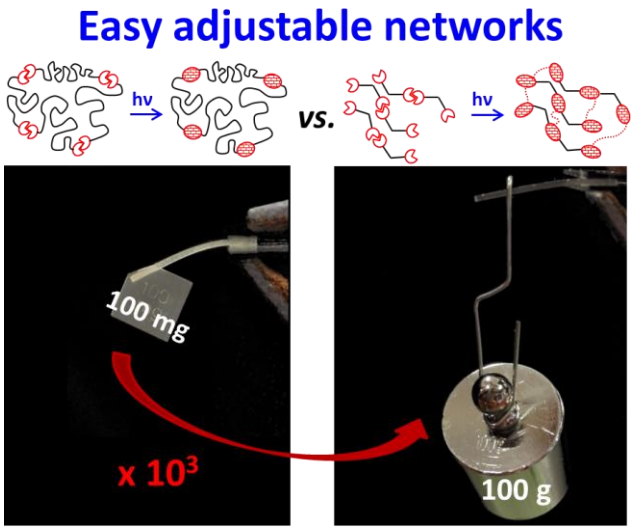

Polymer Chemistry

PAPER

Cite this: *Polym. Chem.*, 2016, **7**, 3100

Photo-polymerizable, low shrinking modular construction kit with high efficiency based on vinylcyclopropanes†

Paul Pineda Contreras and Seema Agarwal*

Received 7th March 2016,
Accepted 10th April 2016

DOI: 10.1039/c6py00411c

www.rsc.org/polymers

The successful development of a universal hydrogen bond (H-bond) concept, specific for bi-functional vinylcyclopropane (VCP) ester–amide derivatives is reported here. Thereby, uniformity within the intermolecular hydrogen bond strength as investigated by variable temperature NMR and FT-IR measurements provides an excellent control of high reactivity, nearly regardless of the chosen spacer-unit, offering the system a possible application as a modular construction kit for cross-linked networks with varied properties. Two entirely diversified VCP ester–amide systems were prepared. The performance benchmark of a flexible, high molar mass macro-monomer VCPPPG$_{2000}$, implementing a polypropyleneglycol Genamine D01/2000 macro-spacer, and two rigid, low molar mass monomers VCP-*m*-phenyl and VCP-*p*-phenyl outlined significantly the strength of the system. Extremely low volume shrinkages between 1.4–4.5% and a wide range of E-moduli could be achieved. An easy control of adjusting final characteristics by varying the co-monomer content in co-networks was shown, especially without obtaining any significant disadvantage in the curing behavior. The VCP ester–amides offer the possibility to replace some currently used dimethacrylate resins within several high-end applications, especially where low volume shrinkage and high polymerization efficiency are required.

Introduction

Bi-functional, cross-linkable resins featuring a variety of precise specifications are of great interest within a wide spectrum of applications, such as electronics,[1] coatings,[2,3] lithography,[4,5] dental applications,[6] 3D microstructures[7] and post-polymerization modifications.[8] However, since the final properties of resins have to match precisely with the complex specifications, there is a demand for monomer-systems providing universality and high precision.[1,9] A suitable method could be to apply low shrinking modular construction kits, merging rather specific techniques within one certain system.

Nevertheless, monomer-systems based on methacrylates pose serious constraints, due to a high discrepancy in photo-curing behaviour, using cross-linkable resins with varied spacer-elements.[10,11] Likewise the observed polymerization shrinkage during curing of methacrylate systems is too high, which can result in high internal compressive stress, leading to microcracks, incomplete fillings, poor adhesion and a short life span of cured resin.[12] Based on these two issues methacrylate systems are not appropriate for low shrinking modular construction kits. An alternative concept, partly developed from the knowledge of low-molecular-weight gelators and supramolecular structures, establishes a further promise on weak forces, such as hydrogen bonds (H-bonds), presuming a partial self-assembly of the molecules. In particular, if a partial self-assembly is taking place selectively at a polymerizable group, a fast and selective curing, as well as targeted control can be assumed, likewise it is required for a modular kit.

Thereby, vinylcyclopropane (VCP) ester–amide derivatives can play a decisive role in the future. Recently we have shown in a special case, that intermolecular amide H-bonds could induce a very effective partial preorganization of bi-functional VCPs molecules, which strongly increased the polymerization behavior.[13] Further, the radical ring-opening polymerization (RROP) of VCP units can significantly reduce the volume shrinkage on polymerization. Therefore, the shrinkage is lower than those recorded for *e.g.* for methacrylate resins, making VCPs attractive as low-shrinking monomers.[14,15]

However, so far the advances within VCP resins have been mainly focused on particular characteristics, *e.g.* reducing the volume shrinkage and improving the reactivity, the ring-

Macromolecular Chemistry II and Bayreuth Center for Colloids and Interfaces, Universität Bayreuth, Universitätsstrasse 30, 95440 Bayreuth, Germany. E-mail: agarwal@uni-bayreuth.de; Tel: +49-921-553397

†Electronic supplementary information (ESI) available: Monomer characterization, TGA curves, ^{13}C solid state NMR, temperature variable IR spectra and X-ray scattering diffractograms. See DOI: 10.1039/c6py00411c

opening efficiency and mechanical properties, especially among researchers in the field of dental fillings.[16–18]

Herein, we report the design of the first highly efficient modular construction kit based on bi-functional VCP ester–amides, extending the general concept of hydrogen-bonding to a universal tool for an extensive application of VCPs as low shrinking resin. The H-bond strength of two diverse VCP ester–amide derivatives was studied in detail, first for a flexible, high molar mass macro-monomer ($VCPPPG_{2000}$, $M_w \sim 2230$ g mol^{-1}), and secondly for a rigid, low molar mass monomer (VCP-*m*-phenyl, $M_w = 468.5$ g mol^{-1}) by temperature dependent NMR- and FT-IR-measurements. Further, a detailed overview of mechanical strength by three point bending experiments, and thermal properties of the cured networks and co-networks by differential scanning calorimetry (DSC) and thermogravimetric (TGA) analysis is provided. In addition to the VCP-*m*-phenyl its constitution isomer of a *para*-phenyl substituted VCP ester–amide resulted in a partial-crystalline system. Thus, the cured and un-cured resins have been studied in detail by nuclear magnetic resonance (NMR) measurements in liquid and solid-state, by temperature dependent polarized microscopy as well as by temperature dependent X-ray diffraction (XRD).

Experimental section

Materials

m-Xylylenediamine (99%), *p*-xylylenediamine (99%), *trans*-1,4-dibromo-2-butene (99%), diethyl malonate (99%), potassium hydroxide (KOH, >85%), *N*,*N*′-dicyclohexylcarbodiimide (DCC, 99%), ethyl 4-(dimethylamino)benzoate (EDMAB, 99%), triethylamine (99%), camphorquinone (CQ, 97%), 1,3,5-trimethylbenzen (mesitylene, >99.8%) and dichloromethane (>99.5%) were supplied by Sigma Aldrich and used without further purification. 1-Hydroxybenzotriazole hydrate (HOBt, >97%, 12% water, Sigma Aldrich) was dried in vacuum prior use. Sodium (>99%, Sigma Aldrich) was purified by melting in dry xylole prior use. Genamine D01/2000 (99%) was provided by Clariant and used as received (determined by (MALDI-TOF-MS): $M_n = 1980$ g mol^{-1}, $M_w = 2027$ g mol^{-1}, $Đ = 1.02$). Urethane-dimethacrylate (UDMA), dodecanediol-dimethacrylate (1,12-DMA) and a 6 : 4 mixture of bisphenol-A-glycidyl methacrylate (BisGMA) and triethylene-glycol-dimethacrylate (TEGDMA) have been provided by the Kettenbach GmbH (Eschenburg, Germany) and were used as received.

Analytical methods

^{1}H- (300 MHz) and ^{13}C-NMR spectra (75 MHz) were recorded on a Bruker Ultrashied-300 spectrometer at room temperature in $CDCl_3$. The spectra were calibrated on the solvent signal ($\delta(^1H) = 7.26$ ppm; $\delta(^{13}C) = 77.16$ ppm). Variable ^{1}H temperature experiments at a concentration of 5 mM in CDl_3 have been performed in a range from 20 °C to 60 °C. High-resolution solid state ^{13}C-CP/MAS (cross polarization/magic angle spinning) NMR Spectra were measured by a Bruker spectrometer operating at 100 MHz, using a pulse experiment with a 30 s pulse delay for 4096 scans. High resolution mass spectra, coupled online to a HPLC system, were recorded on a Q-Exactive Orbitrap (Thermo Scientific). MALDI-TOF MS analysis were performed on a Bruker Reflex III instrument equipped with a N_2 laser ($\lambda = 337$ nm) in linear and reflectron mode. The acceleration voltage was 20 kV. Dithranol (Sigma Aldrich, >98%) was used as matrix material and sodium trifluoroacetate (Sigma Aldrich, 98%) as ionization salt. The samples were prepared with the dried droplet method from THF solution by mixing matrix, polymer and salt in a ratio of 20 : 5 : 1 and applying approximately 1 μL to the target spot. Temperature dependent FT-IR spectra were recorded by a Nicolet Nexus 470 spectrometer with a heated attenuated total reflectance (ATR) unit. Chromatographic purifications were performed using a GRACE Reveleris X2 apparatus. Technical grade solvents, which have been distilled prior use, have been utilized. A dynamic-mechanical analyzer (DMTA IV, Rheometric Scientific) has been used to determine the E-moduli by three-point bending investigations, respectively at 25 °C. A Mettler thermal DSC analyzer (821c) was used for the thermal characterization of the monomer resins and cross-linked polymers. The DSC scans were recorded in nitrogen atmosphere and heating rates of 10 K min^{-1}. Thermogravimetric analysis were done with a TG 209 F1 (Netzsch) by heating the samples up to 800 °C, respectively under nitrogen atmosphere as well as under synthetic air. 85 μm corundum crucibles, heating rates of 10 K min^{-1} and about 10–15 mg of each sample were applied. An AccuPyc 1330 gas pycnometer (Micromeritics) operating with helium gas was used to determine the density of monomers and cross-linked polymers. Temperature dependent XRD patterns were carried out on an X-ray powder diffractometer of the type PANalytical XPert Pro, applying a reaction chamber to measure from 25 to 90 °C in a 2 Theta range from 7 to 35, respectively.

Synthesis of polymer networks

To perform the photo initiation a blue light LED reactor with a light power of ~2.0 mW cm^{-2} at 465 nm was used as radiation source. 1 mol% of the photo-initiator mixture CQ : EDMAB in a molar ratio of 1 : 2 was used. The initiator was dissolved in little DCM and added to the resin. The DCM was evaporated in vaccum prior to curing. For DMTA measurements specimens were produced by filling a stainless steel profile with a dimension of 25 × 3 × 1 mm with the monomer/initiator mixture. The profile was enclosed and fixed both on top and on the bottom with a 50 μm thick hostophan sheet and irradiated for 2 h. The cured specimens were pressed out carefully and stored for 24 h at room temperature prior to further testing. For density measurements the monomer initiator mixture was inserted into a 2 mL standard test tube, flushing the tubes with an argon stream for 30 s and irradiated for 2 h. Afterwards the samples were taken out of the glass tubes and stored for 24 h at 100 °C prior measuring the densities. The partial-crystalline VCP-*p*-phenyl was polymerized in 50 weight% solution of chloroform/toluene (1 : 1). The reaction mixture was

degassed by three freeze–pump–thaw cycles and polymerized within the LED reactor under stirring over 12 h. The polymerization was stopped by putting the test tube into liquid nitrogen; the samples were taken out of the glass tube, transferred into centrifuge tubes and extracted three times by over 25-fold excess of acetone. Afterwards, the resulting polymer was dried in vacuum at 100 °C for 24 h.

Determination of residual monomer amount

The quantification of the residual amount of uncured monomer was performed by ^{1}H-NMR measurements. Therefore the weighed and cured samples have been immediately immersed after radiation in 2.0 mL of $CDCl_3$ (as extraction fluid) in 5 mL bottles for 24 h. The residual monomer amounts have been calculated by comparing the integration areas of the respective ^{1}H-NMR proton signals to the proton signals of mesitylene, which has been added to the $CDCl_3$ as internal standard in 2.8444 mg mL^{-1} amount. To achieve a high signal to noise resolution for each ^{1}H-NMR experiment a number of scans of 2048 has been chosen.

Synthesis of diethyl 2-vinylcyclopropane-1,1-dicarboxylate and 1-(ethoxycarbonyl)-2-vinylcyclopropanecarboxylic acid

Diethyl 2-vinylcyclopropane-1,1-dicarboxylate and the hydrolyzed diethyl 2-vinylcyclopropane-1,1-dicarboxylate were obtained as per published procedure.[14,19]

General procedure to obtain bi-functional VCP ester–amide derivatives

In a round-bottom flask purged with argon 0.5 eq. (0.051 mol) of the diamine compound were dissolved/diluted in 200 mL of anhydrous DCM. The solution was transferred to a funnel, which was connected to 1000 mL three-necked reaction flask, charged with 200 mL of anhydrous DCM, 1.1 eq. (0.112 mol) of 1-(ethoxycarbonyl)-2-vinylcyclopropane-carboxylic acid, 1.1 eq. (0.112 mol) of DCC and 1.15 eq. (0.117 mol) of HOBt. The three-necked reaction flask was stirred for 15 min at room temperature, cooled to 0 °C and then 2.1 eq. (0.214 mol) of triethylamine were added. Afterwards the diamine solution with a drip rate of about 40 mL h^{-1} was added slowly. The reaction solution was stirred for 12 h at room temperature. Subsequently the reaction mixture was filtered, the pale yellow solution was washed two times with water (100 mL), once with 1 molar HCl solution (100 mL) and three times with neutral water (50 mL). After drying over magnesium sulfate, the solution was deposed on silica gel and purified by flash chromatography (general eluents: hexane and ethyl acetate). To the purified organic phase 1500–2500 ppm of butylated hydroxytoluene were added. The organic phase was evaporated in vacuum and the bi-functional VCP–amide derivative dried *in vacuo*. The average yield after purification was 87%. A detailed monomer characterization of the synthesized $VCPPPG_{2000}$, VCP-*m*-phenyl and VCP-*p*-phenyl monomers is provided in the ESI in Fig. S1–S8.†

Results and discussion

The availability of targeted amendments to control selective characteristics by varying the spacer unit, without major transformation *e.g.* in reactivity is crucial for designing a modular construction kit for photo-polymerization purposes. Due to the existence of selective intermolecular H-bonds exactly at the VCP-unit, VCP ester–amide derivatives provide a clear advantage as the curing behaviour is actually independent of the chosen spacer unit. Thereby, Fig. 1A illustrates the universal concept of partial self-assembly for any VCP ester–amide derivative. Moreover, the proposed RROP mechanism of VCP ester–amides (Fig. 1B) clarifies the general efficiency of the intermolecular H-bonds, which are preferred because of N–H···O donor–acceptor interactions and due to chelating effect.

To provide a reasonable illustration, two entirely diversified VCP ester–amide systems were prepared. Thus, first a flexible, high molar mass macro-monomer $VCPPPG_{2000}$ and secondly two rigid, low molar mass monomers VCP-*m*-phenyl and VCP-*p*-phenyl have been synthesized and compared subsequently.

To study the H-bond relationship, both variable-temperature NMR- (Fig. 2) as well as FT-IR-measurements (see Fig. S9 and S10 in the ESI†) have been carried out, for $VCPPPG_{2000}$ and VCP-*m*-phenyl. Thereby the evaluation of the temperature dependency of the amide proton signal revealed the presence of H-bond. The corresponding signal was shifted to higher magnetic field, as with increased temperature a decreased deshielding effect is anticipated.[20,21] The partial regression line of the chemical shift confirmed independently for both VCP ester–amides (R^2 = 0.999), that within the investigated temperature range of 20–60 °C the H-bonds were weaken, but not disrupted. Further, the corresponding slopes of the linear regressions were more or less identical, -4.32×10^{-3} ppm K^{-1} for $VCPPPG_{2000}$ and -4.85×10^{-3} ppm K^{-1} for VCP-*m*-phenyl,

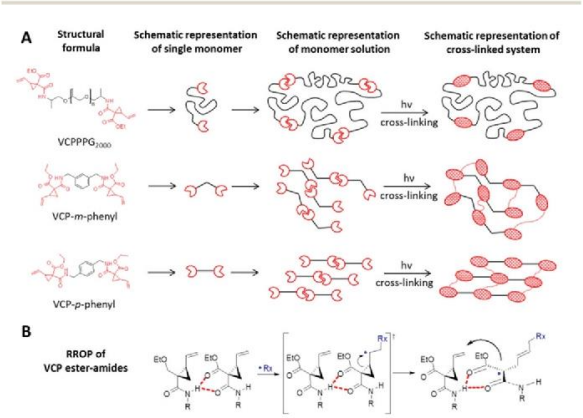

Fig. 1 (A) Schematic aspect of the H-bond mediated partial self-assembly of VCP ester–amide units. The alignment is primary taking place at the functional group. (B) Proposed RROP mechanism of amide-based VCPs. The partial self-assembly and the enhanced orbital arrangements have to be taken into consideration.

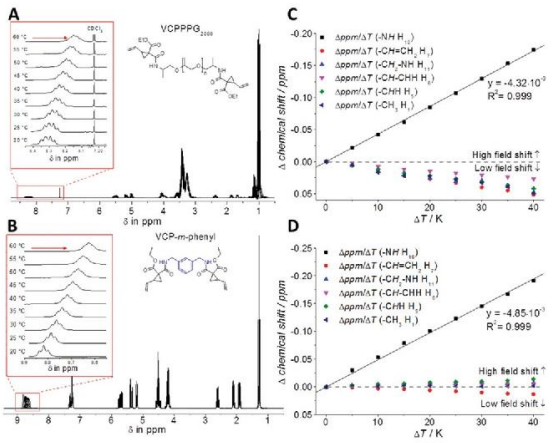

Fig. 2 (A + B) Variable-temperature ^{1}H-NMR experiments of VCPPPG$_{2000}$ and VCPP-*m*-phenyl (0.5 mM in $CDCl_3$) between 20–60 °C. (C + D) Graphical plot of chemical shift within ^{1}H-NMR experiments. With increased temperature a decreased deshielding effect is anticipated, as a partial rupture of the H-bonds occurs.

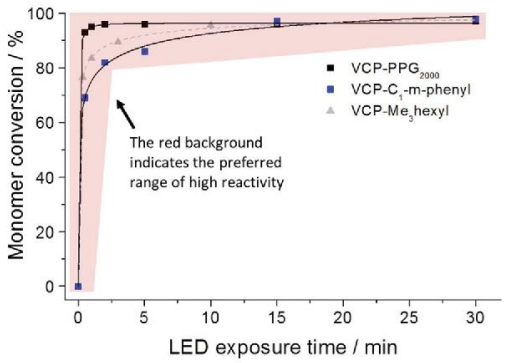

Fig. 3 Determined monomer conversion for the photo-polymerization of VCPPPG$_{2000}$, VCP-*m*-phenyl and VCPMe$_3$hexyl (1 mol% initiator CQ : EDMAB in a molar ratio of 1 : 2). The curing was performed under a controlled atmosphere of nitrogen using a commercial LED source (2.013 mW cm^{-2} for 465 nm).

which confirmed the uniformity of the VCP ester–amide H-bond strength.

In addition to the ^{1}H-NMR experiments, temperature dependent FTIR measurements for the bulk resins underlined this uniformity within the H-bonds. In analogy to the NMR-experiments, an increase in temperature weakened the H-bonds, thus the characteristic IR bands showed an alteration in shape and shift, while non-H-bonded bands remained unchanged. Thus, especially the N–H (3355 cm^{-1}) and C=O stretching vibration (1652 cm^{-1}) shifted to higher frequencies with increased temperature (+4 cm^{-1} and +5 cm^{-1} for VCPPPG$_{2000}$ and VCP-*m*-phenyl, respectively). However, the evidence of the H-bond effect appeared not as pronounced as *e.g.* compared to the well-known urethane-dimethacrylate (UDMA) (see Fig. S11 in the ESI†), since the urethane group contributes to higher coplanarity and higher number of available acceptor atoms compared to VCP ester–amides.[22] Hence for UDMA the N–H (3358 cm^{-1}) and C=O stretching vibration (1702 cm^{-1}) shifted by +20 cm^{-1} and +12 cm^{-1} to higher frequencies. Nevertheless, this did not affect the general curing efficiency of VCP ester–amides, as the H-bonds were sufficiently strong to provide partial preorganization of monomer molecules.

In compliance to the uniform strength of H-bond interaction, for the entirely diversified VCP ester–amides resins VCPPPG$_{2000}$, VCP-*m*-phenyl and VCPMe$_3$hexyl (extended monomer from recently published literature,[13] mentioned for clarification purposes) almost identical curing behaviors were observed (Fig. 3). Hereby curing experiments were carried out by photo-polymerizations using a mixture of camphorquinone (CQ) and ethyl 4-(dimethylamino)-benzoate (EDMAB) in a molar ratio of 1 : 2 as initiator. The exposure with a commercial blue light-emitting diode (LED) could confirm very fast kinetic and high overall conversions. For all investigated VCP ester–amides an overall conversion of >96% could be observed. In comparison, VCP-resins without H-bonded interactions cannot reach high overall conversion even after prolonged curing times.[14] Thus VCP ester–amides like VCPPPG$_{2000}$, VCP-*m*-phenyl as well as the previous studied VCPMe$_3$hexyl have to be seen as pioneers defining a new, universal class of highly efficient and low shrinking resins. However, it is worth noting, that VCPPPG$_{2000}$ reached a conversion of 92% after 30 s of exposure. In this particular case, the slightly enhanced conversion of VCPPPG$_{2000}$ was explained by its low T_g of −55 °C (Table 1). Therefore, a high mobility and continuous diffusion to further radical centers is allowed.

Hence, compared to methacrylate systems, VCP ester–amides show fast curing kinetics irrespective of the spacer unit, but is superior defining the final network characteristics as discussed in Fig. 4.

Thereby, we investigated the mechanical properties of cured VCP ester-amid specimens by three point bending experiments, for VCPPPG$_{2000}$ and VCPP-*m*-phenyl, as well as for the co-networks of VCPPPG$_{2000}$, VCPP-*m*-phenyl and VCPP-*p*-phenyl in different ratios (Fig. 4A). The mechanical pro-

Table 1 Compilation of relevant resin properties

Entry	Polymer	T_g [a]/ °C	$T_{5\%}$ [b] (N_2)/°C	$T_{5\%}$ [c] (air)/°C	Water uptake[d]/%	E_{mod} [e]/ MPa
1	VCPPPG$_{2000}$	−55	340	239	1.3	0.15
2	VCP-*m*-phenyl	147	329	327	2.9	232.3
3	VCP-*p*-phenyl	189	339	321	2.3	—
4	UDMA	119	316	291	2.8	224.1

[a] Determined by DSC. [b] Determined by TGA (50 mL min^{-1} N_2 as purge gas). [c] Determined by TGA (50 mL min^{-1} synthetic air as purge gas). [d] Determined by TGA as mass loss between 30–200 °C, after storage for 48 h at 50 °C in water, respectively. [e] After curing specimens of the dimension 25 × 3 × 1 mm^3 by photo-polymerization and additional annealing for 12 h at 100 °C, respectively.

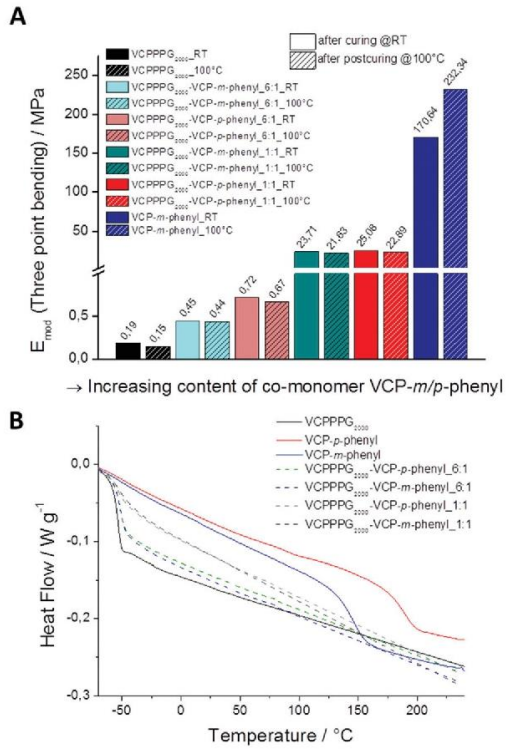

Fig. 4 (A) Determined E-moduli of cured $VCPPPG_{2000}$ and VCPP-*m*-phenyl specimens, as well as by co-networks in ratios of 6 : 1 and 1 : 1 of $VCPPPG_{2000}$, VCPP-*m*-phenyl and VCPP-*p*-phenyl. With increasing content of the co-monomer VCP-*m*/*p*-phenyl, the moduli could be raised up to 1200 times to higher values. (B) Second DSC heating trace of cured VCP specimens, illustrating the glass transition T_g of the cured samples.

perties of the cured specimens have been investigated once directly after curing, and secondly after annealing those 12 h at 100 °C. Thus the additional potential modulus, after partial relaxation of internal network tensions (sub-T_g relaxation) could be determined.[23,24] Subsequent extractions with $CDCl_3$ confirmed conversions higher than 98% for all specimens. Cured $VCPPPG_{2000}$ specimens showed E-moduli of 0.19 ± 0.001 MPa, reflecting predominantly the characteristic of a highly cross-linked organogel. Anealing at 100 °C did not affect significantly the modulus (0.15 ± 0.001 MPa), as the T_g for these cured specimens was much lower as the curing temperature (25 °C). In contrast, for cured VCP-*m*-phenyl specimens the E-modulus could be increased by +36%, since the softening temperature for these specimens was much higher (147 °C).

Further, we could easily control the E-moduli by varying the co-monomer content in the co-networks. With increasing content of the co-monomer VCP-*m*/*p*-phenyl, the moduli could be raised continuously from 0.19 ± 0.001 MPa for $VCPPPG_{2000}$, up to a value of 232.3 ± 0.5 MPa for the cured VCP-*m*-phenyl. Thus, the moduli could be raised up to 1200 times to higher values. Thereby cured VCP-*m*-phenyl resins can compete clearly with commercially available UDMA resins, which provide moduli of 168.8 ± 0.5 MPa and 224.1 ± 0.4 MPa, respectively. In our previous study, $VCPMe_3$hexyl showed E-moduli of 130.9 ± 0.7 MPa and 181.9 ± 0.5 MPa, respectively just after curing and post-curing.[13] This supports the above hypothesis by a third example, that primarily the spacer unit is defining the network properties, whereas the curing behaviour remains constant. Furthermore, according to the high T_g of 147 and 189 °C for the cured VCP-*m*-phenyl and VCP-*p*-phenyl resins (Table 1) the mechanical properties of these networks can be utilized over a wide temperature range.

Moreover, the corresponding thermal characteristics of these cured resins exhibited high potential as well. High overall thermal stabilities could be observed ($T_{5\%}$ > 320 °C) under nitrogen atmosphere as well under air. In contrast, several di-methacrylate networks such as UDMA showed a significant lower stability under identical conditions. In particular, under an atmosphere of air a fast oxidation of the di-methacrylate networks occurred at temperatures of already 290 °C (Table 1 and Fig. S12A in the ESI†). Further, the water absorption of the cured VCP ester–amide networks was less than 3%, as determined by TGA (see Fig. S12B in the ESI†). Especially with regard to the applicability for coatings and dental materials a low water-uptake is required in order to provide durability.[25,26]

Subsequently, the cured VCP ester–amide networks were analyzed by ^{13}C-CP/MAS solid-state spectroscopy. Due to the absence of the carbon atom of the terminal vinyl bond at 119.7 ppm an extraordinary high cross-linking density of the cured networks could be confirmed, respectively for VCP-*m*-phenyl (Fig. 5) and VCP-*p*-phenyl (S13 in the ESI†). Only a very small shoulder remained, hardly perceived, which indicated a negligible amount of remaining vinyl double bonds.

Further to depict the general potential of reducing the volume-shrinkage during polymerization by applying RROP of

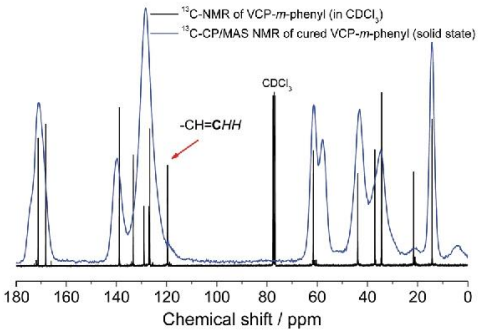

Fig. 5 ^{13}C-NMR comparison: ^{13}C NMR ($CDCl_3$, 75 MHz) of un-cured VCP-*m*-phenyl and ^{13}C-CP/MAS NMR (100 MHz) of cured VCP-*m*-phenyl. The signal at 119.7 ppm defines the carbon atom of the terminal vinyl bond. After curing within the ^{13}C-CP/MAS NMR spectra only a shoulder, hardly perceived at 119.7 ppm, is observed, which indicates a high cross-linking density of the cured VCP-*m*-phenyl.

VCP ester–amide resins, the corresponding state variables volume shrinkage, monomer- and polymer density for cured and uncured states were provided within Fig. 6. Very low volume changes between −4.5% to −1.4% have been determined for the VCP ester–amide resins, as well as for their co-networks in different ratios. It is remarkable, that the cured VCP-*m*-phenyl showed a reduction by 50% in volume shrinkage compared *e.g.* to UDMA, without compromising mechanical performance. $VCPPPG_{2000}$ showed an extremely low volume shrinkage (−1.4%), represented by its increased molecular weight as macro-monomer.[9,27]

In this context we observed a significant difference between the cured isomers VCP-*m*-phenyl and VCP-*p*-phenyl. While VCP-*m*-phenyl showed a volume change of −4.5%, for VCP-*p*-phenyl a volume change of −1.9% was observed. In comparison to the amorphous VCP-*m*-phenyl, its isomer VCP-*p*-phenyl occurs as a heterogeneous system, combining a liquid resin with partial crystallinity. Thereby the DSC curve of VCP-*p*-phenyl showed a melting at T_m = 67 °C, whereas VCP-*m*-phenyl remained completely amorphous (Fig. 7A). In agreement with the DSC measurement, temperature variable polarizing microscopy showed at the same temperature range a transition to an isotropic melt, respectively for VCP-*p*-phenyl (Fig. 7B).

Thus an increased density of VCP-*p*-phenyl (1.139 g cm^{-3}) was observed in comparison to VCP-*m*-phenyl (1.105 g cm^{-3}). A complete crystallization of VCP-*p*-phenyl is hindered, due to the general isomeric structure of VCP ester–amides (see Scheme S1 in the ESI†). Furthermore, once the crystalline phase is melted the reverse crystallization occurs within a longer time lag over weeks, thus within the XRD diffractogram no reflexes returned after cooling the resin back to room temperature (see Fig. S14 within the ESI†).

Generally, the volume change is calculated by the densities of the cured and uncured resins. As in most cases the density of the cured resin is higher, negative volume changes are observed. However, volume expandable resins are known within the literature as well.[28,29] Yet, their applicability is restricted, as the volume expansion is mainly based to the transition of a denser crystalline monomer structure compared to a less compressed, amorphous polymer structure. In fact, this attitude is lost, if the crystalline phase is melted or diluted by any further phase, like it can be observed also for the co-networks of VCP-*p*-phenyl (Fig. 5). In this sense heterogeneous systems, like VCP-*p*-phenyl, have to be seen as an intermediate stage between both physical states, offering a further alternative to reduce the volume shrinkage. Especially the connection of an easy processable wax-like structure and the low volume shrinkage exhibit further potential for composite formulations, and will be investigated in a following work.

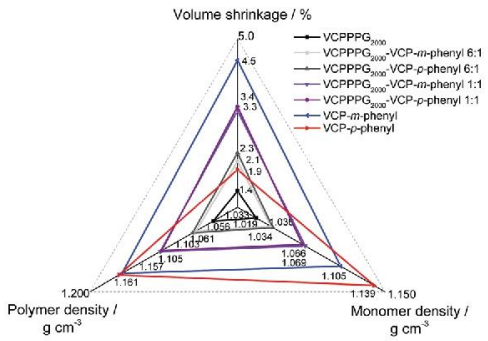

Fig. 6 Spider chart showing the dependency between the monomer- and polymer density to the volume shrinkage. Only the partial-crystalline VCP-*p*-phenyl shows a disproportion within the correlation, based due to the denser partial-crystalline monomer structure of VCP-*p*-phenyl (1.139 g cm^{-3}).

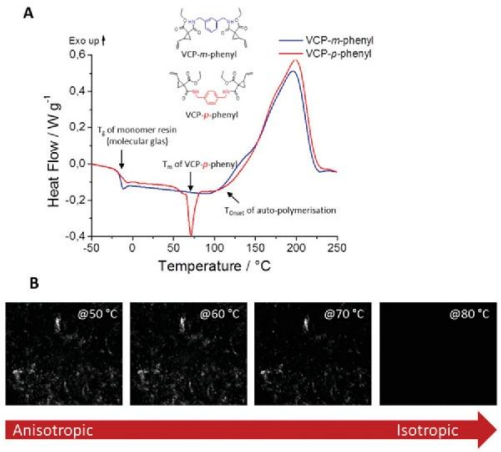

Fig. 7 (A) DSC curves of first heating cycles of un-cured VCP-*m*/*p*-phenyl resins. First the transition from a molecular glass to a resin (T_g – 15 °C) is passed, respectively for both VCPs. In the further heating VCP-*m*-phenyl shows a complete amorphous behavior, whereas for VCP-*p*-phenyl a melting (onset at 67 °C) is observed. At a temperature range of ~99 °C an auto-polymerization of both resins is observed. (B) Polarized microscopy images of the partial-crystalline VCP-*p*-phenyl resin. Beneath the melting transition both amorphous as well as crystalline areas can be observed. When the melting range is passed the VCP-*p*-phenyl resin becomes fully isotropic.

Conclusions

A uniformity of the VCP ester–amide H-bond strength was shown, providing a universal concept of applying VCP ester–amides as suitable low-shrinking resins. With an excellent control of high reactivity, nearly regardless of the spacer-unit chosen, VCP ester–amides offer a clear advantage in comparison to methacrylate based systems. Thus with an appropriate variation of spacer-unit, selective characteristics, like *e.g.* optical properties or mechanical strength could be adjusted in a simple way, without obtaining any significant disadvantage within the curing behaviour. Based on this concept, new VCP ester–amide resins were presented, showing very low volume

changes between −1.4 to −4.5%, a broad variety in mechanical strength between 0.19 to 232 MPa and a high overall thermal stability even under an atmosphere of air. Thereby the network properties could be continuously adjusted by varying the co-monomer content in co-networks. Moreover, due to the inevitable isomeric mixtures of VCP ester–amides, a heterogeneous system could be achieved, combining liquid phase with partial crystallinity, offering an intermediate stage between both physical states. The presented concept of applying VCP ester–amides as low shrinking resins for a modular construction kit is facile and variable. Thus VCP ester–amides offer vast potential for commercial use; especially as the number of combinations possibilities respectively for specified spacer units are yet not exploited.

Acknowledgements

We sincerely thank J. Schöbel for MALDI-TOF analysis, and Dr R. Giesa (MCI), Prof. J. Senker and Dr R. Siegel (both ACIII), Prof. J. Breu and Dr W. Milius (both ACI), Prof. M. Willert-Porada and I. Otto (both Chair of Materials Processing) all of University of Bayreuth for providing diverse access to DMTA, solid-state NMR technique, XRD measurements and a gas-pycnometer.

Notes and references

1 Y. Fuchs, O. Soppera and K. Haupt, *Anal. Chim. Acta*, 2012, **717**, 7.
2 Y. Jian, Y. He, L. Zhao, A. Kowalczyk, W. Yang and J. Nie, *Adv. Polym. Technol.*, 2013, **32**, 21331.
3 E. Andrzejewska, *Prog. Polym. Sci.*, 2001, **26**, 605.
4 C. Decker, *Macromol. Rapid Commun.*, 2002, **23**, 1067.
5 C. Gorsche, K. Seidler, P. Knaack, P. Dorfinger, T. Koch, J. Stampfl, N. Moszner and R. Liska, *Polym. Chem.*, 2016, **7**, 257.
6 K. L. van Landuyt, J. Snauwaert, *et al.*, *Biomaterials*, 2007, **28**, 3757.
7 A. S. Quick, A. de los S. Pereira, M. Bruns, T. Bückmann, C. Rodriguez-Emmenegger, M. Wegener and C. Barner-Kowollik, *Adv. Funct. Mater.*, 2015, **25**, 3735.
8 D. H. Seuyep Ntoukam, G. A. Luinstra and P. Theato, *J. Polym. Sci., Part A: Polym. Chem.*, 2014, **52**, 2841.
9 K. S. Anseth, C. N. Bowman and N. A. Peppas, *J. Polym. Sci., Part A: Polym. Chem.*, 1994, **32**, 139.
10 I. Sideridou, V. Tserki and G. Papanastasiou, *Biomaterials*, 2002, **23**, 1819.
11 S. H. Dickens, J. W. Stansbury, K. M. Choi and C. J. E. Floyd, *Macromolecules*, 2003, **36**, 6043.
12 J. W. Stansbury, M. Trujillo-Lemon, H. Lu, X. Ding, Y. Lin and J. Ge, *Dent. Mater.*, 2005, **21**, 56.
13 P. Pineda Contreras, C. Kuttner, A. Fery, U. Stahlschmidt, V. Jerome, R. Freitag and S. Agarwal, *Chem. Commun.*, 2015, **51**, 11899.
14 P. Pineda Contreras, P. Tyagi and S. Agarwal, *Polym. Chem.*, 2015, **6**, 2297.
15 N. Moszner and U. Salz, *Macromol. Mater. Eng.*, 2007, **292**, 245.
16 N. Moszner, F. Zeuner, T. Völkel and V. Rheinberger, *Macromol. Chem. Phys.*, 1999, **200**, 2173.
17 F. Sanda and T. Endo, *J. Polym. Sci., Part A: Polym. Chem.*, 2001, **39**, 265.
18 V. Alupei and H. Ritter, *e-Polym.*, 2002, **2**, 724.
19 V. Alupei and H. Ritter, *Macromol. Rapid Commun.*, 2001, **22**, 1349.
20 K. D. Kopple, M. Ohnishi and A. Go, *J. Am. Chem. Soc.*, 1969, **91**, 4264.
21 V. Berl, M. Schmutz, M. J. Krische, R. G. Khoury and J.-M. Lehn, *Chem. – Eur. J.*, 2002, **8**, 1227.
22 M. T. Lemon, M. S. Jones and J. W. Stansbury, *J. Biomed. Mater. Res., Part A*, 2007, **83**, 734.
23 J. Lange, S. Toll, J.-A. E. Månson and A. Hult, *Polymer*, 1997, **38**, 809.
24 J. Tu, S. J. Tucker, S. Christensen, A. R. Sayed, W. L. Jarrett and J. S. Wiggins, *Macromolecules*, 2015, **48**, 1748.
25 S. G. Pereira, T. G. Nunes and S. Kalachandra, *Biomaterials*, 2002, **23**, 3799.
26 J. Park, G. Lee, H. Ooshige, A. Nishikata and T. Tsuru, *Corros. Sci.*, 2003, **45**, 1881.
27 J. E. Klee and U. Lehmann, *J. Org. Chem.*, 2009, **5**, 72.
28 H. Chiba, K. Kitazume, S. Yamada and T. Endo, *J. Polym. Sci., Part A: Polym. Chem.*, 2015, **54**, 39.
29 N. Moszner and U. Salz, *Prog. Polym. Sci.*, 2001, **26**, 535.

Supporting Information

Photo-polymerizable, low shrinking modular construction kit with high efficiency based on vinylcyclopropanes

*By Paul Pineda Contreras and Seema Agarwal**

Author information:
Macromolecular Chemistry II, University of Bayreuth and Bayreuth center for Colloids and Interfaces, 95440, Bayreuth, Germany; Fax: +49921-553393; Tel: +49921-553398; E-mail: agarwal@uni-bayreuth.de

Content

Supplementary Information according to Experimental Part 2

Complexness of isomeric structures for bi-functional VCP derivatives 2

Supplementary Analytical Data 8

Temperature variable FT-IR measurements (ATR measurements of bulk material) 9

Thermal analysis by TGA experiments 10

High resolution solid state ^{13}C-NMR spectroscopy of cured VCP ester-amides 12

Further investigation of the partial crystallinity of VCP-p-phenyl 12

References 13

Supplementary Information according to Experimental Part

Complexness of isomeric structures for bi-functional VCP derivatives

The hydrolysis of the racemic 2-vinylcyclopropane-1,1-dicarboxylate results in a racemic mixture of diastereoisomers in a ratio of about 90:10. With continuing synthesis the isomeric complexity is passed on. To avoid losing a general overview over the basic monomer structure, only the most probable isomeric structure is presented within the main part of the manuscript. However, at this point an exemplary structural description of a VCP derivative is presented within Scheme S1.

Scheme S1. Exemplary structural description of the stereo centers and the isomeric complexity of VCP derivatives.

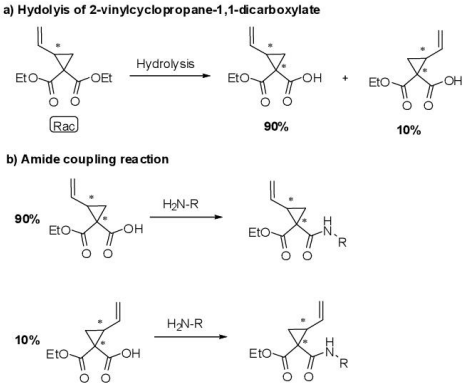

Characterization of polypropyleneglycole Genamine D01/2000 end-capped with two ethyl 1-(carbamoyl)-2-vinylcyclopropanecarboxylate units (in this work abbreviated to VCPPPG2000)

^{1}H-NMR (300 MHz, $CDCl_3$): δ = 8.83-8.32 (m, 2 H, NH), 5,70-5.55 (m, 2 H, CH=CH_2), 5.34-5.26 (m, 2 H, CH=CHH), 5.15-5.11 (m, 2 H, CH=CHH), 4.24-4.02 (m, 2 H, NH-CH, 4 H, O-CH_2), 3.77-3.23 (overlapping of proton signals: 3.77-3.60, m, O-CH_2, 3.60-3.23, m, O-CH_2 and O-CH_3 of PPG repeat unit) 2.55-2.44 (m, 2H, CH-CH), 2.02-1.97 (m, 2H, -CHH), 1.83-1.79 (m, 2H, -CHH), 1.29-1.18 (overlapping of proton signals, m, 2 x 3H, -CH_3), 1.18-1.00 (broad s, -CH_3 of PPG repeat unit); ^{13}C-NMR (75 MHz, $CDCl_3$) δ = 170.6 (NH-C=O), 166.9 (O-C=O), 133.2 (CH=CH_2), 119.0 (CH=CHH), 75.0 (O-CH_2), 73.4-71.8 (backbone of PPG repeat unit), 61.0 (O-CH_2), 45.4 (-CH), 36.2 (CH-CH), 34.0 (C_4), 20.9 (>CHH), 18.0 (CH_3), 17.1 (-CH_3 of PPG repeat unit), 13.9 (-CH_3); FT-IR (attenuated total reflectance (ATR)): ν = 3358 (w), 2971 (m), 2868 (m), 1707 (m), 1655 (m), 1526 (w), 1451 (m), 1373 (s), 1342 (m), 1298 (m), 1260 (w), 1098 (vs), 1015 (s), 920 (m), 864 (m), 833 (w), 733 (m); n_D^{20} = 1.462; determined by DSC: glass transition temperature of monomer T_g = -55 °C, determined by (MALDI-TOF-MS): M_n = 2126 g mol^{-1}, M_w = 2146 g mol^{-1}, PDI = 1.01.

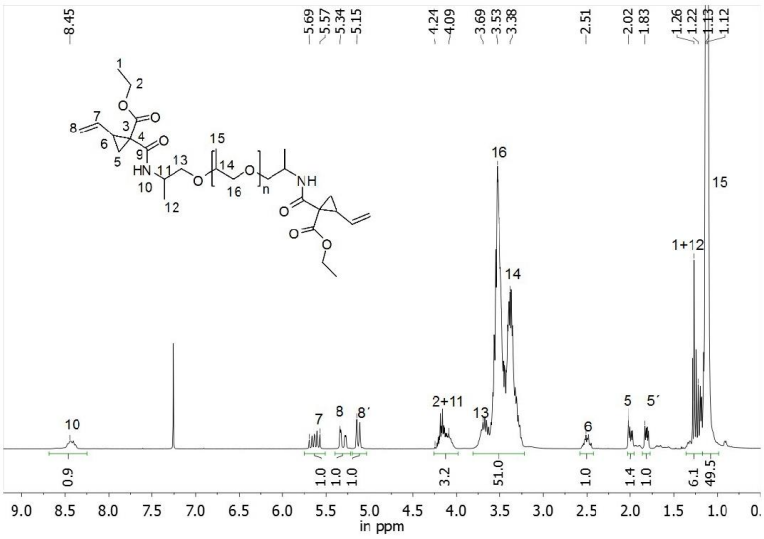

Figure S1: ^{1}H NMR of VCPPPG2000 ($CDCl_3$, 300 MHz).

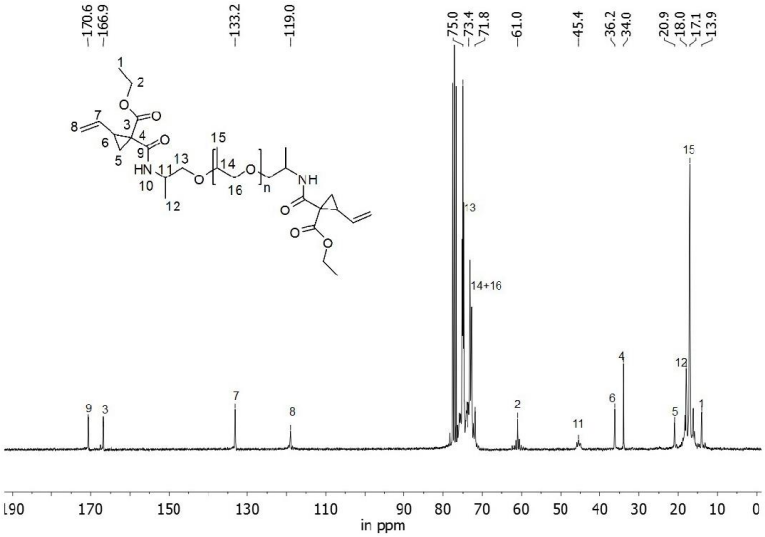

Figure S2: ^{13}C NMR of VCPPPG2000 ($CDCl_3$, 75 MHz).

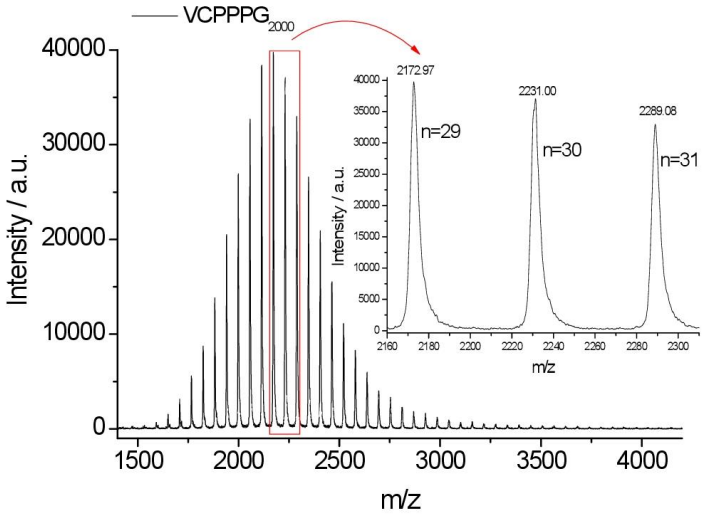

Figure S3: Full MALDI-TOF MS spectrum (linear mode) with an enlargement of 2160-2320 *m/z* region of $VCPPPG_{2000}$.

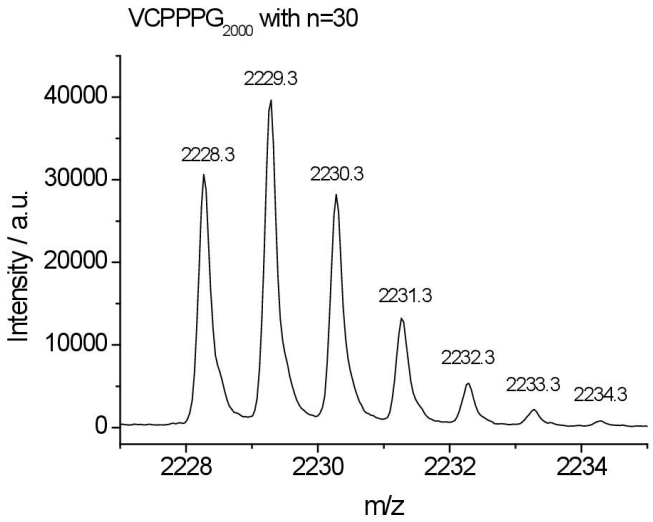

Figure S4: Enlargement of MALDI-TOF MS spectrum within the reflectron mode in the region of 2227-2235 *m/z* region confirms the structural identification of $VCPPPG_{2000}$.

Characterization of diethyl 1,1'-(1,4-phenylenebis(methylene))bis(azanediyl)bis-(oxomethylene)-bis(2-vinylcyclopropanecarboxylate) (in this work abbreviated to "VCP-p-phenyl")

^{1}H-NMR (300 MHz, $CDCl_3$): δ = 8.83-8.45(m, 2 H, NH), 7.32 – 7.22 (s, 4H, aromatic protons) 5.74-5.59 (m, 2 H, CH=CH_2), 5.36-5.29 (m, 2 H, CH=CHH), 5.17-5.12 (m, 2 H, CH=CHH), 4.54-4.37 (m, 4 H, NH-CH_2), 4.23-4.05 (m, 4 H, O-CH_2), 2.62-2.53 (m, 2H, CH-CH), 2.10-2.04(m, 2H, >CHH), 1.90-1.85(m, 2H, >CHH), 1.26-1.22 (t, 3H, -CH_3); ^{13}C-NMR (75 MHz, $CDCl_3$) δ = 171.4 (NH-C=O), 168.1(O-C=O), 137.6 ($C_{arom.}$), 133.4 (CH=CH_2), 128.1 ($C_{arom.}$), 119.7 (CH=CHH), 61.6 (O-CH_2), 43.8 (-CH_2), 37.2 (CH-CH), 34.4 (C_4), 21.6 (-CHH), 14.3 (-CH_3); FT-IR (attenuated total reflectance (ATR)): ν = 3345 (m), 3084 (w), 2983 (w), 2934 (w), 1703 (vs), 1647 (s), 1525 (vs), 1466 (w), 1429 (m), 1372 (m), 1335 (m), 1314 (s), 1196 (m), 1139 (vs), 1071 (w), 1018 (m), 995 (m), 957 (m), 915 (s), 856 (m), 831 (m), 775 (w), 752 (m), 623 (m), 573 (m); HRMS (ESI, pos.) m/z calculated for $C_{26}H_{32}O_6N_2$ $[M + H]^+$ 469.2333, found 469.2331 and 491.2149 $[M + Na]^+$; determined by DSC: glass transition temperature T_g = -15 °C.

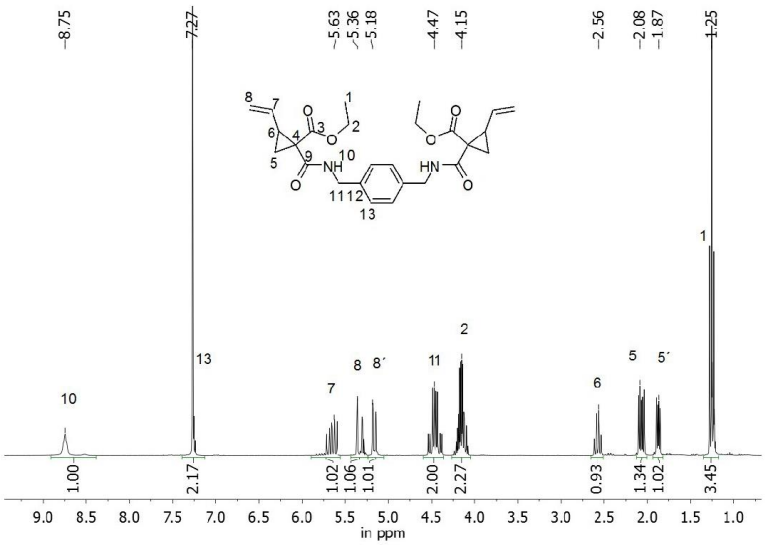

Figure S5: ^{1}H NMR of VCP-p-phenyl ($CDCl_3$, 300 MHz).

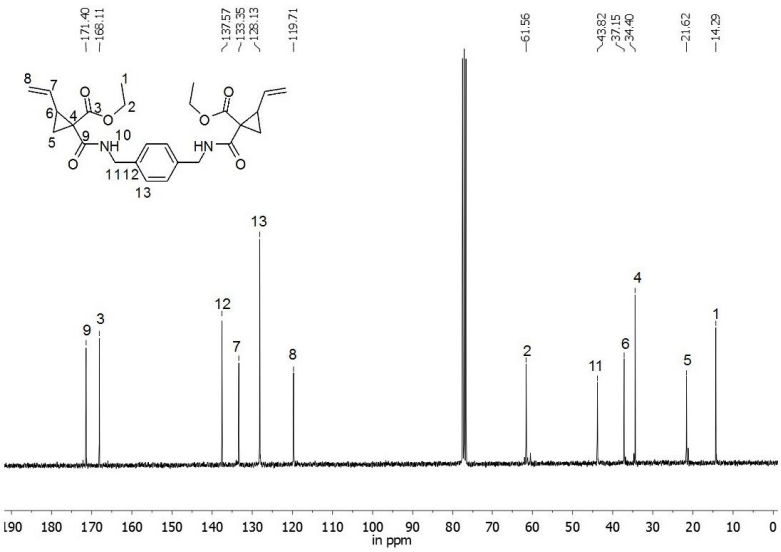

Figure S6: ^{13}C-NMR of VCP-p-phenyl ($CDCl_3$, 75 MHz).

Characterization of diethyl 1,1'-(1,3-phenylenebis(methylene))bis(azanediyl)bis-(oxomethylene)-bis(2-vinylcyclopropanecarboxylate) (in this work abbreviated to "VCP-m-phenyl")

^{1}H-NMR (300 MHz, $CDCl_3$): δ = 8.82-8.45(m, 2 H, NH), 7.32 – 7.17 (m, 4H, aromatic protons) 5.74-5.59 (m, 2 H, $CH=CH_2$), 5.36-5.29 (m, 2 H, CH=CHH), 5.17-5.12 (m, 2 H, CH=CHH), 4.54-4.37 (m, 4 H, $NH-CH_2$), 4.23-4.05 (m, 4 H, $O-CH_2$), 2.62-2.53 (m, 2H, CH-CH), 2.10-2.04(m, 2H, >CHH), 1.90-1.85(m, 2H, >CHH), 1.26-1.22 (t, 3H, $-CH_3$); ^{13}C-NMR (75 MHz, $CDCl_3$) δ = 171.3 (NH-C=O), 168.1(O-C=O), 138.8 ($C_{arom.}$), 133.3 ($CH=CH_2$), 129.1 ($C_{arom.}$), 127.1 ($C_{arom.}$), 126.7 ($C_{arom.}$), 119.7 (CH=CHH), 61.5 ($O-CH_2$), 43.9 ($-CH_2$), 37.1 (CH-CH), 34.3 (C_4), 21.6 (-CHH), 14.2 ($-CH_3$); FT-IR (attenuated total reflectance (ATR)): ν = 3353 (m), 3084 (w), 2983 (w), 2934 (w), 1703 (vs), 1653 (s), 1525 (vs), 1443 (m), 1372 (m), 1335 (w), 1312 (s), 1265 (w), 1198 (m), 1139 (vs), 1071 (w), 1019 (m), 993 (m), 958 (m), 914 (s), 862 (m), 833 (m), 772 (w), 733 (m), 702 (m), 644 (m); n_D^{20} = 1.535; HRMS (ESI, pos.) m/z calculated for $C_{26}H_{32}O_6N_2$ $[M + H]^+$ 469.2333, found 469.2331 and 491.2151 $[M + Na]^+$; determined by DSC: glass transition temperature T_g = -15 °C.

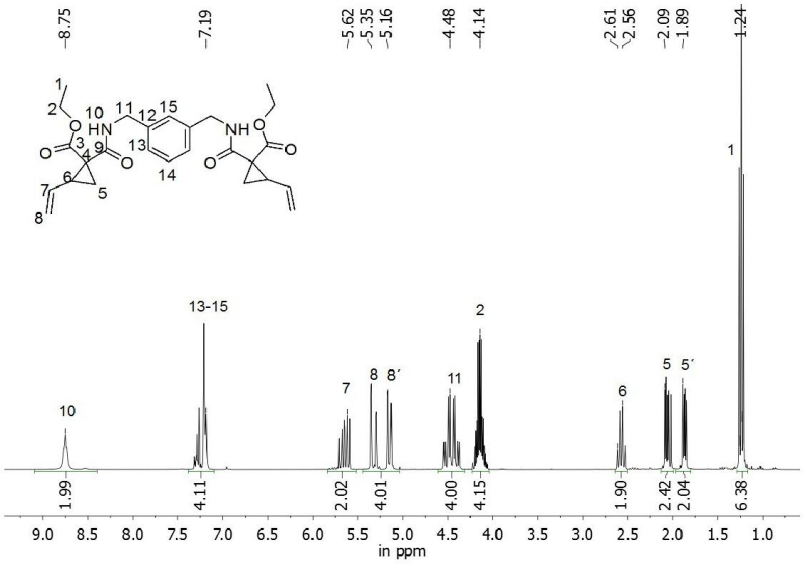

Figure S7: ^{1}H NMR of VCP-m-phenyl ($CDCl_3$, 300 MHz).

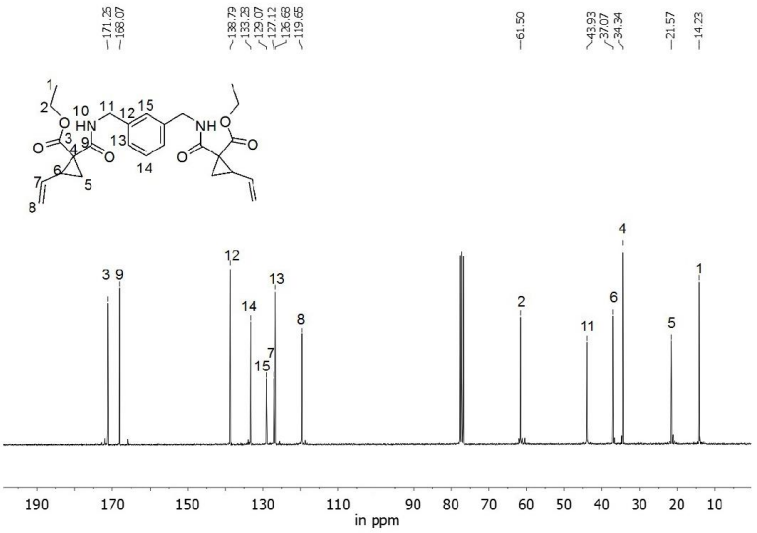

Figure S8: ^{13}C-NMR of VCP-m-phenyl ($CDCl_3$, 75 MHz).

Supplementary Analytical Data

Temperature variable FT-IR measurements (ATR measurements of bulk material)

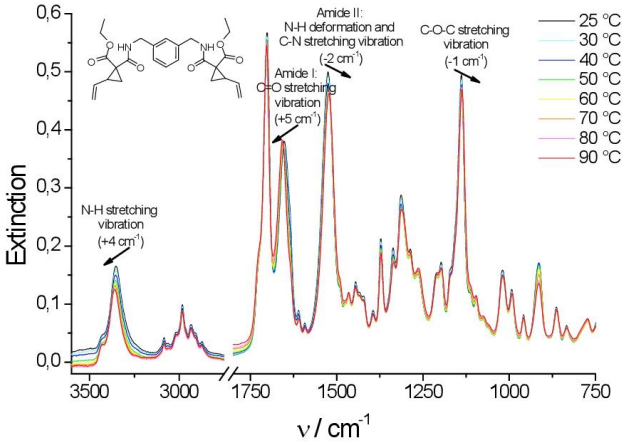

Figure S9: Recorded FT-IR(ATR) spectra of VCP-m-phenyl between temperature ranges of 25 – 90 °C. Due to the temperature dependency of hydrogen bonds, with increased temperature these bonds are weakened and show an alteration in shape and shift. Thus, especially the N-H (3355 cm^{-1}) and C=O (1652 cm^{-1}) stretching vibration of the amide group shift to higher frequencies with increased temperature. Compared to UDMA the shift is less strong, as hydrogen bonds of urethane groups are general more strong than for amides, and secondly for UDMA a higher number of acceptor atoms is available (8 oxygen atoms).

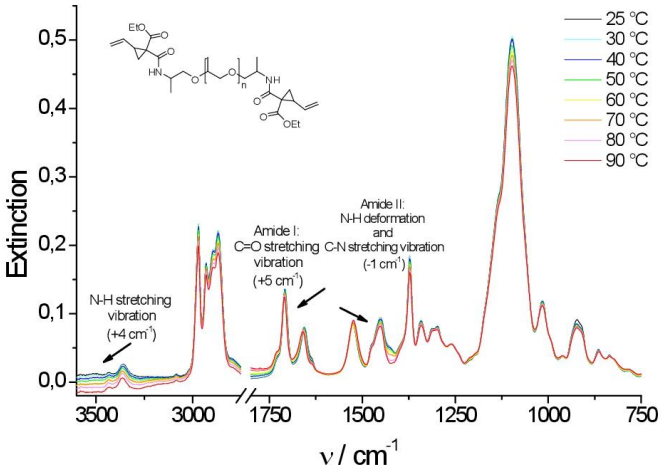

Figure S10: Recorded FT-IR(ATR) spectra of $VCPPPG_{2000}$ between temperature ranges of 25 – 90 °C. Due to the temperature dependency of hydrogen bonds, with increased temperature these bonds are weakened and show an alteration in shape and shift. Thus, especially the N-H (3358 cm^{-1}) and C=O (1656 cm^{-1}) stretching vibration of the amide group shift to higher frequencies with increased temperature. Compared to VCP-m-phenyl the shift of the signals to higher and lower frequencies is equally strong, which confirms that the strength of the hydrogen bonds of VCP-m-phenyl and $VCPPPG_{2000}$ should be at near equal level. However, due the signal intensity of the functional groups of $VCPPPG_{2000}$ is lower, as the signals of the PPG macro-spacer account to the main IR-activity. Nevertheless the tendency is still visible.

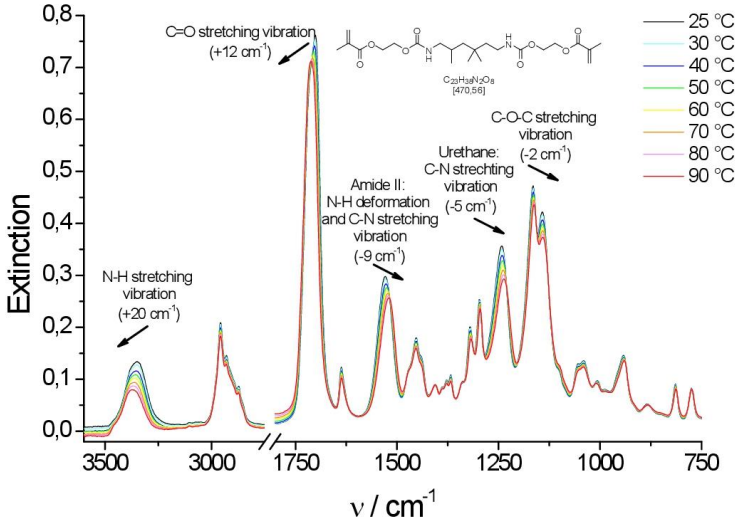

Figure S11: Recorded FT-IR(ATR) spectra of UDMA between temperature ranges of 25 – 90 °C. Due to the temperature dependency of hydrogen bonds, with increased temperature these bonds are weakened and show an alteration in shape and shift. Thus, especially the N-H (3358 cm^{-1}) and C=O (1702 cm^{-1}) stretching vibration shift to higher frequencies with increased temperature. Rather non hydrogen bond affected functional groups are temperature independent and remain constant in their shift and shape.

Thermal analysis by TGA experiments

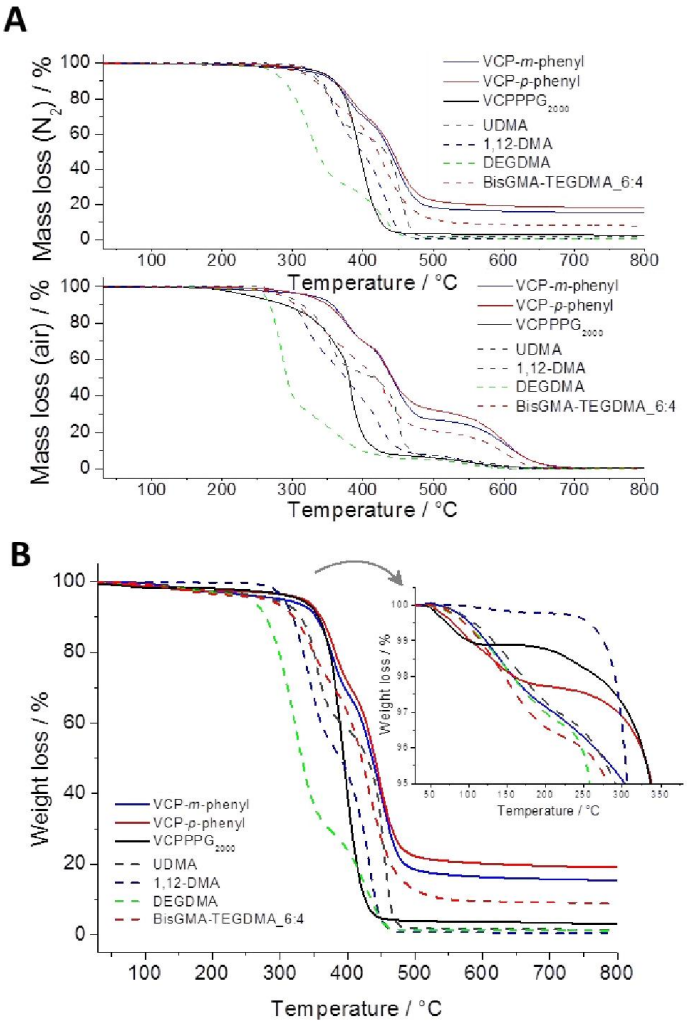

Figure S12: A: Comparison of the thermal stability of cured VCPPPG$_{2000}$, VCP-m/p-phenyl, UDMA, 1,12-DMA, DEGDMA and a mixture of BisGMA-TEGDMA in a ratio of 6:4 by TGA analysis, as well under nitrogen as protections gas as well under synthetic air (heating rate 10 K/min respectively). B: Determination of the maximum water uptake of the cured VCPPPG$_{2000}$, VCP-m/p-phenyl, UDMA, 1,12-DMA, DEGDMA and BisGMA-TEGDMA_6:4 samples by TGA measurements. The mass loss between 25-200°C determines the evaporation of absorbed water.

The oxidative degradation behavior of VCPPPG$_{2000}$ is due to the PPG spacer, and is in accordance with the literature.[1]

High resolution solid state ^{13}C-NMR spectroscopy of cured VCP ester-amides

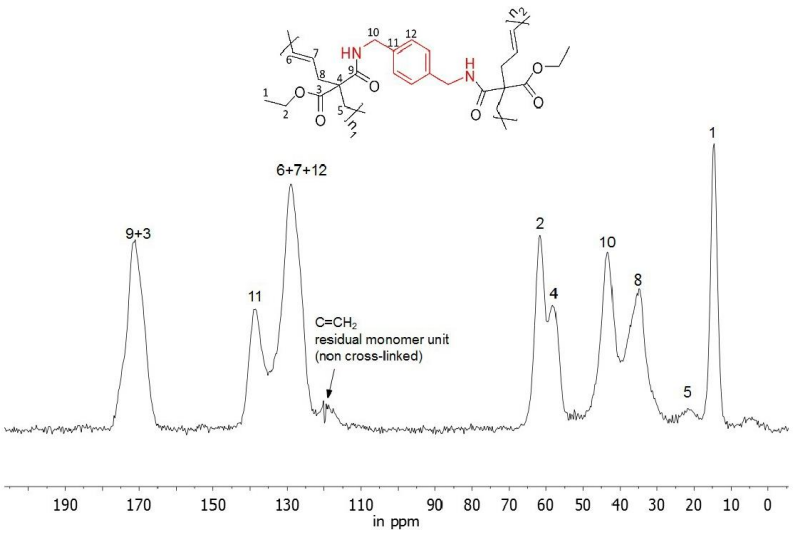

Figure S13: ^{13}C-CP/MAS NMR (100MHz) of cured VCP-*p*-phenyl. The carbon atom of the terminal vinyl unit (CH2=CH-) at 119.7 ppm significantly disappeared after curing. The residual signal indicates the residual non cross-linked VCP-units. Compared to the cured VCP-*m*-phenyl the residual amount of non cross-linked VCP units seems to be slightly higher. However, still a quantification seems not possible, as the signal intensity is outside the current detection limit.

Further investigation of the partial crystallinity of VCP-p-phenyl

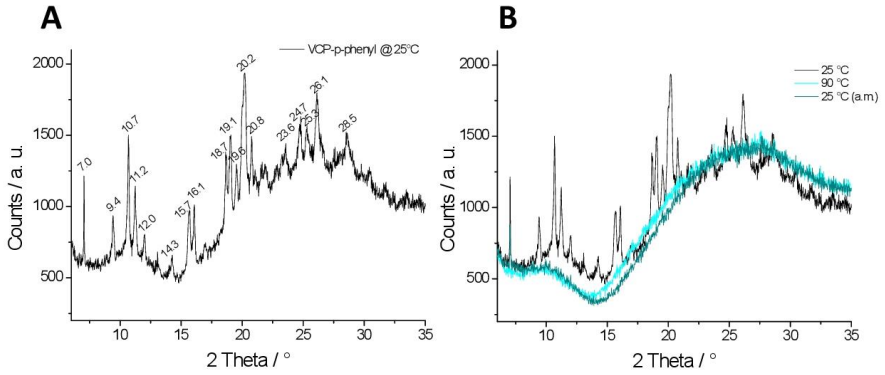

Figure S14: XRD measurements of VCP-p-phenyl. A: XRD diffractogram of VCP-p-phenyl at 25°C after purification, the characteristic XRD reflexes have been signed. B: Temperature dependent XRD measurements of VCP-p-phenyl to illustrate the melting behavior: The first diffractogram was measured at 25 °C, the second diffractogram was measured after heating at 90 °C, the crystalline phase melted completely as no further reflexes remained, the third diffractogram (25 °C a.m.) was measured after cooling the resin again to 25 °C (cooling rate ~5 K/min), no reflexes returned after cooling the resin, only two halos could be observed. After the VCP-p-resin is melted once, the recrystallization process is very slow, providing a partial recrystallization over weeks.

References

1 L. Yang, F. Heatley, T. G. Blease, R. I. Thompson, *Eur. Polym. J.* 1996, **32**, 535.

5 Outlook

Vinylcyclopropane (VCP) monomers and resins that show high polymerization rates and curing efficiencies are promising candidates for coatings, adhesives, 3D laser-writing systems as well as many other medical applications. Thereby both, the light-induced-polymerization technique and the design of partial pre-orientated VCP ester amides offer a sustainable and improved alternative to the commonly used methacrylate systems. Thus, this thesis provides the academic basis for a broad application range of VCP systems, since previous drawbacks of low reactivity and curing inefficiency have been overcome. Therefore, VCP ester amides may allow a facile and versatile implementation as low shrinking, fast polymerizable and post-modifiable system.

Several highly interesting applications seem accessible. Due to their rapid curing and high efficiency during light-induced polymerization, macro-monomers of VCP ester amides may be suitable for reactive electrospinning processes, obtaining spin-able and cross-linked fibers during illumination, as for instance achieved for some photo-cross linkable polymers by *S. Krause et al.* and *H. Wang et al.* (*Macromol. Rapid Commun.*, 2007, **28**, 2062 and *Sci. China Phys. Mech.*, 2012, **55**, 1189). Thereby, investigating the polymerization efficiency of VCPs with other initiators, besides the camphorquinone/amine system, would be promising to achieve an additional increase in polymerization kinetic and control.

Likewise, VCP systems may be auspicious for hydrogel applications as well. By an easy variation of the spacer unit, for instance, water soluble spacers could be incorporated. Such crosslinkable VCP resins may be useful for tissue engineering and other biological purposes. It may be anticipated that the rapid and efficient photo-polymerization, which was shown in this work for bulk polymerizations, is to a certain level transferable to aqueous systems.

Moreover, recently *J. Yue et al.* (*Adv. Funct. Mater.*, 2015, **25**, 6756) developed for the first time an antimicrobial and contact-killing 3D printable material based on dimethacrylate resins. The typical characteristics of VCP polymers like reduced shrinkage, lower internal stress and better durability are very likely to be useful and very valuable to those applications, too.

6 List of Publications

[1] Paul Pineda Contreras, Payal Tyagi, Seema Agarwal

Low volume shrinkage of polymers by photopolymerization of 1,1-bis(ethoxycarbonyl) 2-vinylcyclopropanes

in *Polymer Chemistry*, **2015**, *6*, 2297–2304.

[2] Paul Pineda Contreras, Christian Kuttner, Andreas Fery, Ullrich Stahlschmidt, Valérie Jérôme, Ruth Freitag, Seema Agarwal

Renaissance for low shrinking resins: all-in-one solution by bi-functional vinylcyclopropane-amides

in *Chemical Communications*, **2015**, *51*, 11899-11902.

[3] Paul Pineda Contreras and Seema Agarwal

Photo-polymerizable, low shrinking modular construction kit with high efficiency based on vinylcyclopropanes

in *Polymer Chemistry,* 2016, **7**, 3100–3106

7 Conference Participations

10/2011 **Poster presentation**

by Paul Ksionsko, Susanta Banerjee, Seema Agarwal, Andreas Greiner

FRONTIERS IN POLYMER CHEMISTRY - Kharagpur (IIT), India

Modification of poly(arylether)-membranes by including paracyclophane-elements to achieve copolymers with new and improved properties

09/2013 **Attendance**

BAYREUTH POLYMER SYMPOSIUM (BPS 2013) - Bayreuth, Germany

06/2015 **Poster presentation**

by Paul Pineda Contreras, Payal Tyagi, Seema Agarwal

EUROPEAN POLYMER CONGRESS 2015 (EPF) - Dresden, Germany

Low volume shrinkage polymers by photo polymerization of 1,1-bis(ethoxycarbonyl)-2-vinylcyclopropanes

09/2015 **Attendance**

79. COATING CONGRESS - Schwerin, Germany

09/2015 **Attendance**

BAYREUTH POLYMER SYMPOSIUM (BPS 2015) - Bayreuth, Germany

09/2015 **Poster presentation**

by Paul Pineda Contreras, Seema Agarwal

COVESTRO PH.D. WORKSHOP - Bayreuth, Germany

Renaissance for Low Volume Shrinking Polymers: About the Impact of Hydrogen-Bonding for Vinylcyclopropanes (VCP)

03/2016 **Oral presentation**

by Paul Pineda Contreras, Seema Agarwal

MATERIALS CHEMISTRY 2016 - Valencia, Spain

High efficiency for photo-polymerizable VCP ester-amide resins: A universal concept providing low volume shrinkage, high reactivity and selectivity

8 List of Abbreviations and Symbols

A	absorption
abs.	absolute
AIBN	2,2´-azobisisobutyronitrile
aq.	aqueous
ArC	aromatic carbon
ArH	aromatic proton
AROP	anionic ring opening polymerization
arom.	aromatic
ATR	attenuated total reflection
BHT	butylated hydroxytoluene
BisGMA	bisphenol-A-glycidyl methacrylate
C-C bond	carbon-carbon bond
CQ	camphorquinone
C_6D_6	deuterated-benzene
$CDCl_3$	deuterated-chloroform
CO_2	carbon dioxide
COSY	correlated spectroscopy
CP/MAS	cross polarization/magic angle spinning
CROP	cationic ring opening polymerization
d	doublet (NMR)
3D	three-dimensional space
Da	dalton
DCM	dichloromethane
DCC	*N,N´*-dicyclohexylcarbodiimide
DEA	dielectric analysis
DiMeVCP	2-methyl-2-(prop-1-en-2-yl)cyclopropane-1,1-dicarboxylate
DMAP	4-(dimethylamino)-pyridine
DPIHFP	diphenyliodonium hexafluorphosphate
DTBP	di-*tert.*-butyl-peroxide
DSC	differential scanning calorimetry

1,12-DMA	dodecanediol-dimethacrylate
DMSO	dimethyl sulfoxide
DMTA	dynamic mechanical thermal analysis
δ	chemical shift
EDG	electron donating group
EDMAB	ethyl 4-(dimethylamino)-benzoate
e.g.	for example (Latin “exempli gratia”)
EI	electron impact ionization
ESR/EPR	electron para- magnetic/spin resonance spectroscopy
eq.	equivalent(s)
ET	electron transfer
Et_3N	triethylamine
EtOH	ethanol
ESI	electronic supporting information
et. al.	*et alii; et aliae*
EWG	electron withdrawing group
FT	fourier transformation
GC	gas chromatography
GPC	gel permeation chromatography
H	proton
h	hours
H-bond	hydrogen bond
HCl	hydrochloric acid
H_2O	water
HMBC	heteronuclear multiple bond correlation
HOAc	acetic acid
HOBt	1-hydroxybenzotriazole
HSQC	heteronuclear single quantum coherence
HV	high vacuum
Hz	hertz (unit)
IR	infrared
J	coupling constant (NMR)
KOH	potassium hydroxide

KSCN	potassium thiocyanate
LC-HRMS	liquid chromatography–high resolution mass spectrometry
LD_{50}	lethal dose 50
LED	light emitting diode
lit.	literature
λ	wavelength
m	multiplet (NMR), medium absorption (IR)
MALDI	matrix-assisted laser desorption ionization
mCPBA	*m*-chloroperoxybenzoic acid
MPLC	medium pressure silica gel chromatography
MeOH	methanol
MHz	megahertz
MDO	2-methylene-1,3-dioxepane
Me	methyl group
MeVCP	isomeric mixture of 2-(prop-1-en-2-yl)cyclopropane-1,1-dicarboxylate and 2-methyl-2-vinylcyclopropane-1,1-dicarboxylate
min	minutes
MMA	methyl methacrylate
M_n	number average molar mass
MTT	3-(4,5-dimethylthiazol-2-yl)-2,5-diphenyltetrazolium bromide
MS	mass spectroscopy
M_w	weight average molar mass
Na	sodium
NaOEt	sodium ethanolate
NMR	nuclear magnetic resonance
Nu^-	nucleophile
p.a.	pro analysis
Pd	palladium (metal)
PEG	poly(ethylene glycol)
PMMA	poly(methyl methacrylate)
ppm	parts per million
R	rest (chemical structure)
R·	radical

R_f	retention factor
rpm	revolutions per minute
ROMP	ring opening methatesis polymerization
ROP	ring opening polymerization
RROP	radical ring opening polymerization
RT	room temperature
s	singlet (NMR); strong absorption (IR)
SE	spectroscopic ellipsometry
SOC	spiro orthocarbonate
SOE	spiro orthoester
St	styrene
T	temperature; transmission (IR)
t	triplet (NMR)
$T_{5\%}$	temperature of 5% degradation
T_g	glass transition temperature
TEGDMA	triethylene-glycol-dimethacrylate
TGA	thermogravimetric analysis
THF	tetrahydrofuran
T_m	melting temperature
TMS	tetramethylsilane
TOF	time of flight
UDMA	urethane-dimethacrylate
UV-Vis	ultraviolet-visible
ν	wavenumbers
VCP	vinylcyclopropane (generic term for VCP derivatives)
v.d.W.	van-der-Waals
w	weak absorption (IR)
wt	weight
XRD	X-ray powder diffraction

9 Acknowledgements

I am deeply grateful to Prof. Seema Agarwal for her supervision and the opportunity to work on this interesting and interdisciplinary topic, whereby I obtained a strong overview within the field of materials chemistry. Thus, I gained a deep dive into the field of organic & polymeric chemistry, to materials characterization and their applications. Further, I am thankful for her support and the degree of freedom I received, to develop my own ideas, even if not all of them achieved the original aims.

Also, I would like to thank Prof. Andreas Greiner for his mentoring and support, I received from beginning on my B. Sc. thesis in Nov. 2009 up to the end of my Ph.D. time.

Both, Prof. Agarwal and Prof. Greiner I would like to express my sincere gratitude once again, especially for their help to carry out an external research project at the Indian Institute of Technology (IIT Kharagpur), in India. Working in the group of Prof. Susanta Banerjee gave me an excellent training within cross-cultural competence and increased my interest in novel research topics. In this regard, I gratefully appreciate the financial support I received by the Bayer Science & Education Foundation.

I acknowledge the University of Bayreuth Graduate School and the BayNAT for financial support and training courses. Thereby, I thank Prof. Peter Strohriegel and Prof. Rhett Kempe for being my BayNAT mentors.

For the good cooperation and the regular exchange of ideas within our ZIM project (Zentrales Innovationsprogramm Mittelstand) I thank Dr. Alexander Bublewitz and Dr. Alexander Theis, both from the Kettenbach GmbH.

I am grateful for the help of my research and bachelor students Romina Kirschner, Christian Goldhahn and Philip Schmode. Thank you for your effort and the contributions to this work. All the best for your personal scientific careers.

I would like to thank my labmates, colleagues and friends in a collective for providing many tips, interesting discussions and suggestions. Among them I thank Dr. Ilka Paulus, Dr. Roland Dersch, Dr. Fangyao Liu, Dr. Fabian Mitschang, Dr. Peter Ohlendorf, Dr.Tina Löbling, Dr. Melissa Köhn-Serrano, Viola Buchholz, Judith Schöbel, Lu Chen, Pin Hu,

Michaela Enzeroth, Lisa Hamel, Hui Wang, Amir Bagheri, Matthias Burgard, Tobias Moss, Oliver Hauenstein, Florian Käfer, Steffen Reich, Markus Langner and all the other actual and former MCII members, respectively. Thereby, I want to provide special thanks to Markus, who accompanied me over the last 10 years from beginning of my study. Thanks for thousands of scientific discussions and our good teamwork.

Further, I thank our academic councilor Dr. Holger Schmalz for important scientific discussions and input, and our technicians Kerstin Küspert, Rika Schneider, Bianca Uch, Annika Pfaffenberger and Annette Krökel for their vast contributions concerning monomer synthesis, work-up, installation and repair of analytical instruments and measurements. Thank you for your help and for the nice work together.

I thank also the technical support from Ute Kuhn, Ingrid Otto, Dr. Reneé Siegel, Dr. Reiner Giesa, Dr. Christian Kuttner, Dr. Wolgang Milius and Prof. Peter Strohriegel, all from other departments of the University of Bayreuth, as well as from Dr. Stefan Schmölzer (Netzsch Company).

Many thanks to Gaby Rösner-Oliver, our chair secretary, for her generous support during my Ph.D. time. Thanks for being the soul of the MCII chair.

Moreover, I was lucky to be accompanied by my fellow students and close friends Jürgen Belz, Eric Dameron, Jochen Mogk and Mats Knoop, especially as those encouraged me during the duration of my part-time study.

I deeply appreciate the support of Ute, Karl-Heinz and Dominic Gottier who I call family, due to the vast motivation, love and help during my graduation and grow up. Without their presence, many things would have taken a completely different course.

Further I thank my parents Jadwiga and Reinhard Ksionsko for their education that led me to become who I am today.

Finally, I like to thank my great love Amanda *"mi cielo"*, her parents Beatriz and Benhur, as well as our cute dog Dido alias *"mi pequeño"*. I am so lucky we met and became such a great and colorful family. No words can express how thankful and happy I am.

10 (Eidesstattliche) Versicherung und Erklärung

Entsprechend der Promotionsordnung der Bayreuther Graduiertenschule für Mathematik und Naturwissenschaften/Bayreuth Graduate School of Mathematical and Natural Sciences (BayNAT) vom 20. März 2014

(§ 8 Abs. 2 Nr. 6 PromO)
Hiermit erkläre ich mich damit einverstanden, dass die elektronische Fassung meiner Dissertation unter Wahrung meiner Urheberrechte und des Datenschutzes einer gesonderten Überprüfung hinsichtlich der eigenständigen Anfertigung der Dissertation unterzogen werden kann.

(§ 8 Abs. 2 Nr. 8 PromO)
Hiermit erkläre ich eidesstattlich, dass ich die Dissertation selbstständig verfasst und keine anderen als die von mir angegebenen Quellen und Hilfsmittel benutzt habe.

(§ 8 Abs. 2 Nr. 9 PromO)
Ich habe die Dissertation nicht bereits zur Erlangung eines akademischen Grades anderweitig eingereicht und habe auch nicht bereits diese oder eine gleichartige Doktorprüfung endgültig nicht bestanden.

(§ 8 S. Abs Nr. 10 PromO)
Hiermit erkläre ich, dass ich keine Hilfe von gewerblichen Promotionsberatern bzw. -vermittlern in Anspruch genommen habe und auch künftig nicht in Anspruch nehmen werde.

Ort, Datum, Unterschrift